

Aus der Klinik für Psychosomatische Medizin und Psychotherapie

Direktor: Prof. Dr. Carsten Spitzer

Sektion für Gerontopsychosomatik und dementielle Erkrankungen

Leiter: Prof. Dr. Stefan Teipel

In Kooperation mit dem Deutschen Zentrum für Neurodegenerative Erkrankungen e.V.

Untersuchung des Zusammenhangs zwischen Dysregulation im

Fettstoffwechsel und pathologischen Markern der Alzheimer-Krankheit

(Exploring the relationship between dysregulation in the lipid metabolism and
the pathological hallmarks of Alzheimer's disease)

Kumulative Dissertationsschrift zur Erlangung des akademischen Grades

Doktor der Medizinwissenschaften

der Universitätsmedizin Rostock

vorgelegt von

Fatemah Sakr, geb. am 20.03.1985 in Kairo, Ägypten.

wohnhaft in Bielefeld, Deutschland.

Bielefeld, 24. März 2022

https://doi.org/10.18453/rosdok_id00004328

Gutachter:

Prof. Dr. med. Stefan Teipel.

Klinik und Poliklinik für Psychosomatik und Psychotherapeutische Medizin,
Sektion für Gerontopsychosomatik und demenzielle Erkrankungen,
Universitätsmedizin Rostock,
Rostock, Deutschland.

Prof. Dr. med. Bernd Krause.

Klinik und Poliklinik für Nuklearmedizin,
Universitätsmedizin Rostock,
Rostock, Deutschland.

Priv.-Doz. Dr. Peter Sörös.

Universitätsklinik für Neurologie,
Fakultät für Medizin und Gesundheitswissenschaften, Carl von Ossietzky Universität,
Oldenburg, Deutschland.

Jahr der Einreichung: 2022

Jahr der Verteidigung: 2023

Acknowledgements

I would like to express my warmest thanks and sincere gratitude to the special people who have helped and supported me accomplish this work.

First of all, I would like to express my deep sense of thanks and appreciation to my PhD supervisors, Prof. Dr Stefan Teipel, Prof. Anja Bräuer and Dr Angela Kuhla, for their expertise, valuable support of my work, their critical hints, constructive discussions and their patience.

Furthermore, I would like to thank my colleagues and friends from the Rostock University Medical Centre, the DZNE, the Institute of Experimental surgery and the Anatomy research group in the faculty of Medicine, Carl von Ossietzky University in Oldenburg. Without their advice, motivation and support, this work would not have been possible.

Finally, I would like to give special thanks to my husband Mohammed, my son Malek and my family for their understanding, continuous support and assistance, their love and care in all ups and downs.

Table of Contents

ACKNOWLEDGEMENTS	III
TABLE OF CONTENTS	IV
LIST OF TABLES	V
LIST OF FIGURES	VI
ABBREVIATIONS	VII
SUMMARY	VIII
ZUSAMMENFASSUNG	X
1. INTRODUCTION	1
1.1 AN OVERVIEW OF ALZHEIMER'S DISEASE.	1
1.2 PATHOPHYSIOLOGY OF ALZHEIMER'S DISEASE AND AMYLOID CASCADE THEORY.	1
1.3 NIA-AA 2018 RESEARCH FRAMEWORK.	3
1.4 β -AMYLOID PROGRESSION AND STAGING IN AUTOPSY AND IN-VIVO.	4
1.5 THE OMICS APPROACH UNVEILS THE LINK BETWEEN LIPIDS AND AD PATHOPHYSIOLOGY.	8
1.6 EXPERIMENTAL AIMS AND RESEARCH QUESTIONS.	9
2. METHODS	11
2.1 STUDIES COHORTS OVERVIEW	11
2.2 AMYLOID-PET DATA PRE-PROCESSING AND IN-VIVO STAGING.	13
2.3 VALIDITY OF IN-VIVO AMYLOID STAGES AND ASSOCIATION WITH THE COGNITIVE PERFORMANCE	14
2.4 LIPIDOMICS DATA PREPARATION AND ANALYSIS.	15
3. RESULTS	16
3.1 VALIDITY OF PET-BASED IN-VIVO AMYLOID STAGING SCHEME IN COGNITIVELY NORMAL SENIORS AT HIGHER RISK OF AD	16
3.2 ASSOCIATION OF IN-VIVO AMYLOID STAGES WITH APOE GENOTYPE AND CROSS-SECTIONAL COGNITIVE PERFORMANCE.	18
3.3 ASSOCIATION OF IN-VIVO AMYLOID STAGES WITH LONGITUDINAL COGNITIVE DECLINE.	18
3.4 LIPIDOMIC SIGNATURE IN BLOOD OF PRECLINICAL AND PRODROMAL AD	19
3.5 ASSOCIATION OF LIPID ENDOPHENOTYPES WITH FUTURE COGNITIVE DECLINE	20
4. DISCUSSION	22
4.1 VALIDITY OF PET-BASED IN-VIVO AMYLOID STAGING.	22
4.2 CLINICAL UTILITY OF AMYLOID STAGES AND ADVANTAGE OVER GLOBAL AMYLOID STATUS APPROACH.	23
4.3 LIPIDOMICS SIGNATURE AND CONTRIBUTION TO THE RISK OF AD AND CLINICAL PROGRESSION	24
4.4 CONCLUSION AND FUTURE DIRECTIONS.	25
REFERENCES	26
SELBSTSTÄNDIGKEITSERKLÄRUNG	37
LEBENS LAUF UND WISSENSCHAFTLICHER WERDEGANG	38
FACHPUBLIKATIONEN	39
PRÄSENTATIONEN AUF NATIONALEN UND INTERNATIONALEN FACHKONGRESSEN	39
APPENDIX (STUDIES 1-3)	41

List of Tables

Table 1: Demographic characteristics of INSIGHT-preAD cohort.	11
Table 2: Summary of study samples derived from ADNI and INSIGHT-preAD cohort.	12
Table 3: Summary of demographic characteristics of ADNI cohort used in the third study...	12
Table 4: Distribution of the non-stageable cases across ADNI and INSIGHT-preAD cohorts.	17
Table 5: Distribution of the in vivo amyloid stages among the INSIGHT-preAD participants compared to conventional global amyloid status.	17
Table 6: Results of Cox regression models.....	19
Table 7: Risk of clinical progression among prodromal lipidomic endophenotypes.	21

List of Figures

Figure 1: The sequence of major pathogenic events leading to AD as proposed by the amyloid cascade hypothesis.	3
Figure 2: Hypothetical time course of pathological changes throughout the Alzheimer's disease (AD) continuum.	4
Figure 3: Schematic representation of Thal amyloid deposition phases and their correspondence to the clinical status.	5
Figure 4: Grothe's in-vivo amyloid staging model.	7
Figure 5: Role of lipids in the pathophysiology of AD.	9
Figure 6: In-vivo amyloid stages in INSIGHT-preAD cohort.	16
Figure 7: Dysregulated Lipids in preclinical and prodromal AD.	20

Abbreviations

A β : beta-amyloid plaques.

ABCA7: ATP Binding Cassette Subfamily A Member 7.

AD: Alzheimer's disease.

ADNI: Alzheimer's disease Neuroimaging Initiative.

AIC: Akaike information criterion.

APOE: Apolipoprotein E.

APP: amyloid protein precursor.

BBB: the blood-brain barrier.

CDR: clinical dementia rating scale.

CLU: Clusterin.

CSF: cerebrospinal fluid.

MCI: mild cognitive impairment.

NIA-AA: National Institute on Aging and Alzheimer's Association.

NFT: neurofibrillary tangles.

PET: positron emission tomography.

PIB: ¹¹C Pittsburgh compound B.

PICALM: Phosphatidylinositol Binding Clathrin Assembly Protein.

PLCG2: phospholipase C-gamma.

PLD3: phospholipase-D3

PUFA: polyunsaturated fatty acids.

SCD: subjective cognitive decline.

SORL1: Sortilin Related Receptor 1.

SMC: subjective memory decline.

SUVR: Standardised uptake value ratio.

PVE: partial volume effects.

Summary

Alzheimer's disease (AD) is recognised as a complex, multifactorial disease that manifests itself along a continuum of conditions, ranging from asymptomatic preclinical phase to mild cognitive impairment (MCI) and finally end up with dementia. However, a wide diversity is observed in individuals' clinical course and transition time between continuum phases of the disease. Conventional approaches using established biomarkers are not precise enough to predict the progression of AD and hence individuals' future risk of cognitive decline.

The purpose of this doctoral dissertation is to explore novel biomarker candidates that could reinforce the diagnostic accuracy and predict disease progression at preclinical and early phases of AD. Such biomarkers are expected to allow the stratification of individuals based on the risk associated with their specific pathology burden, i.e., region-specific cortical amyloidosis and lipids dysregulations.

Within the frame of this dissertation, our first study demonstrated the validity and replicability of a recently proposed PET-based in-vivo amyloid staging scheme in a cohort of cognitively normal seniors at higher risk of AD. This amyloid staging scheme allowed for identifying ~ 50 % of individuals having evidence of regional amyloid deposition in the preclinical cohort as opposed to the 21.5 % identified using the conventional global amyloid status. The second study shows the clinical utility of this amyloid staging approach, where higher amyloid stages (from stage II onwards) were associated with a higher risk for clinical progression, particularly in cognitively normal older individuals. These results were robustly replicated across independent samples from two different cohorts. Finally, we identified peripheral lipidomics signature associated with AD pathology biomarkers using data from the ADNI cohort in the third study. Ether-glycerophospholipids, their lyso derivatives, free-fatty acids, cholesterol esters, and complex sphingolipids were altered in the plasma of preclinical and prodromal AD cases. Depletion of PUFA- plasmalogens, long-chain sphingomyelins, and dihydro-ceramides together with higher levels of cholesterol esters, complex ceramides identified a distinct endophenotype associated with a higher risk of progression in prodromal AD cases.

In summary, this work provides evidence for robustness and clinical utility of the in-vivo amyloid staging approach for risk stratification of AD cases, particularly at the preclinical phase. Lipidomics data offers complementary information contributing to AD risk and subsequent clinical trajectories. Both approaches could enable higher precision in research participants' characterisation, which

could be particularly important in guiding and planning clinical trials and adapting intervention regimens to different target subpopulations in prevention trials.

Zusammenfassung

Die Alzheimer-Krankheit (AD) gilt als komplexe, multifaktorielle Erkrankung, die sich entlang eines Kontinuums von Zuständen zeigt, das von der asymptomatischen präklinischen Phase über die leichte kognitive Beeinträchtigung (MCI) bis hin zur Demenz reicht. Der klinische Verlauf und die Übergangszeiten zwischen den einzelnen Phasen der Krankheit sind jedoch sehr unterschiedlich. Herkömmliche Verfahren, die sich auf etablierte Biomarker stützen, sind nicht ausreichend, um das Fortschreiten der Alzheimer-Krankheit und damit das zukünftige Risiko des kognitiven Verfalls von Personen vorherzusagen.

Das Ziel dieser Dissertation ist es, neue Biomarker zu identifizieren, die die diagnostische Genauigkeit unterstützen und das Fortschreiten der Krankheit in präklinischen und frühen Phasen der Alzheimer-Krankheit vorhersagen könnten. Mit Hilfe dieser Biomarker wird eine Stratifizierung von Personen auf der Basis des Risikos ermöglicht, dass mit ihrer spezifischen Pathologiebelastung verbunden ist, d. h. regionsspezifische kortikale Amyloidose und Lipidstörungen.

Im Rahmen dieser Dissertation hat unsere erste Studie die Gültigkeit und Reproduzierbarkeit eines neulich vorgeschlagenen PET-basierten In-vivo-Amyloid-Staging-Schemas in einer Kohorte kognitiv normaler Senioren mit erhöhtem Alzheimer-Risiko nachgewiesen. Mit diesem Amyloid-Staging-Schema konnten ~ 50 % der Personen identifiziert werden, die Anzeichen für regionale Amyloid Ablagerungen in der präklinischen Kohorte aufwiesen, im Gegensatz zu den 21,5 %, die mit dem herkömmlichen globalen Amyloidstatus ermittelt wurden. Die zweite Studie hat den klinischen Nutzen dieses Amyloid-Staging-Ansatzes aufgezeigt, wobei höhere Amyloidstadien (ab Stadium II) mit einem höheren Risiko für ein klinisches Fortschreiten verbunden waren, insbesondere bei kognitiv gesunden älteren Menschen. Diese Ergebnisse konnten in unabhängigen Stichproben aus zwei verschiedenen Kohorten zuverlässig repliziert werden. Schließlich bestimmten wir in der dritten Studie anhand von Daten aus der ADNI-Kohorte eine periphere Lipidomics-Signatur, die mit Biomarkern der AD-Pathologie assoziiert ist. Es wurde festgestellt, dass Ether-Glycerophospholipide, Lyso-Glycerophospholipide, freie Fettsäuren, Cholesterinester und komplexe Sphingolipide im Plasma von präklinischen und Prodromal-AD-Fällen dysreguliert sind. Die Abnahme von PUFA-Plasmalogenen, langkettigen Sphingomyelinen und Dihydroceramiden zusammen mit höheren Gehalten an Cholesterinestern und komplexen Ceramiden ergab einen ausgeprägten Endophänotyp, der mit einem höheren Risiko für das Fortschreiten der Alzheimer-Krankheit im Prodromalstadium verbunden ist.

Insgesamt liefert diese Doktorarbeit Beweise für die Zuverlässigkeit und den klinischen Nutzen des Amyloid-Staging Verfahrens für die Risikostratifizierung von AD-Fällen, insbesondere in der präklinischen Phase. Lipidomics-Daten bieten zusätzliche Informationen, die zum Alzheimer-Risiko und den nachfolgenden klinischen Verläufen beitragen könnten. Beide Ansätze könnten eine genauere Charakterisierung von Forschungsteilnehmern ermöglichen, was besonders wichtig für die Leitung und Planung klinischer Studien und die Anpassung von Interventionsschemata an verschiedene Zielgruppen in Präventionsstudien sein könnte.

1. Introduction

1.1 An overview of Alzheimer's disease.

Alzheimer's disease (AD) is a progressive neurodegenerative disease characterised by initial memory impairment and deterioration in other cognitive abilities that ultimately affect behaviour, speech, visuospatial orientation and interfere with daily living activities in the dementia stage (1). AD is considered the most common cause of dementia in older people above the age of 65 since it accounts for 60-80% of all dementia cases (1-3). 2021 World Alzheimer Report estimated that over 55 million people worldwide live with Alzheimer's disease or a related form of dementia (4), and the prevalence is increasing worldwide. Rising life expectancy contributes to the rapid increase in prevalence (5). Hence, it is anticipated that by 2050 the number of people living with dementia worldwide will be greater than 131 million (5). On a national level, Germany belongs to the top 10 countries with the largest number of people with dementia worldwide (6). The current number of dementia cases is estimated to be over 1.6 million, with an annual incidence of over 300,000 new cases (7).

From an economic perspective, dementia is considered one of the costliest chronic illnesses in old age due to substantial medical and social care burdens, both direct and informal (4,5,7). The 2015 global societal economic cost of dementia was estimated as 818 billion US\$, with a considerable impact on the quality of life both for individuals living with dementia and for their families and caregivers (5). This cost is forecast to steadily increase in the coming years to cross 2 trillion US\$ by 2030 (5). AD has become a tremendous public health and socio-economic challenge of the 21st century (2,8). To date, none of the available pharmacological treatments can halt or slow down the damage and destruction of neurons caused by the disease (2,3), which makes the development of disease-modifying therapeutic procedures an urgent need (8).

1.2 Pathophysiology of Alzheimer's disease and Amyloid cascade theory.

The core pathological hallmark of Alzheimer's disease is the accumulation of two abnormal protein fragments, extracellular beta-amyloid and intracellular abnormal tau, known as beta-amyloid ($A\beta$) plaques and neurofibrillary tangles (NFT) (9,10). $A\beta$ peptides result from sequential cleavage of

Introduction

amyloid precursor protein (APP) by beta- and gamma- secretases (1,8,11,12). On the other hand, A β is cleared from the central nervous system through several mechanisms, including phagocytosis from microglia, enzymatic breakdown, or vascular mechanisms (11) and perivascular drainage of interstitial fluid in the brain (12,13). In AD, A β levels are elevated due to an imbalance between the production and clearance pathways (1,11). Late-onset sporadic AD is usually associated with reduced beta-amyloid clearance, whereas familial early-onset AD is due to overproduction (11). Elevated A β peptides, particularly A β -42, promote their aggregation into higher-order oligomers, fibrils, and plaques (8). Both A β plaques and oligomers contribute to impairment of synaptic activity and synapse loss (11), cerebral capillary blood flow impairment, and direct promotion of tau pathology by stimulating tau hyperphosphorylation (8,12,14,15). A β species can further trigger several downstream events, such as oxidative stress, mitochondrial dysfunction and specifically neuroinflammation (11,12,15).

Tau, a microtubule-associated protein, is the principal constituent of neurofibrillary tangles (16,17). The tau proteins in NFT are formed of paired helical filaments, which are hyperphosphorylated and abnormally folded with an increased affinity to aggregate as intercellular tangles (16,18). Hence, hyperphosphorylated tau loses its ability to bind and stabilise axonal microtubules, which impairs the anterograde transport of nutrients and organelles, including mitochondria, along axons to the synapse and in turn leads to neurodegeneration (11,17,19).

The amyloid cascade hypothesis posits A β as the earliest molecular driver of the disease (20,21), given that A β levels in the brain start to increase decades preceding the development of clinical symptoms (20,22). This hypothesis proposes that A β peptides trigger a cascade of downstream cellular and molecular changes, including tangles aggregation, microgliosis, neuritic dystrophy that finally lead to neurodegenerative changes, cognitive impairment, and dementia (Figure 1) (20,21,23).

A definite AD diagnosis can only be made post-mortem since it requires an extensive neuropathologic evaluation considering the morphology and density of lesions and their topographic distribution (1,24–26). However, advances in biomarkers have enabled the depiction of AD neuropathologic changes in living persons with reasonable validity using cerebrospinal fluid (CSF) or positron emission tomography (PET) imaging biomarkers (24,27,28) as surrogate markers for cerebral beta-amyloid and tau deposition (26,29). A key advantage of PET imaging over fluid biomarkers is the in-vivo depiction of AD pathology biomarkers' magnitude and topographic distribution (24,26–28).

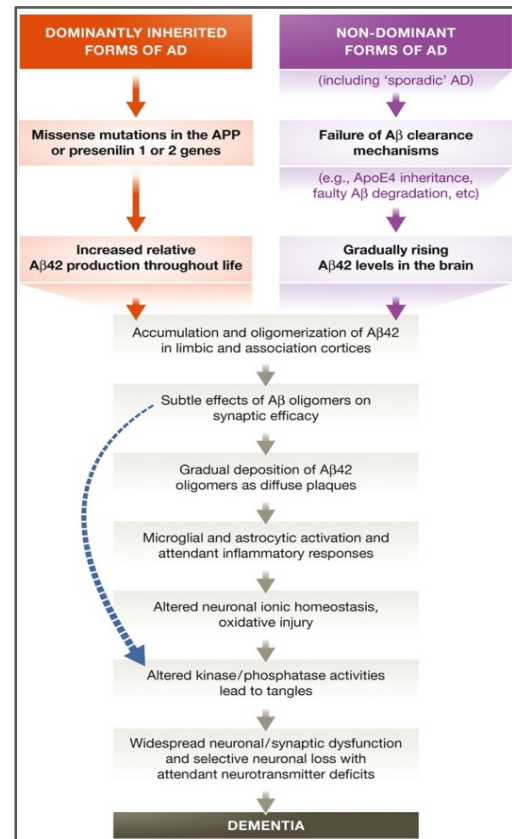


Figure 1: The sequence of major pathogenic events leading to AD as proposed by the amyloid cascade hypothesis.

The curved blue arrow indicates that Aβ oligomers may directly injure the synapses and neurites of brain neurons, in addition to activating microglia and astrocytes. Adapted from Selkoe and Hardy (20).

1.3 NIA-AA 2018 research framework.

In 2018, the National Institute on Aging and Alzheimer's Association (NIA-AA) formulated an updated and unified framework for defining and staging individuals in Alzheimer's disease continuum in the research setting before being adopted into clinical practice (26). According to this research framework, the definition of AD was shifted to a biological construct based on detection of AD neuropathologic changes, for instance, amyloid deposition, pathologic tau, and neurodegeneration [AT(N)], in living subjects using biomarkers rather than the clinical sequence of the disease, i.e., symptoms and signs (26). This definition will ensure a more accurate characterisation of research participants and advance understanding of the sequence of downstream pathologic events that may contribute to the cognitive impairment associated with AD (26). This strategy will additionally enable a more precise approach to interventional trials where specific pathways can be targeted in the disease process and the appropriate people (26).

According to the AT(N) scheme (26), abnormality in both A β deposition and pathological tau biomarkers are mandatory to make a diagnosis of AD (9,26,30). While abnormality in A β deposition alone implies the presence of Alzheimer's pathological changes (26). Consequently β -amyloidosis is widely viewed as the defining signature of AD and the earliest evidence of related neuropathologic change detectable in living persons (31,32). β -amyloidosis is further recognised as being capable of inducing downstream pathologic processes, i.e., tauopathy and neurodegeneration, and ultimately leading to cognitive impairment (Figure 2) (33–35).

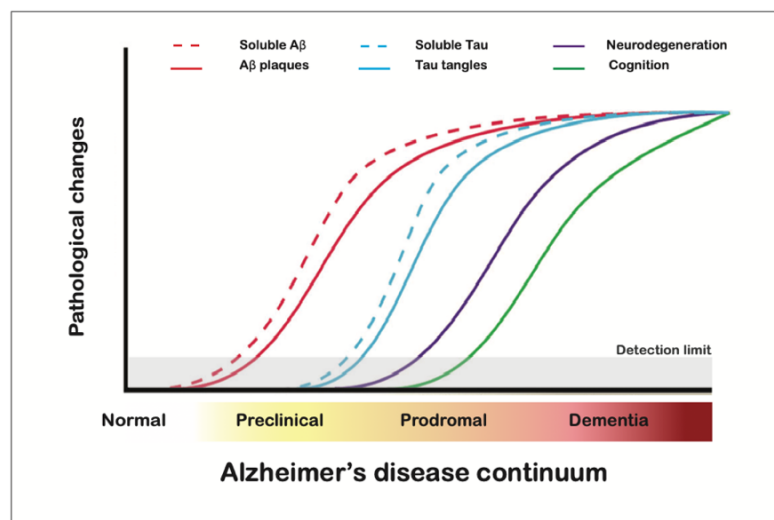


Figure 2: Hypothetical time course of pathological changes throughout the Alzheimer's disease (AD) continuum.

First, biomarkers for amyloid- β become abnormal [cerebrospinal fluid (CSF) amyloid- β 1-42 preceding PET], followed by abnormal tau (CSF p-tau preceding PET), neurodegeneration, and cognitive decline. Adapted from Jack et al. (36,37) and Leuzy et al. (38).

Despite the validity of the established biomarkers, it is crucial to bear in mind that their sensitivity is restricted by the in-vivo limit of detection (26). For instance, PET scans of individuals with early phases of amyloid deposition, as determined by the autopsy, were usually labelled as normal or negative scans regardless ^{11}C Pittsburgh compound B (PIB) (27,28,39) or fluorine (^{18}F) radiolabelled ligands (40–42) were used.

1.4 β -Amyloid progression and staging in autopsy and in-vivo.

Neuropathological studies in autopsy suggested that A β deposition follows a distinct sequence of hierarchical regional involvement (43–46). Dietmar Thal proposed a staging scheme to define phases of amyloid pathology progression in the brain during the course of AD (43). This staging scheme has been later adopted by NIA-AA 2011 for the assessment of A β deposits [A] in the

autopsy gold standard (9,30). In Thal’s scheme, Phase 1, the neocortex is involved, expanding to the allocortex in Phase 2, subcortical nuclei, including the striatum, thalamus and basal forebrain cholinergic nuclei, were involved in Phase 3 (43). Brainstem nuclei were first engaged in Phase 4 and finally the cerebellum in Phase 5 (Figure 3) (43). He observed that AD cases typically exhibit A β phases 4, 5 and occasionally 3, representing a relatively late AD stage (9,30,43). However, early A β phases, particularly 1 and 2, were only observed in asymptomatic individuals; hence these phases could be recognised as preclinical phases of AD (43). He further claimed that the success of AD modifying treatments strongly relies on targeting nondemented individuals in early A β phases, i.e., phases 1 and 2, before the massive expansion of A β and consequently tau pathology in the brain (28,43).







Diagnosis	Normal or non- AD	AD Preclinical stages			AD Clinical stages	
	 A0 = no A β Plaques	 A1 = Phase 1	 A1 = Phase 2	 A2 = Phase 3	 A3 = Phase 4	 A3 = Phase 5
Aβ plaques pathology	NIA-AA score					
	Thal phases	Phase 0 No plaque	Phase 1 Sparse, small groups of diffuse neocortical plaque	Phase 2 + allocortex hippocampus and entorhinal cortex	Phase 3 + striatum Subpial, post cingulate gyrus	Phase 4 + Midbrain-substantia nigra, medulla Oblongata

Figure 3: Schematic representation of Thal amyloid deposition phases and their correspondence to the clinical status.

Different brain regions develop A β deposits in a distinct hierarchical sequence. The red colour shows the newly involved regions in each phase, while the black represents the regions already involved from the previous phase. Adapted from Thal et al. (40) and Koychev et al.(47).

Amyloid sensitive PET imaging is considered a direct in-vivo measure of cortical amyloid load with high specificity and relatively strong correlation with the autopsy gold standard (24,26,28,39,48). Global cortical retention of amyloid-specific radiotracer is conventionally calculated by signal averaging over a meta-region of interest mask, including bilateral prefrontal, orbitofrontal, temporal, parietal, anterior cingulate, posterior cingulate, and precuneus brain regions (49). Then PET scans are binary classified, as positive or negative scan, based on the radiotracers-specific optimised threshold (39). This classification approach was implemented in the clinical setting and basically the inclusion of subjects in clinical trials (39). Several studies have investigated the correspondence

between the global cortical retention and the post-mortem neuropathological evaluation and Thal A β phases (27,28,39–41). However, these studies assumed the low sensitivity of this approach to detect early amyloid deposition (27,28,39–41). Using PIB PET scan, Murray et al. have demonstrated that PIB SUVR of 1.40 corresponds to Thal amyloid Phase 2 (28). They also declared that individuals with Thal phase 1 were labelled as negative PET scans (28). Comparable observations were obtained using fluorine (^{18}F) labelled radiotracers (40–42). Both studies by Thal et al. and Salloway et al. have shown that ^{18}F flutemetamol amyloid PET scans were classified as positive in Thal amyloid phase 4 and 5 cases. In contrast, all Thal amyloid phases 0, 1 and 2 cases were labelled as negative scans (40,42). Only third of the individuals with Thal amyloid phase 3 was assigned as positive for amyloid based on PET scans (40).

Subsequently, a more sensitive approach was suggested to identify early amyloid accumulators while their cognitive functions are still preserved (28,39,41). Many studies recommended using a lower, liberal cut-off than those conventionally used to assign positivity based on global cortical retention (28,39,41). Villeneuve et al. determined an optimal threshold for early amyloid detection (SUVR of 1.21) based on the PIB PET scan (39). They showed that this liberal threshold yielded better sensitivity, yet comparable specificity, to the commonly used conservative threshold (SUVR of 1.40) (39). This approach, however, increased false-positive findings (39).

Alternatively, detailed topographical distribution of amyloid was proposed to characterise and stage amyloid progression in-vivo analogous to Thal amyloid deposition phases in post-mortem autopsy (28,50–54). Grothe et al. adopted a data-driven approach to determine in-vivo regional amyloid progression sequence based on the frequency of regional amyloid positivity across cognitively normal older participants enrolled in the Alzheimer's disease Neuroimaging Initiative (ADNI) study (53). Then a hierarchical four-stage model was constructed (Figure 4), where temporo-basal and fronto-medial areas were initially involved in stage (I), then spread over the remaining associative neocortex in stage (II). The primary sensory-motor cortex and the medial temporal lobe were involved in stage (III), and finally, the subcortical regions, striatum and thalamus, in stage (IV) (53). Given the high consistency of the hierarchical amyloid progression pattern across brain regions, almost all cases profiles (>98%) were classified into one of the four progressive amyloid stages in their study (53). The earliest amyloid deposition stages, \simeq 25% of stage II and 80 % of stage I, were mostly misclassified in the conventional binary assessment of global PET signal, even with more liberal thresholds (50,53,55). Increasing amyloid progression stages correlated well with the drop in CSF A β levels and cognitive deficits in healthy elderly individuals as well as those with mild

cognitive impairment (MCI) (53,56–58). Grothe et al. presented a fine-grained amyloid staging scheme that may be particularly useful for stratifying early and preclinical stages of AD (53,55–58).

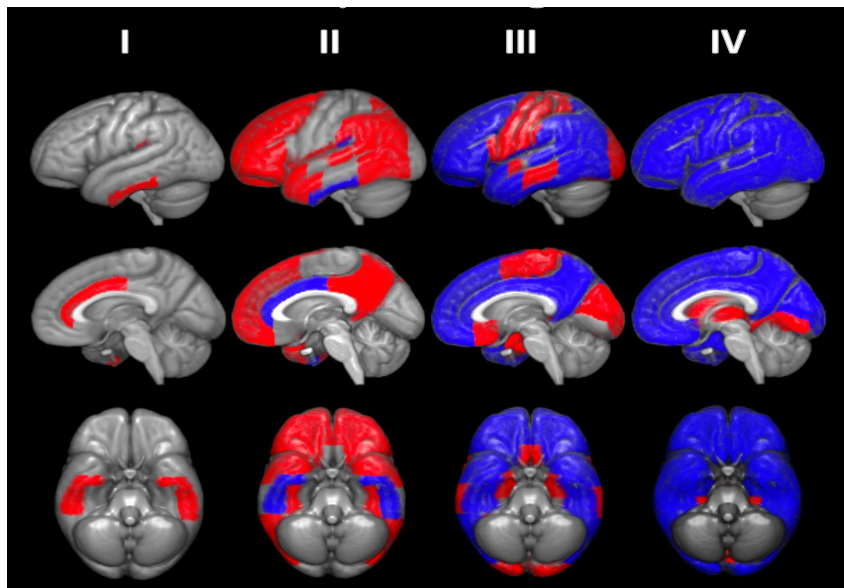


Figure 4: Grothe's in-vivo amyloid staging model.

Amyloid staging is a hierarchical model of four distinct stages representing amyloid deposition progression. Each amyloid stage is derived by the involvement of the corresponding anatomical division (in red) in addition to the previously affected areas (in blue). Figure created in correspondence to the staging model in Grothe et al. (53).

Alternative approaches were proposed for region-based in-vivo amyloid staging schemes (51,52). Hanseeuw et al. considered an a priori distinction between early neocortical and later subcortical amyloid deposition (52). Accordingly, they classified participants into three PET stages; Stage 0: low cortical and low striatal PET signal, Stage 1 high cortical and low striatal and Stage 2 high cortical and high striatal (52). Their staging scheme correlated well with tau burden, hippocampal atrophy and predicted future cognitive impairment (52). Conversely, Mattsson et al. made use of the time lag, up to 10 years, between amyloid positivity based on CSF biomarker and global PET signal to distinguish regions of early versus late amyloid accumulation (51,59–61). They identified three composites of early, intermediate, and late amyloid deposition; then their final staging scheme included four stages; Stage 0: all three composites were negative for amyloid, Stage 1: only early composite was positive, Stage 2: early and intermediate composites were positive and Stage 3: all three composites were positive (51). They validated their staging scheme in an independent cohort using a different radiolabelled ligand (51). Furthermore, they showed a sequential increase of CSF p-Tau levels in Stage 1, CSF Tau in Stage 2, and accelerated atrophy in Stage 3 (51).

1.5 The omics approach unveils the link between lipids and AD pathophysiology.

AD is increasingly recognised as a complex and multifactorial disease that manifests itself along a continuum of conditions, ranging from asymptomatic preclinical phase to mild cognitive impairment (MCI) and finally end up with dementia (62). Heterogeneity was observed in individuals' specific clinical course and transition rates between continuum phases of the disease (62,63). However, established AD biomarkers fall short in explaining individual clinical trajectories and precisely predicting future risk of cognitive decline (62). Thus, high-throughput 'Omics', an unbiased data-drive approach, was recently deployed for a more comprehensive and deeper insight into individuals' molecular and metabolic pathways (62,64,65). Alterations in these pathways may reflect ongoing downstream pathologic events due to AD pathology as well as individual's specific comorbidities and genetic characteristics (62,65).

Growing evidence supports the role of lipid dysregulation in the aetiology of AD as early as preclinical phases of the disease (66–68). Lipids play critical structural and physio-chemical roles in the brain since they are an essential membrane constituent of the cell and its organelles and are actively involved in cellular transport, energy storage, and signalling pathways (69–71). Changes in membranes' lipid composition and organisation interfere with the processing and trafficking of proteins and metabolites, hence modulating the activity of transmembrane proteins, e.g., amyloid protein precursor (APP) and its secretases as well as ion-channels (69,71). Moreover, perturbation of membrane lipids can have devastating consequences on cellular signalling, energy balance, blood-brain barrier (BBB) function and myelin and synapses integrity (71). Essentially, lipids, particularly polyunsaturated fatty acids (PUFA), play a crucial role in regulating inflammatory response through pro-inflammatory and pro-resolving lipid mediators, as well as response to oxidative stress (71).

Regarding AD genetic risk, the APOE gene, particularly its E4 allele, is the strongest common genetic risk factor for late-onset sporadic form. APOE is the primary lipoprotein in the brain, which has an abundant role in the lipids' transport and metabolism (71). Recent genome-wide association studies (GWAS) identified several genes involved in lipid metabolism and are significantly associated with increased risk for AD (72,73). For instance, genes involved in cholesterol metabolism and transport such as Clusterin (CLU) (74), SORL1, ABCA7 and APOE (72,73,75). Additional potential loci were identified including, PICALM (72–75), phospholipase-D3 (PLD3)

(75,76) and the microglia related phospholipase C-gamma (PLCG2) (77,78). PICALM is involved in the intracellular trafficking of proteins and lipids (79), while PLD3 and PLCG2 are involved in lipid metabolism and crucial downstream signalling pathways (76–78). Taken together by biological and genetic evidence, lipid metabolism can capture several facets in the complex pathophysiology of AD (Figure 5) and, therefore could serve as a potential biomarker in early asymptomatic stages of AD (71,80).

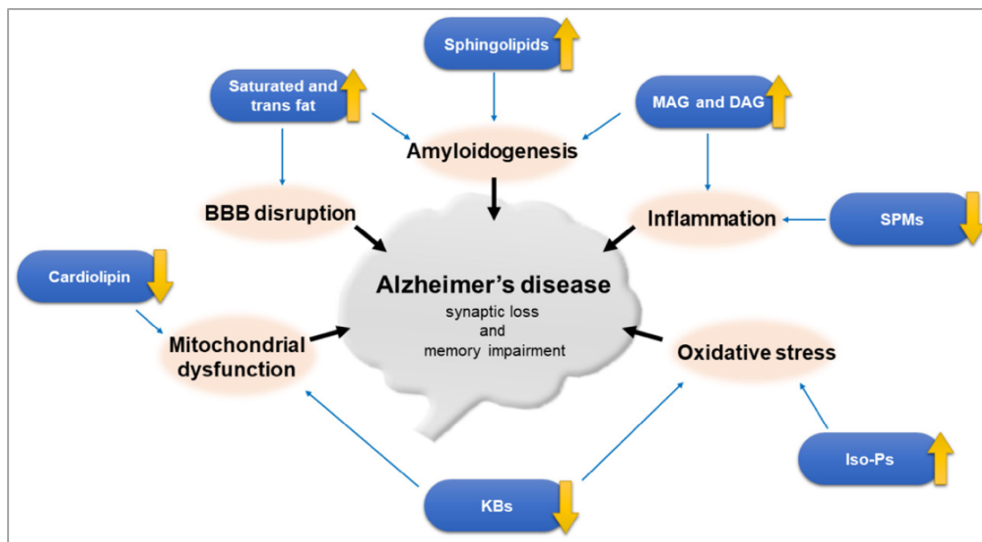


Figure 5: Role of lipids in the pathophysiology of AD.

Several mechanisms link lipids dysregulation and AD, including modulating transmembrane proteins, neuronal signalling pathway, BBB disruption, mitochondrial dysfunction, oxidative stress, and inflammation, leading to synaptic loss and ultimately memory impairment. Adapted from Kao et al.(80).

Lipidomics, an omics approach, aims to quantitatively and comprehensively analyse lipid pathways and networks in biological systems (70,81). Advances in lipidomics platforms enabled identifying thousands of lipid species with a high level of sensitivity and precision (70,81). Plasma lipidome is complex and consists of many lipid species that share similar elemental composition, yet they might display specific associations with biological outcomes (65). Now, it is feasible to examine in detail the comprehensive plasma lipidome in a human population or clinical study using recent ultra-high-performance high-resolution mass spectrometry and high-performance liquid chromatography (65).

1.6 Experimental aims and research questions.

The purpose of this doctoral dissertation was to explore novel biomarkers that could reinforce the diagnostic accuracy and predict disease progression at preclinical and early phases of AD when the utility of clinical data is limited. We believe that these biomarkers will enable the stratification of

individuals based on the risk associated with their specific pathology burden, i.e., region-specific cortical amyloidosis and lipids dysregulations. Such stratification could be of particular importance in guiding the selection of individuals in clinical trials and adaptation of intervention regimens to different target subpopulations in prevention trials (62,64). Our aim was addressed through the following objectives in three different studies:

I- Investigate the validity and replicability of a fine-grained PET-based in-vivo amyloid staging scheme in a cohort of cognitively normal seniors at higher risk of AD (55):

The first study used 18F-florbetapir PET data of cognitively intact older individuals with subjective memory decline (SMC) from an independent monocentric cohort (INSIGHT-preAD). We projected their regional amyloid uptake signal into the previously designated hierarchical regional amyloid staging. Subsequently, we determined the adherence to this model across all cases. Finally, we tested the association between increasing in vivo amyloid stage and cognitive performance using ANCOVA models as well as the frequency of the APOE- ϵ 4 allele.

II- Evaluate the associated risk of the amyloid stages with future cognitive decline in cognitively normal seniors at higher risk of AD (58):

In the second study, we were interested in determining the usefulness of the previously designated regional amyloid staging to predict conversion of cognitively normal people with and without subjective cognitive/memory decline (SCD/ SMC) to MCI or AD dementia. We additionally evaluated the risk of MCI cases conversion to dementia. We used clinical dementia rating scale (CDR) scores as the primary endpoint to assess change in cognitive function.

III- Identifying the lipid dysregulations in the blood associated with AD pathology biomarkers in preclinical and prodromal AD cases and inspecting their possible contribution to the risk of future cognitive decline (82):

We identified dysregulated lipids in the blood (plasma) of preclinical and prodromal AD cases using targeted lipidomics data derived from the ADNI cohort. We adopted a Bayesian elastic net regression method to select salient plasma lipid classes associated with CSF pTau/A β 42 ratio as a combined biomarker of AD pathology. Then we determined lipidomic endophenotypes within prodromal and preclinical cases, respectively, using a consensus clustering approach applied to the selected lipid classes. Finally, we investigated the possible contribution of these lipid endophenotypes to the risk of future cognitive decline.

2. Methods

2.1 Studies cohorts overview

As explained below, we used different cohorts to achieve our goals and objectives.

Study 1: (55) We used the INSIGHT-preAD cohort, which consisted of 318 cognitively normal Caucasian individuals with subjective memory complaints between 70 and 85 years old. All the study participants underwent comprehensive neuropsychological evaluation as well as amyloid PET scans to define their brain amyloid status. Demographic characteristics of the study cohort are summarised in Table 1.

Table 1: Demographic characteristics of INSIGHT-preAD cohort.

	N	Age (sd) [years]	Gender (F/M)	APOE- ϵ 4	MMSE score (sd) [0-30]	Education (sd) [0-8]
Amyloid +ve	68	76.6 \pm 3.6	44 / 24	38.2 %	28.5 \pm 0.91	6.0 \pm 2.1
Amyloid -ve	250	75.9 \pm 3.5	157 / 93	12.8 %	28.7 \pm 0.96	6.2 \pm 2.0
All subjects	318	76.1 \pm 3.5	201 / 117	18.2%	28.67 \pm 0.95	6.2 \pm 2.0

Study 2: (58) We used three samples derived from two independent cohorts, i.e., ADNI and INSIGHT-preAD. The first sample (ADNI-A) consists of cognitively normal seniors and MCI subjects. Participants of the (ADNI-A) sample were previously used to construct the in-vivo amyloid staging model. The second sample (ADNI-B) consists of cognitively normal seniors and MCI subjects, in addition to participants with SCD. Finally, the third sample was derived from (INSIGHT-preAD), the same sample used in our first study. Both ADNI and INSIGHT-preAD participants underwent amyloid PET imaging and comprehensive neuropsychological examinations at least every 12 months. The Mini-Mental State Examination (83) was available for both cohorts to assess global cognition. We used the CDR score (84) as the primary endpoint to evaluate change in functional status.

Table 2: Summary of study samples derived from ADNI and INSIGHT-preAD cohort.

Cohorts / Diagnoses	N	M/F	Age (SD) [years]	MMSE (SD)	Median follow-up [months] (interquartile range)
ADNI-A					
Controls	179	88/91	73.8 (6.5)	29.1 (1.2)	65 (54; 68)
MCI	403	220/183	71.8 (7.6)	28.1 (1.7)	47 (43; 51)
ADNI-B					
Controls	75	36/39	79.2 (5.2)	29.2 (1.3)	64 (60; 71)
MCI	124	79/45	75.4 (8.1)	27.8 (1.8)	52 (49; 56)
SCD	103	42/61	72.4 (5.6)	29.0 (1.2)	51 (38; 59)
INSIGHT-preAD					
SMC	318	114/204	76.5 (3.5)	28.7 (1.0)	

Key: MMSE, Mini-Mental State Examination; SCD, subjective cognitive decline according to the definition in the ADNI cohort (85). SMC, subjective memory complaints as defined in the INSIGHT-preAD cohort (86).

Study 3: (82) We used a cohort of 529 participants derived from the ADNI cohort. All the participants have a baseline diagnosis of cognitively normal or MCI, in addition to complete CSF-biomarkers, plasma Lipidomics, APOE genotype and BMI data. Based on their CSF- biomarkers status and baseline clinical diagnosis, the final cohort was classified into three diagnostic groups: 1. The cognitively normal control group (CN) with negative CSF biomarkers and baseline diagnosis of cognitively normal (CDR= 0), 2. The preclinical group with positive CSF biomarkers and baseline diagnosis of cognitively normal (CDR= 0) and 3. The prodromal group with positive CSF biomarkers and baseline diagnosis of mild cognitive impairment (CDR= 0.5) (Table 3).

Table 3: Summary of demographic characteristics of ADNI cohort used in the third study.

Characteristics are described as Number (N) and the corresponding percentage (per cent %) or Mean value and standard deviation (sd) as convenient. Group differences were tested using Bayesian ANOVA (a) and Bayesian test of association (b). Results were interpreted in terms of Bayes Factor (BF) in favour of the presence of group differences in the tested variables, where BF of (3–20) represented moderate evidence (*), BF of (20–150) expressed

strong evidence (**). In contrast, BF of (>150) represented very strong evidence (***). Differences in CSF biomarkers levels between Preclinical and Prodromal are marked by (#).

	CN	Preclinical	Prodromal	Whole cohort
N	182	73	274	529
Mean age (sd) ^a	73.2 (5.9)	75.9 (5.2)	73.3 (7.0)	73.6 (6.5)
Sex – Females ^b N (percent %)	88 (48 %)	41 (56 %)	109 (40 %)	238 (45 %)
APOE4 carriers ^{b***} N (percent %)	32 (18 %)	43 (59 %)	195 (71 %)	270 (51 %)
BMI ^{b***} N (percent %)				
- Low	50 (27%)	38 (52%)	113 (41%)	201 (38%)
- Medium	85 (47%)	21 (29%)	126 (46%)	232 (44%)
- high	47 (26 %)	14 (19 %)	35 (13%)	96 (18%)
Mean Education years (sd) ^a	16.3 (2.7)	16.0 (2.8)	15.9 (2.9)	16.1 (2.8)
CSF biomarkers				
Mean A β 42 (sd) ^{*****}	1727.0 (524.0)	634.0 (185.0)	630.0 (167.0)	1007.8 (620.4)
Mean pTau (sd) ^{*****}	20.1 (6.6)	28.8 (10.4) [#]	35.4 (14.1) [#]	29.2 (13.4)
Mean pTau/ A β 42 ratio (sd) ^{*****}	0.012 (0.003)	0.049 (0.025) [#]	0.059 (0.028) [#]	0.042 (0.03)

2.2 Amyloid-PET data pre-processing and in-vivo staging.

Both structural MRI (T1-weighted) images and 18F-Florbetapir amyloid PET images were acquired in ADNI and INSIGHT-preAD cohorts (87–89). The pre-processing pipeline followed the previously described procedures in the study by Grothe et al. (53). Briefly, MRI images were realigned, segmented into tissue types, and spatially normalised to an ageing/AD-specific reference template space using Statistical Parametric Mapping software (SPM8, the Wellcome Trust Centre for Neuroimaging) implemented in MATLAB 2013. Averaged PET frames were co-registered to their corresponding structural MRI scan in native space and corrected for partial volume effects (PVE) using the 3-compartmental “Müller-Gärtner” method (90,91). Then corrected PET images were spatially normalised to the reference template space using transformation parameters from the corresponding MRI. Fifty-two brain regions of interest were defined using the Harvard–Oxford structural atlas (<https://fsl.fmrib.ox.ac.uk/fsl/fslwiki/Atlases>) (92), which included forty-eight cortical regions in addition to the subcortical regions. Regional standard uptake value ratios (SUVR_{cereb}) were computed by scaling the mean tracer uptake values by the mean uptake value of the whole cerebellum, estimated in non-PVE-corrected PET data (53,90,93,94).

The pre-processed PET data were then projected into Grothe in-vivo amyloid staging scheme (53) (Figure 4). In the staging scheme, the 52 brain regions were merged into a simplified progression model across four broader anatomical divisions (53,55). Each anatomical division was considered positive for amyloid pathology if at least 50% of regions of interest within this division displayed suprathreshold signal, i.e., $SUVR_{cereb} = 0.92$ in the ADNI cohort (58) and $SUVR_{cereb} = 0.98$ in the INSIGHT-preAD cohort (55). The individual in-vivo amyloid stage was then assigned based on the estimated hierarchical involvement of anatomical divisions (53). Stage I was defined as positive in the first anatomical division but negative in all following divisions (53). Then, the successive stages II-IV were determined by the additional involvement of their corresponding divisions 2, 3, and 4, respectively (53). Individuals who exhibited amyloid positivity in any division without concurrent amyloid positivity in the preceding divisions were classified as non-stageable (53).

2.3 Validity of in-vivo amyloid stages and association with the cognitive performance

In our first study (55), we assessed the validity of Grothe's in-vivo amyloid staging scheme in a completely independent sample derived from a cohort of cognitively normal seniors at higher risk of AD, "INSIGHT-preAD". Then we investigated the association between increasing in vivo amyloid stage and cross-sectional cognitive performance using ANCOVA models as well as the frequency of APOE- $\epsilon 4$ allele.

The second study (58) explored the association between in-vivo amyloid stages and the longitudinal decline in global cognition in the three different samples from ADNI and INSIGHT-preAD cohorts (58). Hence, we used Cox regression to predict time to conversion in CDR status (from 0 to 0.5 or higher, and from 0.5 to 1 or higher) while adjusting for age and sex (58). The Cox regression models performance was determined by the Akaike information criterion (AIC) as a measure of overall model fit (58).

Additionally, we compared the clinical utility of the amyloid stages against the current analytical approach based on the global amyloid status in both the first and second studies (55,58). Thus, we determined the amyloid positivity based on global mean uptake using the thresholds ($SUVR_{cereb} > 1.17$) (58) for the ADNI cohort and (non-PVE corrected $SUVR_{cereb} > 1.1$) (55) in the first study and (PVE corrected $SUVR_{cereb} > 0.88$) (58) in the second study for the INSIGHT-preAD.

2.4 Lipidomics data preparation and analysis.

Targeted high-resolution Lipidomics data were derived from the plasma samples of ADNI cases using ultra-high-performance liquid chromatography (82). Lipid species (692) were then merged into one hundred and seven (107) composite scores through applying a hierarchical clustering approach within each of the lipid subclasses/classes (82). We used Bayesian elastic net regression to identify lipid classes/ subclasses alterations associated with the CSF pTau/A β 42 ratio as a combined biomarker of AD pathology in preclinical and prodromal AD cases (82). Consensus clustering of the selected lipid classes/ sub-classes was used to identify distinctive lipidomic endophenotypes and study their association with clinical progression (82).

3. Results

3.1 Validity of PET-based in-vivo amyloid staging scheme in cognitively normal seniors at higher risk of AD

We determined the validity of the hierarchical amyloid staging scheme by the proportion of participants that adhere to the regional hierarchy implied by the progression model. In the INSIGHT-preAD cohort, one hundred fifty-six participants (49%) showed evidence of regional amyloid deposition (Figure 6) as opposed to the 21.5% identified using the conventional global amyloid status. Only two (0.6%) out of the whole cohort subjects (318) violated the proposed regional hierarchy and thus were labelled non-stageable. Across all the inspected samples from ADNI and INSIGHT-preAD cohorts, 1.4% (17 out of 1202 cases) were marked non-stageable. The distribution of non-stageable cases across cohorts and diagnoses is shown in Table 4.

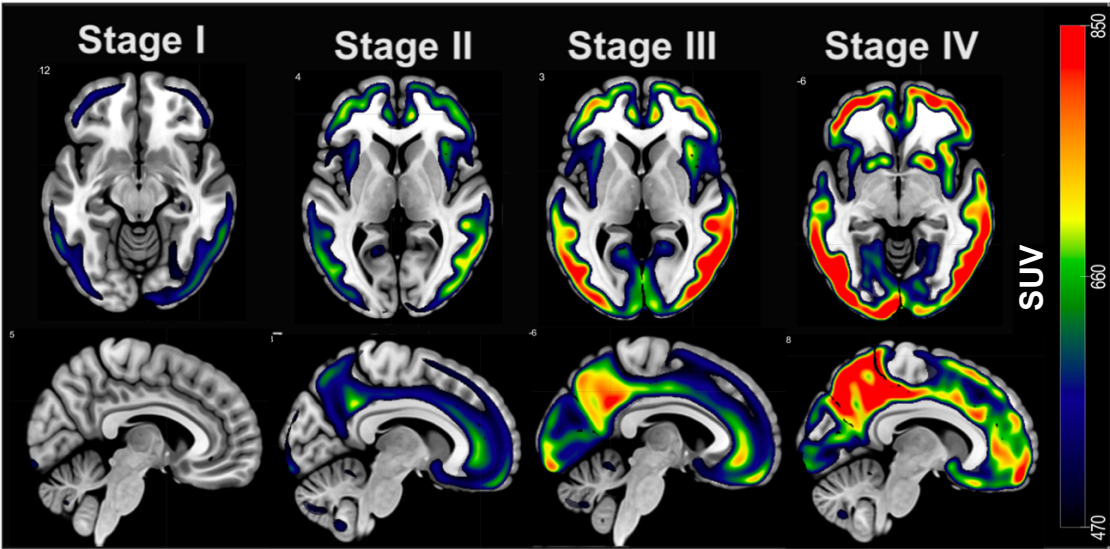


Figure 6: In-vivo amyloid stages in INSIGHT-preAD cohort.

Mean PET images representative for each stage of the amyloid progression model in the INSIGHT-preAD cohort are displayed on both axial and sagittal views.

Table 4: Distribution of the non-stageable cases across ADNI and INSIGHT-preAD cohorts.

Cohorts / Diagnoses	N	Non-stageable
ADNI-A	582	
Controls	179	3 (1.7%)
MCI	403	4 (0.7%)
ADNI-B	302	
Controls	75	1 (1.3%)
MCI	124	3 (2.4%)
SCD	103	4 (3.9%)
INSIGHT-preAD	318	
SMC	318	2 (0.6%)

We further explored the correspondence between the amyloid stages and the conventional binary classification based on a global signal and threshold of $SUVR_{cereb} > 1.10$ in the INSIGHT-preAD cohort. Almost all stage III or IV (96.8% and 100%, respectively) cases were classified as amyloid positive, while most of stage I (98.7%) and $\sim 30\%$ of stage II were classified as amyloid-negative (Table 5).

Table 5: Distribution of the in vivo amyloid stages among the INSIGHT-preAD participants compared to conventional global amyloid status.

Data represents the number of participants with global cortical retention exceeding the thresholds of ($SUVR = 1.1$) and ($SUVR = 1.135$), respectively, and their percentage among the total participants comprising the respective stage. The cut-off of ($SUVR = 1.1$) is the most used threshold to detect early amyloid positivity, while the cut-off of ($SUVR = 1.135$) is equivalent to the threshold used to assign regional positivity.

	Stage 0	Stage 1	Stage 2	Stage 3	Stage 4	Non-stageable
SUVR > 1.1	3 (1.9%)	1 (1.3%)	29 (72.5%)	31 (96.9%)	4 (100%)	0 (0%)
SUVR > 1.135	0 (0%)	0 (0%)	24 (60%)	31 (96.9%)	4 (100%)	0 (0%)
Number of subjects	162	78	40	32	4	2

3.2 Association of in-vivo amyloid stages with APOE genotype and cross-sectional cognitive performance.

In vivo amyloid stages was significantly associated with ApoE- ϵ 4 status, such that the percentage of ApoE- ϵ 4 carriers increased with increasing amyloid stage (chi-squared (χ^2) test, $p = 0.001$). Neither the in-vivo amyloid stage nor the global amyloid status showed significant association with cross-sectional cognitive performance in the INSIGHT-preAD cohort.

3.3 Association of in-vivo amyloid stages with longitudinal cognitive decline.

In almost all cohorts and diagnostic sub-groups, in-vivo amyloid stages III/IV were associated with increased risk of CDR conversion from 0 to 0.5 or higher in cognitively normal and SCD/SMC cases and from 0.5 to 1 or higher in MCI cases. In cognitively normal subjects from ADNI-A and ADNI-B samples, amyloid stage II was also associated with a higher rate of CDR conversion than stage 0 cases. Based on the global amyloid status, amyloid positive cases showed a higher rate of CDR conversion relative to negative amyloid cases in almost all comparisons, except for ADNI-B SCD cases. Using AIC, we assessed the performance of all Cox regression models using in-vivo amyloid stages compared to global amyloid status. A better performance was reported in all comparisons favouring amyloid staging over the global amyloid status models except for the ADNI-B controls model. The probability for the global amyloid status to provide a better fit than the staging model was below 0.002 for the ADNI-A controls and the ADNI-B MCI and SCD cases, and below 0.3 for the ADNI-A MCI and the INSIGHT-preAD SMC cases. Table 6 summarises the results and performance parameters of all the conducted Cox regression models.

Compared to global amyloid status, regional amyloid stages allowed identifying a subsample of people with a very high risk of conversion, i.e., amyloid stage III/IV cases. For example, MCI cases with amyloid stage IV had a 47% rate of conversion to dementia compared with 38% estimated for the global amyloid-positive cases in the ADNI-A sample. Analogously, in the INSIGHT-preAD cohort, 22% of stage III/IV individuals with SMC converted to CDR 0.5 or higher compared with only 14% in the global amyloid-positive cases.

Table 6: Results of Cox regression models.

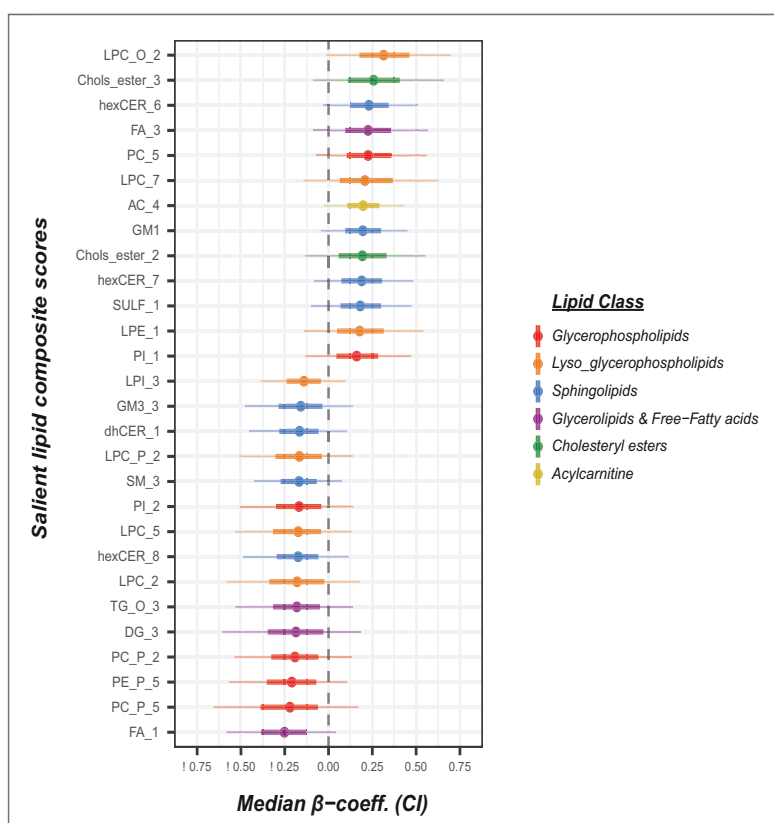
For both staging and global amyloid status-based models, the number of cases (N), Hazards ratio (HR) and corresponding standard error (SE) and p-value were provided. The performance of models was compared regarding the AIC and probability of the global amyloid status model to minimise AIC compared with the staging model.

Key: Amyloid stages (I-IV); A+: amyloid positive according to the global threshold; n.s.: non-significant.

Clinical diagnosis	Model	Sample													
		ADNI-A				ADNI-B				INSIGHT-preAD					
		N	HR (SE)	p	AIC	N	HR (SE)	p	AIC	N	HR (SE)	p	AIC		
Cognitively normal	Staging model	0	95				0	37							
		I	27	< 0.1	n.s.		I	9	1.3 (0.82)	n.s.					
		II	15	4.4 (0.49)	< 0.003	237	II	11	4.1 (0.60)	< 0.02	173				
		III	20	1.8 (0.60)	n.s.		III/IV	13	8.7 (0.56)	< 0.0002					
	Global amyloid status	A ⁻	132			260	A ⁻	48			170				
		A ⁺	40	3.1(0.40)	< 0.004	(p < 0.0001)	A ⁺	23	6.2 (0.47)	< 0.0001					
SMC/SCD	Staging model	0				0	49				0	162			
		I				I	14	0.9 (0.81)	n.s.		I	78	1.0 (0.64)	n.s.	211
		II				II	11	1.1 (0.86)	n.s.	176	II	40	0.48 (1.1)	n.s.	
		III				III	13	3.2 (0.62)	n.s.		III/IV	36	5.5 (0.52)	< 0.002	
	Global amyloid status	A ⁻					A ⁻	62				A ⁻	255		
		A ⁺					A ⁺	37	1.9 (0.43)	n.s.	193 (p < 0.002)	A ⁺	63	3.2 (0.45)	< 0.02
MCI	Staging model	0	136			0	39								
		I	34	0.7 (1.1)	n.s.		I	11	< 0.1	n.s.					
		II	44	1.6 (0.59)	n.s.	790	II	14	6.0 (1.2)	n.s.	173				
		III	75	7.0 (0.38)	< 0.0001		III	20	18.0 (1.06)	< 0.007					
	IV	85	9.6 (0.36)	< 0.0001		IV	21	27.1 (1.06)	< 0.002						
	Global amyloid status	A ⁻	194			794	A ⁻	50			186				
A ⁺		183	7.7 (0.32)	< 0.0001	(p = 0.13)	A ⁺	58	23.5 (1.03)	< 0.0003	(p < 0.002)					

3.4 Lipidomic signature in blood of preclinical and prodromal AD.

Bayesian elastic net regression identified lipid classes/ subclasses which were dysregulated in the blood (plasma) of preclinical and prodromal AD participants (Figure 7). lyso-glycerophospholipids (specifically LPC), glycerophospholipids (acyl, alkyl, and alkenyl), free fatty acids (FFA), cholesterol esters and sphingolipids (complex ceramides) lipid classes/subclasses were accounted on top of the list. Lipid species harbouring polyunsaturated fatty acids (PUFA) and ether bonds were particularly affected.

**Key:**

LPC-O-2: Lyso-alkyl-phosphatidylcholine (long FA), Choles ester-3: Cholesteryl ester (PUFA), hexCER: Hexosylceramide, FA-3: Free fatty acid (AA), PC-5: Phosphatidylcholine (AA), LPC-7: Lysophosphatidylcholine (PUFA), AC-4: Acylcarnitine (PUFA), GM1: GM1 gangliosides, Choles ester-2: Cholesteryl ester, SULF-1: Sulfatides, LPE-1: Lyso-phosphatidylethanolamine (saturated FA), PI-1: Phosphatidylinositol (PUFA), LPI-3: Lyso-phosphatidylinositol (AA), GM3-3: GM3 gangliosides (very long FA), dhCER: Dihydroceramide, LPC-P-2: Lyso-alkenyl-phosphatidylcholine (long FA), SM-3: Sphingomyelin (very long saturated FA), PI-2: Phosphatidylinositol (saturated, monounsaturated FA), LPC-5: Lysophosphatidylcholine (long, very long FA), LPC-2: Lysophosphatidylcholine (odd numbered FA), TG O 3: Alkyl-diacylglycerol, DG 3: diacylglycerol (EPA & DHA), PC-P-2: Alkenyl-phosphatidylcholine (saturated and mono-unsaturated FA), PE-P-5: Alkenyl-phosphatidylethanolamine (AA, DHA), PC-P-5: Alkenyl-phosphatidylcholine (DHA & EPA) and FA 1: Free fatty acid.

Figure 7: Dysregulated Lipids in preclinical and prodromal AD.

Salient lipid scores are represented as posterior β -coefficients (points) with their respective 50% and 90% credibility intervals as thick and thin error bars, respectively, points' colour codes for their corresponding lipid class.

3.5 Association of lipid endophenotypes with future cognitive decline

Consensus clustering identified five distinct lipid endophenotypes within prodromal participants. Two specific lipid endophenotypes (cluster II and V) were associated with a higher risk for cognitive decline (Table 7). Sex differences were also noted in the association of lipids with anticipated cognitive decline. In women, only cluster (II) showed a high risk of conversion, while cluster (III) showed a lower risk of conversion relative to the reference cluster (IV), yet only in men. Endophenotypes at high risk of conversion to dementia were distinguished by depletion of PUFA-plasmalogens associated with a compensatory increase of species containing saturated and monounsaturated FAs. Additionally, we observed higher levels of cholesterol esters and complex ceramides together with the depletion of long-chain sphingomyelins and dihydro-ceramides in this subgroup of high-risk prodromals.

Results

Table 7: Risk of clinical progression among prodromal lipidomic endophenotypes.

Bayesian survival analysis was conducted to estimate the relative risk of progression to dementia among prodromal lipidomic endophenotypes while adjusting for APOE4. Then, this model was replicated on male and female subsets separately to explore the sex-specific effect of lipidomic endophenotypes on clinical progression. We set cluster (IV) as our reference group throughout the analysis. Results were interpreted in terms of credibility intervals (CI) of posterior distributions, where hazard ratios with CI not covering (1) were considered relevant and reported in red.

Model	Cluster + APOE4			Male subset			Female subset		
	Median (MAD)	Hazard ratio	CI	Median (MAD)	Hazard ratio	CI	Median (MAD)	Hazard ratio	CI
Intercept: IV	-9.03 (1.80)			-8.46 (2.20)			-9.24 (2.72)		
I	0.02 (0.26)	1.02	0.68-1.52	-0.16 (0.32)	0.85	0.54- 1.51	0.28 (0.42)	1.33	0.68- 2.72
II	0.68 (0.28)	1.97	1.26- 3.10	0.56 (0.35)	1.75	1.04- 3.16	0.84 (0.43)	2.32	1.15- 4.57
III	-0.41 (0.42)	0.66	0.36- 1.22	-1.08 (0.58)	0.34	0.13- 0.89	0.09 (0.54)	1.10	0.48- 2.56
V	0.69 (0.26)	1.99	1.30- 3.00	0.85 (0.34)	2.35	1.38- 4.06	0.55 (0.43)	1.74	0.89- 3.53
APOE4	0.39 (0.21)	1.48	1.07- 2.05	0.40 (0.27)	1.50	1.00- 2.25	0.27 (0.33)	1.31	0.76- 2.23

4. Discussion

In light of our research questions, I will discuss the major findings of our studies integrated into the existing literature in the field. Finally, the chapter will be wrapped up with a general conclusion while pointing out future research directions.

4.1 Validity of PET-based in-vivo amyloid staging.

Our first study provided evidence for the general validity of Grothe's in-vivo amyloid staging scheme in an independent sample enriched for preclinical AD derived from the "INSIGHT-preAD" cohort (55). Indeed ~ 99% of cases adhered to the regional hierarchy implied by the four-stage model (55). Essentially identical findings were observed on an extended sample, including preclinical and prodromal AD cases (58). A crucial advantage of the regional amyloid stages is identifying individuals with incipient amyloid deposition, i.e., amyloid confined to the neocortex, corresponding to the earliest Thal phase (Phase 1) in autopsy (55). Conversely, global amyloid status usually misinterprets early Thal amyloid phases as negative scans (27,28,40–42,48,54). A follow-up study further confirmed the strong association between the regional amyloid stages and neuropathological Thal phases as well as CERAD ratings of neuritic and diffuse plaque densities in autopsy (50). In a Bayesian framework, regional amyloid stages were forty-four times more likely to associate with Thal phases than global amyloid status (50).

Hanseeuw et al. and Mattsson et al. also proposed alternative region-based amyloid staging schemes (51,52). Hanseeuw et al.'s three-stage scheme employed a distinction between striatal and neocortical amyloid load (52), while Mattsson et al. constructed their staging scheme based on the frequency of longitudinal regional involvements (51). Despite the different approaches, the results converged in many aspects. Overall, the amyloid staging schemes predicted a relatively similar pattern of amyloid progression in the brain (51,53,55,56). A β deposition in the orbitofrontal cortex, anterior and posterior cingulate gyri, precuneus and insula precedes the late accumulator brain regions, namely precentral, postcentral, lingual and calcarine cortices (51,53,55–57). Subcortical, particularly striatal, A β occurs later in the course of the disease following cortical amyloidosis (52,53,55–57). Keeping with Cho et al.'s study, we also observed early amyloid deposition in the temporal neocortex, whereas the medial temporal lobe was the least involved (53–55). A recent study demonstrated that individuals' longitudinal amyloid progression closely follows the initial cross-sectionally estimated staging scheme (56).

Several methodological considerations were raised against our initial amyloid staging approach, for example, using global versus region-specific threshold for defining regional positivity and the validity of our approach using different PET radiotracer or DVR instead of SUVR values. First, our focus was assessing the validity of the initial staging approach proposed by Grothe, adopting a constant global threshold and the widely used SUVR values. We also believe that the methodological choices offered by the initial approach could easily enable its future implementation in the clinical setting (55,58). The sensitivity analysis in (53) also suggested limited variability of inter-regional noise levels after PVE correction of PET images since it accounts for the spill-in effects from high non-specific white matter signals (90). Finally, follow up studies from our group (56,57) further addressed all these considerations. Although using different methodological choices resulted in some alterations in the temporal ordering of the neocortical regions, the overall amyloid progression pattern remained consistent. Among all the methodological factors, the region-specific threshold exerted the most remarkable effect (56,57).

4.2 Clinical utility of amyloid stages and advantage over global amyloid status approach.

As per the preclinical AD (INSIGHT-preAD) cohort, we presumed the lack of associations between cross-sectional cognitive performance and amyloid burden regardless regional amyloid stages or global amyloid status approach was used (55). Our findings contradict previous studies that reported subtle episodic memory changes associated with amyloid burden in preclinical stages of AD (95–97). Further studies adopting our regional amyloid stages showed that higher amyloid stages were associated with worse memory scores, i.e., delayed recall score, in cognitively normal seniors (53,56). This contradiction may be attributable to the inclusion criteria of the INSIGHT-preAD cohort, which implied normal performance on cognitive tests, i.e., the FCSRT total recall. Hence, the amyloid burden association with cross-sectional memory scores is possibly masked by the limited variability in episodic memory performance in this cohort (55).

Based on a larger sample, including preclinical and prodromal AD cases, advanced amyloid stages, specifically III and IV, were associated with a higher risk of cognitive decline (58). Comparable results were also obtained using the global amyloid status (58). However, the added value of the regional amyloid stages over global amyloid status is the stratification of individuals into subsamples that differ for their risk of cognitive decline (58). This risk stratification could be of particular relevance in future clinical trials since it allows the selection of participants to match the trial specific aims, thus targeting earlier or later preclinical or prodromal Alzheimer's stages (52,58).

For instance, some amyloid targeted clinical trials may consider including participants at very high risk of cognitive decline, i.e., stage IV, which would translate into shorter times to progression and follow up duration (52,58). Other prevention trials may prefer to enrol participants exclusively with incipient amyloidosis, i.e., stage I or II (52). Although this approach will imply a greater screening effort in clinical trials, the cost benefit is reasonably justifiable compared to including many cases with a low risk of conversion (52,58). Suppose a 20% reduction of conversion rate should be detected at a significance level of 5% with 80% power. Then a trial would need to enrol 429 cases in case of stage IV MCI cases, having an initial conversion rate of 47%, whereas this sample size should be expanded to 607 cases in case of global amyloid-positive MCI with an initial conversion rate of 38% (58).

Following the same notion, Hanseeuw et al. and Mattsson et al. explored the association of their region-based staging schemes with rates of cognitive decline (51,52). In the Hanseeuw staging scheme, Stage 2, having high neocortical and striatal signal predicted faster cognitive decline than elevated cortical signal alone (Stage 1) (52). Their Stage 2 roughly corresponds to Stage IV in our regional staging scheme; however, our staging scheme offers a fine-grained differentiation of cortical involvement. Analogously Mattsson et al. showed that advanced amyloid stages were associated with high rates of cognitive decline (51). In contrast to both studies, we further assessed the stage-specific risk of functional conversion and compared it to standard global amyloid status, thus providing evidence for significant risk enrichment in advanced stages of amyloid progression (58).

4.3 Lipidomics signature and contribution to the risk of AD and clinical progression

Our third study (82) identified subsets of functionally similar lipid species that were altered early in the blood of preclinical and prodromal AD cases using high-resolution lipidomics data, considering fatty acids saturation and chain length. In agreement with previous studies, ether and PUFA containing glycerophospholipids, their lyso derivatives, sphingolipids, free fatty acids, and cholesterol esters lipid classes were dysregulated (65,66,98–101). A remarkable finding in our analysis was the depletion of plasmalogen ether glycerophospholipids in AD cases. Plasmalogens depletion was frequently linked to AD pathology (102–108) as well as age and APOE4, as two major risk factors (109). Consistent with Toledo's study (98), our results suggested an early role of arachidonated phosphatidylcholines, particularly long-chain alkyl isomers and their lyso

derivatives, in AD pathogenesis. These phosphatidylcholine species are key precursors of potent inflammatory mediators, including platelet-activating factor (PAF) and arachidonic acid (110,111). We also presumed that a higher risk of AD progression was associated with distinct lipid endophenotype in prodromal cases (82). For instance, the abundance of cholesterol esters, alterations in ether-glycerophospholipids and sphingolipids profile was observed among high-risk AD cases. A recent study found that cholesterol esters could trigger both amyloidosis and tau pathological changes through independent pathways (112). Ether-glycerophospholipids profile remodelling occurred such that species susceptible to oxidative stress were depleted compared to the preserved or increased more stable species, harbouring saturated fatty acids and/or alkyl bonds (82). Such remodelling could suggest a compensatory mechanism to overcome the increasing oxidative stress due to ageing and β -amyloid and thus subsequent lipid peroxidation and inflammatory mediator's release. Keeping with literature, we found a shift in sphingolipids metabolism towards accumulating ceramides accompanied by depletion of long-chain sphingomyelins and di-hydro-ceramides (113–117). Alterations in sphingolipids' metabolism could reflect cell signalling disturbances mediated by ceramide, sphingosine, and their respective 1-phosphates (C1P and S1P) (118). These signalling molecules are actively involved in cell survival and regulation of pro and anti-inflammatory responses (118).

4.4 Conclusion and Future directions

Briefly, our dissertation provides evidence for robustness and clinical utility of the in-vivo amyloid staging approach for risk stratification of AD cases, particularly at the preclinical phase. Given the multifactorial nature of AD, amyloid stages may need to be combined with other markers of the associated pathological mechanisms to precisely predict individuals' cognitive trajectories and progression risk. Lipidomics data offers comprehensive information encompassing additional pathological mechanisms, namely neuroinflammation, mitochondrial dysfunction, response to oxidative stress and cell survival, contributing to AD risk. Hence, the lipidomic profile could provide complementary information reflecting individual-specific vulnerability or resilience to AD pathology. Refining and validating lipidomic/ metabolic profiling could further open a new avenue to exploring possible adjuvant therapies modulating metabolic pathways and targeting the appropriate subpopulations in prevention trials. Future studies will be needed to evaluate the usefulness of combining lipidomic/metabolic profiling with amyloid burden in characterising AD cases and stratifying individuals based on their cumulative risk.

References

1. DeTure MA, Dickson DW. The neuropathological diagnosis of Alzheimer's disease. *Mol Neurodegener* [Internet]. 2019;14(1):32. Available from: <https://doi.org/10.1186/s13024-019-0333-5>
2. Jellinger KA. Neuropathology of the Alzheimer's continuum: an update. *Free Neuropathol* [Internet]. 2020 Nov 11;1(0 SE-Reviews):32. Available from: <https://www.uni-muenster.de/Ejournals/index.php/fnp/article/view/3050>
3. 2020 Alzheimer's disease facts and figures. *Alzheimer's Dement* [Internet]. 2020 Mar 10;16(3):391–460. Available from: <https://onlinelibrary.wiley.com/doi/10.1002/alz.12068>
4. Gauthier S, Rosa-Neto P, Morais JA, Webster C. *World Alzheimer Report 2021: Journey through the diagnosis of dementia*. London, England: Alzheimer's Disease International.; 2021.
5. Prince M, Wimo A, Guerchet M, Ali G-C, Wu Y-T, Prina M. *World Alzheimer Report 2015. The Global Impact of Dementia. An Analysis of Prevalence, Incidence, Cost and Trends*. 2015.
6. Doblhammer G, Fink A, Zylla S, Willekens F. Compression or expansion of dementia in Germany? An observational study of short-term trends in incidence and death rates of dementia between 2006/07 and 2009/10 based on German health insurance data. *Alzheimers Res Ther* [Internet]. 2015 Nov 5;7(1):66. Available from: <https://pubmed.ncbi.nlm.nih.gov/26537590>
7. Michalowsky B, Flessa S, Hertel J, Goetz O, Hoffmann W, Teipel S, et al. Cost of diagnosing dementia in a German memory clinic. *Alzheimers Res Ther* [Internet]. 2017;9(1):65. Available from: <https://doi.org/10.1186/s13195-017-0290-6>
8. Long JM, Holtzman DM. Alzheimer Disease: An Update on Pathobiology and Treatment Strategies. *Cell* [Internet]. 2019;179(2):312–39. Available from: <https://www.sciencedirect.com/science/article/pii/S0092867419310074>
9. Hyman BT, Phelps CH, Beach TG, Bigio EH, Cairns NJ, Carrillo MC, et al. National Institute on Aging-Alzheimer's Association guidelines for the neuropathologic assessment of Alzheimer's disease. *Alzheimers Dement* [Internet]. 2012 Jan;8(1):1–13. Available from: <https://pubmed.ncbi.nlm.nih.gov/22265587>
10. Price JL, McKeel Jr DW, Buckles VD, Roe CM, Xiong C, Grundman M, et al. Neuropathology of nondemented aging: presumptive evidence for preclinical Alzheimer disease. *Neurobiol Aging* [Internet]. 2009/04/18. 2009 Jul;30(7):1026–36. Available from: <https://pubmed.ncbi.nlm.nih.gov/19376612>
11. Raskin J, Cummings J, Hardy J, Schuh K, Dean RA. Neurobiology of Alzheimer's Disease: Integrated Molecular, Physiological, Anatomical, Biomarker, and Cognitive Dimensions. *Curr Alzheimer Res* [Internet]. 2015;12(8):712–22. Available from: <https://pubmed.ncbi.nlm.nih.gov/26412218>

References

12. Kumar A, Singh A, Ekavali. A review on Alzheimer's disease pathophysiology and its management: an update. *Pharmacol Reports* [Internet]. 2015;67(2):195–203. Available from: <https://www.sciencedirect.com/science/article/pii/S1734114014002886>
13. Weller RO, Subash M, Preston SD, Mazanti I, Carare RO. Perivascular drainage of amyloid-beta peptides from the brain and its failure in cerebral amyloid angiopathy and Alzheimer's disease. *Brain Pathol* [Internet]. 2008 Apr;18(2):253–66. Available from: <https://pubmed.ncbi.nlm.nih.gov/18363936>
14. O'Brien RJ, Wong PC. Amyloid precursor protein processing and Alzheimer's disease. *Annu Rev Neurosci* [Internet]. 2011;34:185–204. Available from: <https://pubmed.ncbi.nlm.nih.gov/21456963>
15. Mattson MP. Pathways towards and away from Alzheimer's disease. *Nature* [Internet]. 2004;430(7000):631–9. Available from: <https://doi.org/10.1038/nature02621>
16. Ballard C, Gauthier S, Corbett A, Brayne C, Aarsland D, Jones E. Alzheimer's disease. *Lancet* [Internet]. 2011;377(9770):1019–31. Available from: <https://www.sciencedirect.com/science/article/pii/S0140673610613499>
17. Arendt T, Stieler JT, Holzer M. Tau and tauopathies. *Brain Res Bull* [Internet]. 2016;126:238–92. Available from: <https://www.sciencedirect.com/science/article/pii/S0361923016302325>
18. Alonso A del C, Grundke-Iqbal I, Iqbal K. Alzheimer's disease hyperphosphorylated tau sequesters normal tau into tangles of filaments and disassembles microtubules. *Nat Med* [Internet]. 1996;2(7):783–7. Available from: <https://doi.org/10.1038/nm0796-783>
19. Aisen PS, Cummings J, Jack Jr CR, Morris JC, Sperling R, Frölich L, et al. On the path to 2025: understanding the Alzheimer's disease continuum. *Alzheimers Res Ther* [Internet]. 2017 Aug 9;9(1):60. Available from: <https://pubmed.ncbi.nlm.nih.gov/28793924>
20. Selkoe DJ, Hardy J. The amyloid hypothesis of Alzheimer's disease at 25 years. *EMBO Mol Med* [Internet]. 2016 Jun 1;8(6):595–608. Available from: <https://pubmed.ncbi.nlm.nih.gov/27025652>
21. Karran E, Mercken M, Strooper B De. The amyloid cascade hypothesis for Alzheimer's disease: an appraisal for the development of therapeutics. *Nat Rev Drug Discov* [Internet]. 2011;10(9):698–712. Available from: <https://doi.org/10.1038/nrd3505>
22. Jack Jr CR, Knopman DS, Jagust WJ, Shaw LM, Aisen PS, Weiner MW, et al. Hypothetical model of dynamic biomarkers of the Alzheimer's pathological cascade. *Lancet Neurol* [Internet]. 2010 Jan;9(1):119–28. Available from: <https://pubmed.ncbi.nlm.nih.gov/20083042>
23. Barage SH, Sonawane KD. Amyloid cascade hypothesis: Pathogenesis and therapeutic strategies in Alzheimer's disease. *Neuropeptides* [Internet]. 2015;52:1–18. Available from: <https://www.sciencedirect.com/science/article/pii/S0143417915000657>

References

24. Thal DR, Ronisz A, Tousseyn T, Rijal Upadhaya A, Balakrishnan K, Vandenberghe R, et al. Different aspects of Alzheimer's disease-related amyloid β -peptide pathology and their relationship to amyloid positron emission tomography imaging and dementia. *Acta Neuropathol Commun* [Internet]. 2019;7(1):178. Available from: <https://doi.org/10.1186/s40478-019-0837-9>
25. Thal DR, Capetillo-Zarate E, Del Tredici K, Braak H. The development of amyloid beta protein deposits in the aged brain. *Sci Aging Knowledge Environ* [Internet]. 2006 Mar 8;2006(6):re1. Available from: <https://doi.org/10.1126/sageke.2006.6.re1>
26. Jack CR, Bennett DA, Blennow K, Carrillo MC, Dunn B, Haeberlein SB, et al. NIA-AA Research Framework: Toward a biological definition of Alzheimer's disease. *Alzheimer's Dement* [Internet]. 2018 Apr;14(4):535–62. Available from: <https://onlinelibrary.wiley.com/doi/10.1016/j.jalz.2018.02.018>
27. Seo SW, Ayakta N, Grinberg LT, Villeneuve S, Lehmann M, Reed B, et al. Regional correlations between [11C]PIB PET and post-mortem burden of amyloid-beta pathology in a diverse neuropathological cohort. *NeuroImage Clin* [Internet]. 2017;13:130–7. Available from: <https://www.sciencedirect.com/science/article/pii/S2213158216302145>
28. Murray ME, Lowe VJ, Graff-Radford NR, Liesinger AM, Cannon A, Przybelski SA, et al. Clinicopathologic and 11C-Pittsburgh compound B implications of Thal amyloid phase across the Alzheimer's disease spectrum. *Brain* [Internet]. 2015/03/23. 2015 May;138(Pt 5):1370–81. Available from: <https://pubmed.ncbi.nlm.nih.gov/25805643>
29. Lowe VJ, Lundt ES, Albertson SM, Przybelski SA, Senjem ML, Parisi JE, et al. Neuroimaging correlates with neuropathologic schemes in neurodegenerative disease. *Alzheimer's Dement* [Internet]. 2019;15(7):927–39. Available from: <https://www.sciencedirect.com/science/article/pii/S1552526019300913>
30. Montine TJ, Phelps CH, Beach TG, Bigio EH, Cairns NJ, Dickson DW, et al. National Institute on Aging–Alzheimer's Association guidelines for the neuropathologic assessment of Alzheimer's disease: a practical approach. *Acta Neuropathol* [Internet]. 2012;123(1):1–11. Available from: <https://doi.org/10.1007/s00401-011-0910-3>
31. Bateman RJ, Xiong C, Benzinger TLS, Fagan AM, Goate A, Fox NC, et al. Clinical and Biomarker Changes in Dominantly Inherited Alzheimer's Disease. *N Engl J Med* [Internet]. 2012 Jul 11;367(9):795–804. Available from: <https://doi.org/10.1056/NEJMoa1202753>
32. Young AL, Oxtoby NP, Daga P, Cash DM, Fox NC, Ourselin S, et al. A data-driven model of biomarker changes in sporadic Alzheimer's disease. *Brain* [Internet]. 2014 Sep 1;137(9):2564–77. Available from: <https://doi.org/10.1093/brain/awu176>
33. Mortimer JA, Snowden DA, Markesbery WR. The Effect of APOE- ϵ 4 on Dementia is Mediated by Alzheimer Neuropathology. *Alzheimer Dis Assoc Disord* [Internet]. 2009;23(2). Available from: https://journals.lww.com/alzheimerjournal/Fulltext/2009/04000/The_Effect_of_APOE__4_on_Dementia_is_Mediated_by.9.aspx

References

34. Bennett DA, Schneider JA, Wilson RS, Bienias JL, Arnold SE. Neurofibrillary Tangles Mediate the Association of Amyloid Load With Clinical Alzheimer Disease and Level of Cognitive Function. *Arch Neurol* [Internet]. 2004 Mar 1;61(3):378–84. Available from: <https://doi.org/10.1001/archneur.61.3.378>
35. Therriault J, Pascoal T, Sefranek M, Mathotaarachchi S, Benedet A, Chamoun M, et al. Amyloid-dependent and amyloid-independent effects of Tau in individuals without dementia. *Ann Clin Transl Neurol*. 2021 Oct 7;8.
36. Jack CR, Knopman DS, Jagust WJ, Shaw LM, Aisen PS, Weiner MW, et al. Hypothetical model of dynamic biomarkers of the Alzheimer’s pathological cascade. *Lancet Neurol* [Internet]. 2010;9(1):119–28. Available from: <https://www.sciencedirect.com/science/article/pii/S1474442209702996>
37. Jack CR, Knopman DS, Jagust WJ, Petersen RC, Weiner MW, Aisen PS, et al. Tracking pathophysiological processes in Alzheimer’s disease: an updated hypothetical model of dynamic biomarkers. *Lancet Neurol* [Internet]. 2013;12(2):207–16. Available from: <https://www.sciencedirect.com/science/article/pii/S1474442212702910>
38. Leuzy A, Chiotis K, Lemoine L, Gillberg P-G, Almkvist O, Rodriguez-Vieitez E, et al. Tau PET imaging in neurodegenerative tauopathies—still a challenge. *Mol Psychiatry* [Internet]. 2019 Aug 11;24(8):1112–34. Available from: <http://www.nature.com/articles/s41380-018-0342-8>
39. Villeneuve S, Rabinovici GD, Cohn-Sheehy BI, Madison C, Ayakta N, Ghosh PM, et al. Existing Pittsburgh Compound-B positron emission tomography thresholds are too high: statistical and pathological evaluation. *Brain* [Internet]. 2015 Jul 1;138(7):2020–33. Available from: <https://doi.org/10.1093/brain/awv112>
40. Thal DR, Beach TG, Zantette M, Heurling K, Chakrabarty A, Ismail A, et al. [18F]flutemetamol amyloid positron emission tomography in preclinical and symptomatic Alzheimer’s disease: Specific detection of advanced phases of amyloid- β pathology. *Alzheimer’s Dement* [Internet]. 2015;11(8):975–85. Available from: <https://www.sciencedirect.com/science/article/pii/S1552526015002162>
41. Fleisher AS, Chen K, Liu X, Roontiva A, Thiyyagura P, Ayutyanont N, et al. Using Positron Emission Tomography and Florbetapir F 18 to Image Cortical Amyloid in Patients With Mild Cognitive Impairment or Dementia Due to Alzheimer Disease. *Arch Neurol* [Internet]. 2011 Nov 1;68(11):1404–11. Available from: <https://doi.org/10.1001/archneurol.2011.150>
42. Salloway S, Gamez J, Singh U, Sadowsky C, Villena T, Sabbagh M, et al. Performance of [18 F]flutemetamol amyloid imaging against the neuritic plaque component of CERAD and the current (2012) NIA-AA recommendations for the neuropathologic diagnosis of Alzheimer’s disease. *Alzheimer’s Dement Diagnosis, Assess Dis Monit*. 2017 Jul 1;9.
43. Thal DR, Rüb U, Orantes M, Braak H. Phases of A β -deposition in the human brain and its relevance for the development of AD. *Neurology* [Internet]. 2002 Jun

- 25;58(12):1791 LP – 1800. Available from:
<http://n.neurology.org/content/58/12/1791.abstract>
44. Braak H, Braak E. Frequency of Stages of Alzheimer-Related Lesions in Different Age Categories. *Neurobiol Aging* [Internet]. 1997;18(4):351–7. Available from:
<https://www.sciencedirect.com/science/article/pii/S0197458097000560>
 45. Näslund J, Haroutunian V, Mohs R, Davis KL, Davies P, Greengard P, et al. Correlation Between Elevated Levels of Amyloid β -Peptide in the Brain and Cognitive Decline. *JAMA* [Internet]. 2000 Mar 22;283(12):1571–7. Available from:
<https://doi.org/10.1001/jama.283.12.1571>
 46. Braak H, Braak E. Neuropathological staging of Alzheimer-related changes. *Acta Neuropathol* [Internet]. 1991;82(4):239–59. Available from:
<https://doi.org/10.1007/BF00308809>
 47. Koychev I, Hofer M, Friedman N. Correlation of Alzheimer Disease Neuropathologic Staging with Amyloid and Tau Scintigraphic Imaging Biomarkers. *J Nucl Med* [Internet]. 2020 Oct 1;61(10):1413 LP – 1418. Available from:
<http://jnm.snmjournals.org/content/61/10/1413.abstract>
 48. Ikonomic MD, Buckley CJ, Heurling K, Sherwin P, Jones PA, Zanette M, et al. Post-mortem histopathology underlying β -amyloid PET imaging following flutemetamol F 18 injection. *Acta Neuropathol Commun* [Internet]. 2016;4(1):130. Available from: <https://doi.org/10.1186/s40478-016-0399-z>
 49. Jack Jr CR, Lowe VJ, Senjem ML, Weigand SD, Kemp BJ, Shiung MM, et al. 11C PiB and structural MRI provide complementary information in imaging of Alzheimer's disease and amnesic mild cognitive impairment. *Brain* [Internet]. 2008 Mar 1;131(3):665–80. Available from: <https://doi.org/10.1093/brain/awm336>
 50. Teipel SJ, Temp AGM, Levin F, Dyrba M, Grothe MJ, Initiative ADN. Association of PET-based stages of amyloid deposition with neuropathological markers of A β pathology. *Ann Clin Transl Neurol* [Internet]. 2020/11/02. 2021 Jan;8(1):29–42. Available from: <https://pubmed.ncbi.nlm.nih.gov/33137247>
 51. Mattsson N, Palmqvist S, Stomrud E, Vogel J, Hansson O. Staging β -Amyloid Pathology With Amyloid Positron Emission Tomography. *JAMA Neurol* [Internet]. 2019 Nov 1;76(11):1319–29. Available from:
<https://doi.org/10.1001/jamaneurol.2019.2214>
 52. Hanseeuw BJ, Betensky RA, Mormino EC, Schultz AP, Sepulcre J, Becker JA, et al. PET staging of amyloidosis using striatum. *Alzheimer's Dement* [Internet]. 2018;14(10):1281–92. Available from:
<https://www.sciencedirect.com/science/article/pii/S155252601830133X>
 53. Grothe MJ, Barthel H, Sepulcre J, Dyrba M, Sabri O, Teipel SJ. In vivo staging of regional amyloid deposition. *Neurology*. 2017;
 54. Cho H, Choi JY, Hwang MS, Kim YJ, Lee HM, Lee HS, et al. In vivo cortical spreading pattern of tau and amyloid in the Alzheimer disease spectrum. *Ann Neurol*

- [Internet]. 2016 Aug 1;80(2):247–58. Available from: <https://doi.org/10.1002/ana.24711>
55. Sakr FA, Grothe MJ, Cavedo E, Jelistratova I, Habert M-O, Dyrba M, et al. Applicability of in vivo staging of regional amyloid burden in a cognitively normal cohort with subjective memory complaints: The INSIGHT-preAD study. *Alzheimer's Res Ther*. 2019;11(1).
 56. Jelistratova I, Teipel SJ, Grothe MJ. Longitudinal validity of PET-based staging of regional amyloid deposition. *Hum Brain Mapp* [Internet]. 2020/07/10. 2020 Oct 15;41(15):4219–31. Available from: <https://pubmed.ncbi.nlm.nih.gov/32648624>
 57. Levin F, Jelistratova I, Betthausen TJ, Okonkwo O, Johnson SC, Teipel SJ, et al. In vivo staging of regional amyloid progression in healthy middle-aged to older people at risk of Alzheimer's disease. *Alzheimers Res Ther* [Internet]. 2021 Oct 21;13(1):178. Available from: <https://pubmed.ncbi.nlm.nih.gov/34674764>
 58. Teipel SJ, Dyrba M, Chiesa PA, Sakr F, Jelistratova I, Lista S, et al. In vivo staging of regional amyloid deposition predicts functional conversion in the preclinical and prodromal phases of Alzheimer's disease. *Neurobiol Aging* [Internet]. 2020;93:98–108. Available from: <https://www.sciencedirect.com/science/article/pii/S0197458020300907>
 59. Vlassenko AG, McCue L, Jasielec MS, Su Y, Gordon BA, Xiong C, et al. Imaging and cerebrospinal fluid biomarkers in early preclinical alzheimer disease. *Ann Neurol* [Internet]. 2016 Sep 1;80(3):379–87. Available from: <https://doi.org/10.1002/ana.24719>
 60. Palmqvist S, Mattsson N, Hansson O, Initiative for the ADN. Cerebrospinal fluid analysis detects cerebral amyloid- β accumulation earlier than positron emission tomography. *Brain* [Internet]. 2016 Apr 1;139(4):1226–36. Available from: <https://doi.org/10.1093/brain/aww015>
 61. Palmqvist S, Schöll M, Strandberg O, Mattsson N, Stomrud E, Zetterberg H, et al. Earliest accumulation of β -amyloid occurs within the default-mode network and concurrently affects brain connectivity. *Nat Commun* [Internet]. 2017;8(1):1214. Available from: <https://doi.org/10.1038/s41467-017-01150-x>
 62. Badhwar AP, McFall GP, Sapkota S, Black SE, Chertkow H, Duchesne S, et al. A multiomics approach to heterogeneity in Alzheimer's disease: focused review and roadmap. *Brain*. 2020;143(5):1315–31.
 63. Goyal D, Tjandra D, Migrino R, Giordani B, Syed Z, Wiens J. Characterizing heterogeneity in the progression of Alzheimer's disease using longitudinal clinical and neuroimaging biomarkers. *Alzheimer's Dement Diagnosis, Assess Dis Monit*. 2018 Aug 1;10.
 64. Hampel H, O'Bryant SE, Molinuevo JL, Zetterberg H, Masters CL, Lista S, et al. Blood-based biomarkers for Alzheimer disease: mapping the road to the clinic. *Nat Rev Neurol* [Internet]. 2018 Nov;14(11):639–52. Available from: <https://pubmed.ncbi.nlm.nih.gov/30297701>

65. Huynh K, Lim WLF, Giles C, Jayawardana KS, Salim A, Mellett NA, et al. Concordant peripheral lipidome signatures in two large clinical studies of Alzheimer's disease. *Nat Commun*. 2020;11(1):5698.
66. Mapstone M, Cheema AK, Fiandaca MS, Zhong X, Mhyre TR, Macarthur LH, et al. Plasma phospholipids identify antecedent memory impairment in older adults. *Nat Med*. 2014;20(4):415–8.
67. Cheng H, Wang M, Li J-L, Cairns NJ, Han X. Specific changes of sulfatide levels in individuals with pre-clinical Alzheimer's disease: an early event in disease pathogenesis. *J Neurochem* [Internet]. 2013/07/30. 2013 Dec;127(6):733–8. Available from: <https://pubmed.ncbi.nlm.nih.gov/23865640>
68. Fonteh AN, Chiang AJ, Arakaki X, Edminster SP, Harrington MG. Accumulation of Cerebrospinal Fluid Glycerophospholipids and Sphingolipids in Cognitively Healthy Participants With Alzheimer's Biomarkers Precedes Lipolysis in the Dementia Stage [Internet]. Vol. 14, *Frontiers in Neuroscience* . 2020. Available from: <https://www.frontiersin.org/article/10.3389/fnins.2020.611393>
69. Wong MW, Braidy N, Poljak A, Pickford R, Thambisetty M, Sachdev PS. Dysregulation of lipids in Alzheimer's disease and their role as potential biomarkers. *Alzheimer's Dement*. 2017;13(7):810–27.
70. Brügger B. Lipidomics: Analysis of the Lipid Composition of Cells and Subcellular Organelles by Electrospray Ionization Mass Spectrometry. *Annu Rev Biochem* [Internet]. 2014 Jun 2;83(1):79–98. Available from: <https://doi.org/10.1146/annurev-biochem-060713-035324>
71. Chew H, Solomon VA, Fonteh AN. Involvement of Lipids in Alzheimer's Disease Pathology and Potential Therapies. *Front Physiol* [Internet]. 2020 Jun 9;11:598. Available from: <https://www.frontiersin.org/article/10.3389/fphys.2020.00598>
72. Lambert J-C, Ibrahim-Verbaas CA, Harold D, Naj AC, Sims R, Bellenguez C, et al. Meta-analysis of 74,046 individuals identifies 11 new susceptibility loci for Alzheimer's disease. *Nat Genet* [Internet]. 2013;45(12):1452–8. Available from: <https://doi.org/10.1038/ng.2802>
73. Kunkle BW, Grenier-Boley B, Sims R, Bis JC, Damotte V, Naj AC, et al. Genetic meta-analysis of diagnosed Alzheimer's disease identifies new risk loci and implicates A β , tau, immunity and lipid processing. *Nat Genet* [Internet]. 2019;51(3):414–30. Available from: <https://doi.org/10.1038/s41588-019-0358-2>
74. Harold D, Abraham R, Hollingworth P, Sims R, Gerrish A, Hamshere ML, et al. Genome-wide association study identifies variants at CLU and PICALM associated with Alzheimer's disease. *Nat Genet* [Internet]. 2009;41(10):1088–93. Available from: <https://doi.org/10.1038/ng.440>
75. Giri M, Zhang M, Lü Y. Genes associated with Alzheimer's disease: An overview and current status. *Clin Interv Aging*. 2016;11:665–681.
76. Cruchaga C, Karch CM, Jin SC, Benitez BA, Cai Y, Guerreiro R, et al. Rare coding

- variants in the phospholipase D3 gene confer risk for Alzheimer's disease. *Nature* [Internet]. 2014;505(7484):550–4. Available from: <https://doi.org/10.1038/nature12825>
77. Magno L, Lessard CB, Martins M, Lang V, Cruz P, Asi Y, et al. Alzheimer's disease phospholipase C-gamma-2 (PLCG2) protective variant is a functional hypermorph. *Alzheimer's Res Ther*. 2019;11(1):16.
 78. Andreone BJ, Przybyla L, Llapashtica C, Rana A, Davis SS, van Lengerich B, et al. Alzheimer's-associated PLC γ 2 is a signaling node required for both TREM2 function and the inflammatory response in human microglia. *Nat Neurosci* [Internet]. 2020;23(8):927–38. Available from: <https://doi.org/10.1038/s41593-020-0650-6>
 79. Grimm MOW, Michaelson DM, Hartmann T. Omega-3 fatty acids, lipids, and apoE lipidation in Alzheimer's disease: A rationale for multi-nutrient dementia prevention. *J Lipid Res*. 2017;
 80. Kao Y-C, Ho P-C, Tu Y-K, Jou I-M, Tsai K-J. Lipids and Alzheimer's Disease. Vol. 21, *International Journal of Molecular Sciences* . 2020.
 81. Sousa BC, Wakelam MJO, Lopez-Clavijo AF. Chapter 2 - Methods of lipid analysis. In: Ridgway ND, McLeod Lipoproteins and Membranes (Seventh Edition) RSBT-B of L, editors. Elsevier; 2021. p. 53–83. Available from: <https://www.sciencedirect.com/science/article/pii/B9780128240489000109>
 82. Sakr F, Dyrba M, Bräuer A, Teipel S. Association of Lipidomics Signatures in Blood with Clinical Progression in Preclinical and Prodromal Alzheimer's Disease. *J Alzheimer's Dis* [Internet]. 2022 Feb 1;85(3):1115–27. Available from: <https://www.medra.org/servlet/aliasResolver?alias=iospress&doi=10.3233/JAD-201504>
 83. Folstein MF, Folstein SE, McHugh PR. "Mini-mental state": A practical method for grading the cognitive state of patients for the clinician. *J Psychiatr Res* [Internet]. 1975;12(3):189–98. Available from: <https://www.sciencedirect.com/science/article/pii/0022395675900266>
 84. Berg L. Clinical Dementia Rating (CDR). *Psychopharmacol Bull*. 1988;24(4):637–9.
 85. Risacher SL, Kim S, Nho K, Foroud T, Shen L, Petersen RC, et al. APOE effect on Alzheimer's disease biomarkers in older adults with significant memory concern. *Alzheimer's Dement*. 2015;11(12):1417–29.
 86. Dubois B, Epelbaum S, Nyasse F, Bakardjian H, Gagliardi G, Uspenskaya O, et al. Cognitive and neuroimaging features and brain β -amyloidosis in individuals at risk of Alzheimer's disease (INSIGHT-preAD): a longitudinal observational study. *Lancet Neurol* [Internet]. 2018;17(4):335–46. Available from: <https://www.sciencedirect.com/science/article/pii/S1474442218300292>
 87. Habert M-O, Bertin H, Labit M, Diallo M, Marie S, Martineau K, et al. Evaluation of amyloid status in a cohort of elderly individuals with memory complaints: validation of the method of quantification and determination of positivity thresholds. *Ann Nucl*

- Med [Internet]. 2018;32(2):75–86. Available from: <https://doi.org/10.1007/s12149-017-1221-0>
88. Jagust W, Landau S, Koeppe R, Reiman E, Chen K, Mathis C, et al. The Alzheimer's Disease Neuroimaging Initiative 2 PET Core: 2015. *Alzheimers Dement*. 2015 Jul 1;11:757–71.
 89. Jack Jr CR, Bernstein MA, Fox NC, Thompson P, Alexander G, Harvey D, et al. The Alzheimer's Disease Neuroimaging Initiative (ADNI): MRI methods. *J Magn Reson Imaging* [Internet]. 2008 Apr;27(4):685–91. Available from: <https://pubmed.ncbi.nlm.nih.gov/18302232>
 90. Gonzalez-Escamilla G, Lange C, Teipel S, Buchert R, Grothe MJ. PETPVE12: an SPM toolbox for Partial Volume Effects correction in brain PET – Application to amyloid imaging with AV45-PET. *Neuroimage* [Internet]. 2017;147:669–77. Available from: <https://www.sciencedirect.com/science/article/pii/S1053811916308023>
 91. Müller-Gärtner HW, Links JM, Prince JL, Bryan RN, McVeigh E, Leal JP, et al. Measurement of Radiotracer Concentration in Brain Gray Matter Using Positron Emission Tomography: MRI-Based Correction for Partial Volume Effects. *J Cereb Blood Flow Metab* [Internet]. 1992 Jul 1;12(4):571–83. Available from: <https://doi.org/10.1038/jcbfm.1992.81>
 92. Desikan RS, Ségonne F, Fischl B, Quinn BT, Dickerson BC, Blacker D, et al. An automated labeling system for subdividing the human cerebral cortex on MRI scans into gyral based regions of interest. *Neuroimage* [Internet]. 2006;31(3):968–80. Available from: <https://www.sciencedirect.com/science/article/pii/S1053811906000437>
 93. Catafau AM, Bullich S, Seibyl JP, Barthel H, Ghetti B, Leverenz J, et al. Cerebellar Amyloid- β Plaques: How Frequent Are They, and Do They Influence ^{18}F -Florbetaben SUV Ratios? *J Nucl Med* [Internet]. 2016 Nov 1;57(11):1740 LP – 1745. Available from: <http://jnm.snmjournals.org/content/57/11/1740.abstract>
 94. Klunk WE, Koeppe RA, Price JC, Benzinger TL, Devous Sr MD, Jagust WJ, et al. The Centiloid Project: standardizing quantitative amyloid plaque estimation by PET. *Alzheimers Dement* [Internet]. 2014/10/28. 2015 Jan;11(1):1-15.e154. Available from: <https://pubmed.ncbi.nlm.nih.gov/25443857>
 95. Bilgel M, An Y, Lang A, Prince J, Ferrucci L, Jernigan B, et al. Trajectories of Alzheimer disease-related cognitive measures in a longitudinal sample. *Alzheimers Dement* [Internet]. 2014/07/14. 2014 Nov;10(6):735-742.e4. Available from: <https://pubmed.ncbi.nlm.nih.gov/25035155>
 96. Amariglio RE, Becker JA, Carmasin J, Wadsworth LP, Lorusso N, Sullivan C, et al. Subjective cognitive complaints and amyloid burden in cognitively normal older individuals. *Neuropsychologia* [Internet]. 2012/08/23. 2012 Oct;50(12):2880–6. Available from: <https://pubmed.ncbi.nlm.nih.gov/22940426>

References

97. Mowrey WB, Lipton RB, Katz MJ, Ramratan WS, Loewenstein DA, Zimmerman ME, et al. Memory Binding Test Predicts Incident Amnesic Mild Cognitive Impairment. *J Alzheimer's Dis.* 2016;53:1585–95.
98. Toledo JB, Arnold M, Kastenmüller G, Chang R, Baillie RA, Han X, et al. Metabolic network failures in Alzheimer's disease: A biochemical road map. *Alzheimer's Dement.* 2017;13(9):965–84.
99. Ma YH, Shen XN, Xu W, Huang YY, Li HQ, Tan L, et al. A panel of blood lipids associated with cognitive performance, brain atrophy, and Alzheimer's diagnosis: A longitudinal study of elders without dementia. *Alzheimer's Dement Diagnosis, Assess Dis Monit* [Internet]. 2020 Jan 15;12(1):e12041. Available from: <https://onlinelibrary.wiley.com/doi/10.1002/dad2.12041>
100. Mielke MM, Bandaru VVR, Haughey NJ, Rabins P V., Lyketsos CG, Carlson MC. Serum sphingomyelins and ceramides are early predictors of memory impairment. *Neurobiol Aging.* 2010;31(1):17–24.
101. Casanova R, Varma S, Simpson B, Kim M, An Y, Saldana S, et al. Blood metabolite markers of preclinical Alzheimer's disease in two longitudinally followed cohorts of older individuals. *Alzheimer's Dement.* 2016;12(7):815–22.
102. Su XQ, Wang J, Sinclair AJ. Plasmalogens and Alzheimer's disease: A review. *Lipids Health Dis.* 2019;18:100.
103. Grimm MOW, Kuchenbecker J, Rothhaar TL, Grösgen S, Hundsdörfer B, Burg VK, et al. Plasmalogen synthesis is regulated via alkyl-dihydroxyacetonephosphate- synthase by amyloid precursor protein processing and is affected in Alzheimer's disease. *J Neurochem.* 2011;116(5):916–25.
104. Ginsberg L, Rafique S, Xuereb JH, Rapoport SI, Gershfeld NL. Disease and anatomic specificity of ethanolamine plasmalogen deficiency in Alzheimer's disease brain. *Brain Res.* 1995;698(1–2):223–6.
105. Goodenowe DB, Cook LL, Liu J, Lu Y, Jayasinghe DA, Ahiahonu PWK, et al. Peripheral ethanolamine plasmalogen deficiency: A logical causative factor in Alzheimer's disease and dementia. *J Lipid Res.* 2007;48(11):2485–98.
106. Wood PL, Barnette BL, Kaye JA, Quinn JF, Woltjer RL. Non-targeted lipidomics of CSF and frontal cortex grey and white matter in control, mild cognitive impairment, and Alzheimer's disease subjects. *Acta Neuropsychiatr.* 2015;27(5):270–8.
107. Yamashita S, Kiko T, Fujiwara H, Hashimoto M, Nakagawa K, Kinoshita M, et al. Alterations in the levels of amyloid- β , phospholipid hydroperoxide, and plasmalogen in the blood of patients with Alzheimer's disease: Possible interactions between amyloid- β and these lipids. *J Alzheimer's Dis.* 2016;50(2):527–37.
108. Wood PL, Mankidy R, Ritchie S, Heath D, Wood JA, Flax J, et al. Circulating plasmalogen levels and Alzheimer Disease Assessment Scale-Cognitive scores in Alzheimer patients. *J Psychiatry Neurosci.* 2010;35(1):59–62.

References

109. Lim WLF, Huynh K, Chatterjee P, Martins I, Jayawardana KS, Giles C, et al. Relationships Between Plasma Lipids Species, Gender, Risk Factors, and Alzheimer's Disease. *J Alzheimers Dis.* 2020;76(1):303–15.
110. Wykle RL. Arachidonate remodeling and PAF synthesis in human neutrophils. In: *Arachidonate Remodeling and Inflammation.* Basel: Birkhäuser, Basel; 2004. p. 73–87.
111. Prescott SM, Zimmerman GA, Stafforini DM, McIntyre TM. Platelet-activating factor and related lipid mediators. *Annu Rev Biochem.* 2000;69:419–45.
112. van der Kant R, Langness VF, Herrera CM, Williams DA, Fong LK, Leestemaker Y, et al. Cholesterol Metabolism Is a Druggable Axis that Independently Regulates Tau and Amyloid- β in iPSC-Derived Alzheimer's Disease Neurons. *Cell Stem Cell* [Internet]. 2019/01/24. 2019 Mar 7;24(3):363-375.e9. Available from: <https://pubmed.ncbi.nlm.nih.gov/30686764>
113. He X, Huang Y, Li B, Gong CX, Schuchman EH. Deregulation of sphingolipid metabolism in Alzheimer's disease. *Neurobiol Aging.* 2010;31(3):398–408.
114. Han X, Rozen S, Boyle SH, Hellegers C, Cheng H, Burke JR, et al. Metabolomics in early Alzheimer's disease: Identification of altered plasma sphingolipidome using shotgun lipidomics. *PLoS One.* 2011;6(7):e21643.
115. Han X, Holtzman DM, McKeel DW, Kelley J, Morris JC. Substantial sulfatide deficiency and ceramide elevation in very early Alzheimer's disease: Potential role in disease pathogenesis. *J Neurochem.* 2002;82(4):809–18.
116. Filippov V, Song MA, Zhang K, Vinters H V, Tung S, Kirsch WM, et al. Increased Ceramide in Brains with Alzheimer's and Other Neurodegenerative Diseases. *J Alzheimer's Dis.* 2012;29:537–47.
117. Katsel P, Li C, Haroutunian V. Gene Expression Alterations in the Sphingolipid Metabolism Pathways during Progression of Dementia and Alzheimer's Disease: A Shift Toward Ceramide Accumulation at the Earliest Recognizable Stages of Alzheimer's Disease? *Neurochem Res* [Internet]. 2007;32(4):845–56. Available from: <https://doi.org/10.1007/s11064-007-9297-x>
118. Jana A, Hogan EL, Pahan K. Ceramide and neurodegeneration: Susceptibility of neurons and oligodendrocytes to cell damage and death. *J Neurol Sci* [Internet]. 2009;278(1):5–15. Available from: <https://www.sciencedirect.com/science/article/pii/S0022510X08006011>

Selbstständigkeitserklärung

Ich erkläre hiermit, dass ich die vorliegende Arbeit ohne unzulässige Hilfe Dritter und ohne Benutzung anderer als der angegebenen Hilfsmittel angefertigt habe. Die aus anderen Quellen direkt oder indirekt übernommenen Informationen und Konzepte sind unter Angabe der Quelle gekennzeichnet.

Die Regeln zur Sicherung guter wissenschaftlicher Praxis wurden beachtet.

Ich versichere, dass ich für die inhaltliche Erstellung der vorliegenden Arbeit nicht die entgeltliche Hilfe von Vermittlungs- und Beratungsdiensten (Promotionsberater oder andere Personen) in Anspruch genommen habe. Niemand hat von mir unmittelbar oder mittelbar geldwerte Leistungen für Arbeiten erhalten, die im Zusammenhang mit dem Inhalt der vorgelegten Dissertation stehen.

Die Arbeit wurde bisher weder im In- noch im Ausland in gleicher oder ähnlicher Form einer anderen Prüfungsbehörde vorgelegt.

Declaration:

I hereby declare that I have prepared the present work without undue help from third parties and without using any aids other than those specified. The information and concepts taken directly or indirectly from other sources are identified with an indication of the source.

The rules for safeguarding good scientific practice were observed.

I assure you that I did not use the paid help of mediation and advisory services (doctoral advisors or other people) to prepare the content of this thesis. Nobody has received direct or indirect monetary benefits from me for work related to the content of the submitted dissertation.

So far, the thesis has not been submitted to another examination authority in the same or a similar form, either in Germany or abroad.

Bielefeld, den 26.04.20

Fachpublikationen

2022

Sakr F, Dyrba M, Bräuer A, Teipel S.

Association of Lipidomics Signatures in Blood with Clinical Progression in Preclinical and Prodromal Alzheimer's Disease. *J Alzheimer's Dis* [Internet]. 2022 Feb 1;85(3):1115–27.

Available from:

<https://www.medra.org/servlet/aliasResolver?alias=iospress&doi=10.3233/JAD-201504>

2020

Teipel SJ, Dyrba M, Chiesa PA, Sakr F, Jelistratova I, Lista S, et al.

In vivo staging of regional amyloid deposition predicts functional conversion in the preclinical and prodromal phases of Alzheimer's disease. *Neurobiol Aging* [Internet]. 2020;93:98–108. Available from:

2020;93:98–108. Available from:

<https://www.sciencedirect.com/science/article/pii/S0197458020300907>

Eke CS, Sakr F, Jammeh E, Zhao P, Ifeakor E.

A Robust Blood-based Signature of Cerebrospinal Fluid $A\beta^{42}$ Status. In: 2020 42nd Annual International Conference of the IEEE Engineering in Medicine & Biology Society (EMBC). 2020. p. 5523–6.

2019

Sakr FA, Grothe MJ, Cavedo E, Jelistratova I, Habert M-O, Dyrba M, et al.

Applicability of in vivo staging of regional amyloid burden in a cognitively normal cohort with subjective memory complaints: The INSIGHT-preAD study. *Alzheimer's Res Ther*. 2019;11(1).

Präsentationen auf nationalen und internationalen Fachkongressen

2020

Sakr FA, Dybra M, Gräler M, Teipel SJ, Braeuer A. What can lipidomics tell about pathomechanisms at the early phases of Alzheimer's disease? *Alzheimer's Dement*. 2020;16(S4). Alzheimer's Association International Conference (AAIC).

2019

Sakr FA, Kuhla A, Ruehlmann C, Dybra M, Lindner T, Hadlich S, et al. IC-P-020:

Investigating the progression of neuroimaging biomarkers in the appswe/ps1de9 transgenic mouse model of alzheimer's disease. *Alzheimer's Dement*. 2019;15. Alzheimer's Association International Conference (AAIC), Los Angeles, USA.

Sakr FA, Grothe MJ, Cavedo E, Habert M-O, Bertin H, Locatelli M, et al.

Clinical significance of in-vivo staging of regional amyloid deposition in subjective memory complainers. Alzheimer's Research Conference, UK, 2019.

Sakr FA, Grothe MJ, Dybra M, Kuhla A, Bräuer A, Teipel S. What do lipids do with β -Amyloid and Alzheimer's disease ?. Summer school within the frame of the EU funded (H2020) project Blood Biomarker-based Diagnostic tools or early stage Alzheimer's disease (BBDiag), Rostock, Germany, June 2019.

Sakr FA, Grothe MJ, Dybra M, Kuhla A, Bräuer A, Teipel S. What do lipids do with β -Amyloid and Alzheimer's disease ?. Residential workshop within the frame of the EU funded (H2020) project Blood Biomarker-based Diagnostic tools or early stage Alzheimer's disease (BBDiag), Milan, Italy, October 2019.

2018

Sakr FA, Grothe MJ, Cavedo E, Habert M-O, Bertin H, Locatelli M, et al. P3-411: Clinical significance of in-vivo staging of regional amyloid deposition in subjective memory complainers. Alzheimer's dement. 2018;14(7s_part_23). Alzheimer's Association International Conference (AAIC), Chicago, USA.

Kuhla A, Sakr FA, Ruehlmann C, Lindner T, Polei S, Hadlich S, et al.: APP^{swe}/PS1^{dE9} mice with cortical amyloid pathology show a reduced NAA/Cr ratio without apparent brain atrophy: A MRS and MRI stud. Joint Annual Meeting International Society for Magnetic Resonance in medicine-European Society for Magnetic Resonance in Medicine and Biology, Paris, France 2018

Sakr FA, Grothe MJ, Bräuer A, Teipel S. Exploring patho-mechanistic targets of Alzheimer's disease in its initial stages. Anatomische Gesellschaft meeting, Rostock, Germany 2018.

Sakr FA, Grothe MJ, Bräuer A, Teipel S. Patho-mechanistic targets of Alzheimer's disease in its initial stages. China-Europe Alzheimer's Disease Symposium – Biomarkers & Early Diagnosis, Beijing, China, May 2018.

Sakr FA, Grothe MJ, Dybra M, Kuhla A, Bräuer A, Teipel S. Initiating new approaches targeting the patho-mechanics of Alzheimer's disease in its initial stages. Residential workshop within the frame of the EU funded (H2020) project Blood Biomarker-based Diagnostic tools or early stage Alzheimer's disease (BBDiag), Rome, Italy, March 2018.

Sakr FA, Grothe MJ, Dybra M, Kuhla A, Bräuer A, Teipel S. What do lipids do with β -Amyloid and Alzheimer's disease ?. Residential workshop within the frame of the EU funded (H2020) project Blood Biomarker-based Diagnostic tools or early stage Alzheimer's disease (BBDiag), Madrid, Spain, October 2018.


Appendix (Studies 1-3)

RESEARCH

Open Access



Applicability of in vivo staging of regional amyloid burden in a cognitively normal cohort with subjective memory complaints: the INSIGHT-preAD study

Fatemah A. Sakr^{1,2*} , Michel J. Grothe^{2†}, Enrica Cavedo^{3,4,5,6,7}, Irina Jelistratova², Marie-Odile Habert^{8,9,10}, Martin Dyrba², Gabriel Gonzalez-Escamilla¹¹, Hugo Bertin⁹, Maxime Locatelli^{8,9,10}, Stephane Lehericy^{5,9,12,13}, Stefan Teipel^{1,2}, Bruno Dubois^{4,5,6}, Harald Hampel^{3,4,5,6}, for the INSIGHT-preAD study group and the Alzheimer Precision Medicine Initiative (APMI)

Abstract

Background: Current methods of amyloid PET interpretation based on the binary classification of global amyloid signal fail to identify early phases of amyloid deposition. A recent analysis of 18F-florbetapir PET data from the Alzheimer's disease Neuroimaging Initiative cohort suggested a hierarchical four-stage model of regional amyloid deposition that resembles neuropathologic estimates and can be used to stage an individual's amyloid burden in vivo. Here, we evaluated the validity of this in vivo amyloid staging model in an independent cohort of older people with subjective memory complaints (SMC). We further examined its potential association with subtle cognitive impairments in this population at elevated risk for Alzheimer's disease (AD).

Methods: The monocentric INSIGHT-preAD cohort includes 318 cognitively intact older individuals with SMC. All individuals underwent 18F-florbetapir PET scanning and extensive neuropsychological testing. We projected the regional amyloid uptake signal into the previously proposed hierarchical staging model of in vivo amyloid progression. We determined the adherence to this model across all cases and tested the association between increasing in vivo amyloid stage and cognitive performance using ANCOVA models.

Results: In total, 156 participants (49%) showed evidence of regional amyloid deposition, and all but 2 of these (99%) adhered to the hierarchical regional pattern implied by the in vivo amyloid progression model. According to a conventional binary classification based on global signal ($SUVR_{Cereb} = 1.10$), individuals in stages III and IV were classified as amyloid-positive (except one in stage III), but 99% of individuals in stage I and even 28% of individuals in stage II were classified as amyloid-negative. Neither in vivo amyloid stage nor conventional binary amyloid status was significantly associated with cognitive performance in this preclinical cohort.

(Continued on next page)

* Correspondence: fatemah.sakr@med.uni-rostock.de

†Fatemah A. Sakr and Michel J. Grothe contributed equally to this work.

¹Department of Psychosomatic Medicine, Clinical Dementia Research, Faculty of Medicine, Rostock University, Rostock, Germany

²German Center for Neurodegenerative Diseases (DZNE), Rostock, Germany

Full list of author information is available at the end of the article



(Continued from previous page)

Conclusions: The proposed hierarchical staging scheme of PET-evidenced amyloid deposition generalizes well to data from an independent cohort of older people at elevated risk for AD. Future studies will determine the prognostic value of the staging approach for predicting longitudinal cognitive decline in older individuals at increased risk for AD.

Keywords: Amyloid PET, In vivo staging, Subjective memory complaint,

Background

Amyloid PET imaging is considered a direct in vivo measure of cortical amyloid load with a high specificity and a relatively strong correlation between the in vivo amyloid signal in PET and the post-mortem quantification of neuritic amyloid plaque load [1–3]. Currently, the majority of studies use a binary classification of global amyloid signal into positive and negative categories. Several postmortem studies, however, suggest a relatively consistent pattern of sequential regional amyloid involvement, with initial amyloid accumulation in the associative neocortex, then spreading through the primary sensory-motor cortex and the medial temporal allocortex to subcortical regions (striatum, thalamus, and cholinergic basal forebrain) and finally to the brain stem and cerebellum [3–6]. Based on these findings, two recent studies explored the topographical pattern of amyloid spread in vivo using regional analysis of amyloid PET signal in cognitively normal (CN), mild cognitive impairment (MCI), and Alzheimer's disease (AD) individuals, which revealed highly consistent results with the findings described by post-mortem studies [6, 7].

Grothe et al. further tested the utility of this progression model for staging of individual deposition patterns [7]. They found that the individual deposition patterns closely adhered to the regional hierarchy implied by the progression model, allowing them to classify over 95% of participants with detectable regional amyloid deposition into one of four successive amyloid stages. Although the earliest in vivo amyloid stages were mostly missed by conventional binary classification approaches based on global amyloid signal, they were associated with significantly reduced cerebrospinal fluid (CSF) A β 42 levels, corroborating the pathologic origin of these PET signal elevations [7]. Moreover, advanced in vivo amyloid stages were most frequently observed in cognitively impaired patients (MCI or AD dementia) and correlated with cognitive deficits in healthy elderly individuals [7].

The primary goal of the current study was to explore the validity of this recently proposed in vivo staging scheme [7] and its association with cognitive function in independent data from a large cohort of cognitively intact older individuals with subjective memory complaints, the "INSIGHT-preAD" cohort [8–10].

Methods

Participants

All the data for this project were collected for the INSIGHT-preAD study which is a mono-centric academic university-based cohort derived from the Institute for Memory and Alzheimer's Disease (IM2A) at the Pitié-Salpêtrière University Hospital in Paris, France, with the objective of investigating the earliest preclinical stages of AD and its development including influencing factors and markers of progression [11].

The INSIGHT-preAD study includes 318 cognitively normal Caucasian individuals from the Paris area, between 70 and 85 years old, with subjective memory complaints and with defined brain amyloid status. The study aims at 7 years of follow-up, with the 2-year follow-up being completed in 2017. Demographic, cognitive, functional, nutritional, biological, genetic, genomic, imaging, electrophysiological, and other assessments were performed at baseline. Subjective memory complaints were confirmed by an affirmative answer to both of the following questions: (i) "Are you complaining about your memory?", and (ii) "Is it a regular complaint which lasts more than 6 months?"

Demographic characteristics, including cognitive performance and ApoE genotype, are shown in Table 1. Each participant had a total recall at the Free and Cued Selective Reminding Test in the normal range (mean 46.1 ± 2.0). Written informed consent was provided by all participants. The study was approved by the local Institutional Review Board and has been conducted in accord with the Helsinki Declaration of 1975.

Cognitive tests

A comprehensive neuropsychological battery was administered to all participants of the INSIGHT-preAD cohort including the Mini-Mental State Examination (MMSE) [14] to assess global cognition, the Free and Cued Selective Reminding Test (FCSRT) and Memory Binding Test (MBT) [15–17] for episodic memory, Letter and Category Verbal Fluency test [18–20] for instrumental and executive functions, the Rey-Osterrieth Complex Figure Copy [21] for visuo-spatial abilities; Digit span (forward and backward) [22, 23], the Trail Making Test (TMT) [24], and the Frontal Assessment Battery [25] for the

Table 1 Summary of participants' demographics

	N	Age (years)	Gender (F/M)	ApoE-ε4	MMSE score (0–30)	Education (0–8)
Amyloid +ve	68	76.6 ± 3.6	44/24	38.2%	28.5 ± 0.91	6.0 ± 2.1
Amyloid –ve	250	75.9 ± 3.5	157/93	12.8%	28.7 ± 0.96	6.2 ± 2.0
All subjects	318	76.1 ± 3.5	201/117	18.2%	28.67 ± 0.95	6.2 ± 2.0

The table presents the demographic features among the whole INSIGHT-preAD cohort as well as the distribution within two main categories, amyloid-positive and amyloid-negative as classified using the conventional threshold of SUVR = 1.10 applied to global 18F-florbetapir PET signal intensity normalized to the average signal in the whole cerebellum [12, 13]. Data are mean values ± standard deviation

N number of participants in each category, ApoE-ε4 percent of participants positive for ε4 allele, MMSE Mini Mental State Examination

assessment of working memory and executive function. In order to reduce the high dimensionality of the detailed cognitive test data, we ran a principal component analysis (PCA) on standardized z-scores of the 15 available cognitive test scores to sum up the covariates into representative eigenvectors. However, we excluded from the PCA analysis the scores of MMSE, Frontal Assessment Battery, and total (free and cued) delayed recall of FCSRT (index test for study inclusion) due to lack of variance in their scores among participants.

ApoE genotype

DNA was prepared from frozen blood samples using the 5Prime Archive Pure DNA purification system according to the manufacturer's instructions. ApoE genotypes were determined for each individual using PCR-based Sanger sequencing. Exon 4 from ApoE gene containing the SNP corresponding to the ε3/ε4 alleles was amplified using PCR with the following primers: ApoE sense, 5'-TAAG CTTGGCACGGCTGTCCAAGGA-3'; ApoE antisense, 5'-ACAGAATTCGCCCGGCCTGGTACAC-3'. For each sample, the reaction mixture (50 μl) contained 200 ng of genomic DNA, 10 μl PCR Flexi buffer (5×), 3 μl MgCl₂ (25 mM), 1 μl dNTPs (10 mM), 1 μl of each forward and reverse primers (10 μM), and 0.25 μl GO Taq DNA polymerase (Promega). The cycling program was carried out after a preheating step at 95 °C for 2 min and 35 cycles of denaturation at 95 °C for 1 min, annealing at 68 °C for 1 min and extension at 72 °C for 1 min. The amplified fragments were then purified and sequenced using the same primers [11].

Imaging data acquisition

In the Pitié-Salpêtrière University Hospital in Paris, all the amyloid PET scans were acquired in a single session on a CT-PET scanner (Gemini GXL, Philips, Cleveland, USA) 50 ± 5 min after the injection of approximately 370 MBq (333–407 MBq) of 18F-florbetapir (AVID radiopharmaceuticals). PET acquisition consisted of 3 × 5-min frames, in a 128 × 128 acquisition matrix, with a voxel size of 2 × 2 × 2 mm³.

Images were then reconstructed using the iterative LOR-RAMLA algorithm (10 iterations). Reduction of noise was modulated by the relaxation parameter

lambda, which was set to 0.7. All corrections (attenuation, scatter, and random coincidence) were integrated in the reconstruction [26]. The reconstructed PET image resolution was 7.5 mm FWHM.

MRI scans were acquired on a Siemens Verio 3 T scanner at the CENIR in the Brain and Spine Institute, Paris, France. A T1-weighted image was acquired using a fast three-dimensional gradient echo pulse sequence using a magnetization preparation pulse (Turbo FLASH) and with the parameters of TR = 2300 ms; TE = 2.98 ms; IT = 900 ms; flip angle = 9°; 1-mm isotropic voxel size; matrix 256 × 240; bandwidth 240 Hz/Px [26].

Imaging data pre-processing

Images were preprocessed using Statistical Parametric Mapping software version 12 (SPM12) (The Wellcome Trust Centre for Neuroimaging, Institute of Neurology, University College London) implemented in Matlab 2013. The pre-processing pipeline followed the routine previously described in Grothe et al. [7]. First, each subject's averaged PET frames were co-registered to their corresponding T1-weighted MRI scan. Then, partial volume effects (PVE) were corrected in native space using the three-compartmental voxel-based post-reconstruction method as described by Müller-Gärtner and colleagues (MG method) [27]. The corrected PET images were spatially normalized to an aging/AD-specific reference template using the deformation parameters derived from the normalization of their corresponding MRI. The pre-processing pipeline is summarized in the schematic diagram provided in Additional file 1: Figure S1.

The regional 18F-florbetapir PET mean uptake values were estimated for 52 brain regions defined by the Harvard–Oxford structural atlas [28], including both cortical and subcortical regions (<https://fsl.fmrib.ox.ac.uk/fsl/fslwiki/Atlases>). Standard uptake value ratios (SUVR_{cereb}) were computed for the 52 brain regions by dividing the mean uptake values by the mean uptake value of the whole cerebellum as estimated in non-PVE-corrected PET data [7, 29–31].

In accordance with the methods used for the published PET-based amyloid staging approach, we based the cutoff used for determining regional amyloid positivity on a cutoff value of SUVR_{cereb} = 1.135 [7], which lies

in between the two most widely used global signal cutoffs for non-PVE-corrected 18F-florbetapir PET SUVRs, i.e., $SUVR_{cereb} = 1.10$ [12, 13, 32], which represents the upper limit of observed signal in a group of healthy controls, and $SUVR_{cereb} = 1.17$, which corresponds to the lowest signal observed in a group of AD dementia patients [33, 34]. This threshold was converted to PVE-corrected data employed in the regional staging approach using linear regression. Thus, global 18F-florbetapir PET uptake mean values within a cortical composite mask were calculated on PET data both corrected and non-corrected for PVE and these were scaled to the mean signal of the whole cerebellum (extracted from non-PVE-corrected data). Global 18F-Florbetapir PET $SUVR_{cereb}$ of both non-corrected (X -axis) and PVE-corrected PET (Y -axis) data were plotted, and linear regression analysis indicated a very strong correlation between the two values ($R = 0.94$). The linear regression equation was used to transform the mean cutoff value of $SUVR_{cereb} = 1.135$ to a value of $SUVR_{cereb} = 0.98$ in the PVE-corrected PET data used in our present study [7] (Additional file 2: Figure S2).

Data analysis

Individual staging of amyloid deposition according to previously reported four-stage model

We projected our regional $SUVR_{cereb}$ values on the previously published four-stage model of amyloid pathology progression derived from 18F-Florbetapir PET data of cognitively normal older individuals enrolled in the Alzheimer's disease Neuroimaging Initiative (ADNI) study [7]. This four-stage model was estimated by counting the frequency of amyloid positivity across the 52 brain regions defined in the Harvard–Oxford structural atlas and then merging the regions into four broader anatomical divisions based on equal proportions of the observed range of involvement frequencies. The four anatomical divisions defining the staging scheme are illustrated in Additional file 3: Figure S3, and full details on the development of this staging approach are provided in the original publication [7].

Following the approach described in [7], an anatomical division was considered positive for amyloid pathology if at least 50% of the regions included in this division exceeded the cutoff value ($SUVR_{cereb} = 0.98$) in the respective participant. Subsequently, participants were classified as stage I if only the first division was considered positive. Then, the successive stages II–IV were defined by the additional involvement of their corresponding divisions 2, 3, and 4, respectively. Participants who exhibited amyloid positivity in any division without concurrent amyloid positivity in the preceding divisions were classified as non-stageable (mismatch).

For comparison, 18F-Florbetapir PET scans were also conventionally classified into global amyloid-positive or amyloid-negative categories based on a commonly used cutoff of $SUVR_{cereb} > 1.10$, applied to the global composite $SUVR_{Cereb}$ values (non-PVE-corrected).

Reproducibility of the amyloid progression model

In order to assess the reproducibility of the regional progression model underlying the hierarchical staging scheme, we re-estimated the model by calculating the regional frequency of amyloid positivity across the 18F-Florbetapir PET scans of the INSIGHT-preAD cohort. Correspondence between the model derived from the INSIGHT-preAD cohort and the original model derived from the ADNI cohort was assessed quantitatively using the Spearman correlation between the respective ranks of the 52 studied brain regions.

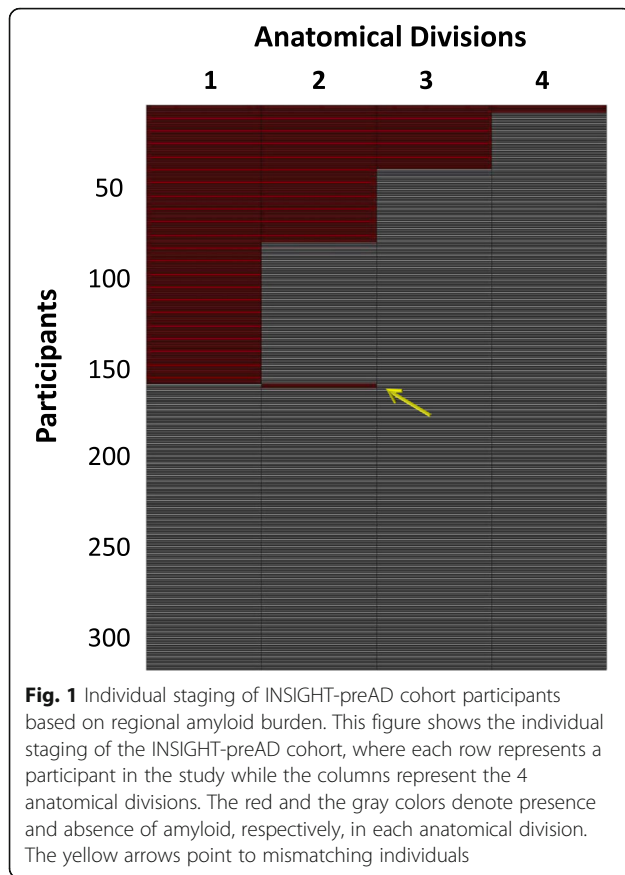
Statistical analysis

All the data were statistically analyzed using the SPSS Statistics software package, version 23.0, developed by IBM. An association between in vivo amyloid stage and ApoE- $\epsilon 4$ allele frequency was assessed using chi-squared (χ^2) test. Analysis of covariance (ANCOVA) was used to examine the covariation between amyloid stage and scores of the cognitive principal components, as well as the cognitive tests scores being most representatives for each of these components, while adjusting for the covariates age and gender. For comparison, we also applied the ANCOVA analysis to the conventional binary amyloid status. P values were corrected for multiple comparisons using the Bonferroni correction.

Results

Individual staging based on hierarchical four-stage model of regional amyloid deposition

The individual staging of INSIGHT-preAD participants based on regional amyloid burden is displayed in Fig. 1. One hundred fifty-six participants (49%) showed evidence of regional amyloid deposition, and only two of these (1.3%) were found to violate the proposed regional hierarchy implied by the four-stage model, providing evidence for the consistency of this stage model across different cohorts. Both mismatching individuals were found to be positive for the second anatomical division while lacking amyloid positivity for the regions of the first anatomical division. Among the five regions comprising the first anatomical division, the mismatching individuals exhibited positivity for the inferior temporal gyrus (both anterior and posterior divisions) while lacking amyloid deposition in the remaining regions, namely anterior cingulate gyrus, temporal fusiform cortex, and parietal operculum.



Exploring the distribution of the different stages of the model against the conventional binary classification model (based on a global signal threshold of $SUVR_{cereb} > 1.10$), we observed that almost all the subjects in stage III or IV (96.8% and 100%, respectively) were classified as amyloid-positive. By contrast, almost all the subjects who belonged to stages 0 and I were classified as amyloid-negative (98.1% and 98.7%, respectively). Moreover, about 30% of individuals in stage II were classified as amyloid-negative (Table 2). When matching the global signal cutoff to the cutoff used for determining regional positivity ($SUVR_{cereb} = 1.135$), the percentage of negatively classified individuals in stage II rose to 40%.

Association of amyloid stage with APOE genotype and cognitive performance

In vivo amyloid stage was significantly associated with ApoE-ε4 status, such that the percentage of ApoE-ε4 carriers increased with increasing amyloid stage (chi-squared (χ^2) test, $p = 0.001$) (Table 3).

The principal component analysis of the cognitive tests, including memory, executive, and attention functions, identified three main components that accounted for 45.5% of the variance in the data (Additional file 4: Table S1). The highest loading in the first component was for FCSRT “Total free recall scores” and in the second component for the MCT “Immediate Total Free Recall List 1 and 2.” The third component mainly represented tests of executive and attention functions and showed highest loadings on “TMT-B scores.”

In vivo amyloid stage was not significantly associated with any of the principal component scores, but showed relatively weak effects on FCSRT total recall scores ($p = 0.022$, partial $\eta^2 = 0.063$) and TMT-B scores ($p = 0.036$, partial $\eta^2 = 0.056$), which did not survive correction for multiple comparisons. Moreover, the effects appeared to be primarily driven by low cognitive scores of the few participants in amyloid stage IV ($N = 4$) and did not remain (nominally) significant when these participants were removed. The binary conventional approach had no significant effect on any of the three principal components or their most representative individual tests scores (full statistics for all tests and plots of the data are reported in Additional file 5: Table S2).

In vivo amyloid progression model based on frequency of regional involvement

In the INSGHT-preAD cohort, the inferior temporal gyri showed the highest frequency of involvement (about ~ 90%) followed by the lateral occipital cortices and middle temporal gyri (~ 70% and ~ 60% respectively) and the other associative cortex regions. The precuneus cortex and the cingulate gyri surprisingly showed an intermediate frequency of involvement (~ 20%) which was rather close to the primary sensory-motor regions (~ 15–20%). The brain areas less involved were the striatum and the parahippocampal regions (~ 2–5%), while no regional amyloid pathology was detected in the thalamus and hippocampus (Additional file 6: Figure S4).

Table 2 Comparing individual amyloid stages to conventional binary amyloid status

	Stage 0	Stage 1	Stage 2	Stage 3	Stage 4
SUVR > 1.1	3 (1.9%)	1 (1.3%)	29 (72.5%)	31 (96.9%)	4 (100%)
SUVR > 1.135	0 (0%)	0 (0%)	24 (60%)	31 (96.9%)	4 (100%)
Number of subjects	162	78	40	32	4

The table presents the distribution of the stages of the in vivo amyloid staging model among the INSGHT-preAD participants compared to conventional binary amyloid status. Data represents the number of participants with global cortical measure exceeding the cutoff of ($SUVR = 1.1$) and cutoff of ($SUVR = 1.135$), respectively, and their percentage among the total participants comprising the respective stage

Table 3 Amyloid progression model stages and ApoE-ε4 status

	N	Stage 0	Stage 1	Stage 2	Stage 3	Stage 4
ApoE-ε4 (+ve)	58	17 (10.5%)	12 (15.4%)	15 (37.5%)	13 (40.6%)	1 (25.0%)
ApoE-ε4 (-ve)	258	145 (89.9%)	66 (84.6%)	25 (62.5%)	19 (59.4%)	3 (75.0%)
All subjects	316	162	78	40	32	4

The table presents the distribution of stageable participants (316 out of 318) in the INSIGHT-preAD cohort among the in vivo amyloid stages and their corresponding ApoE-ε4 status

N number of participants in each category, ApoE-ε4 apolipoprotein E (ε4 allele)

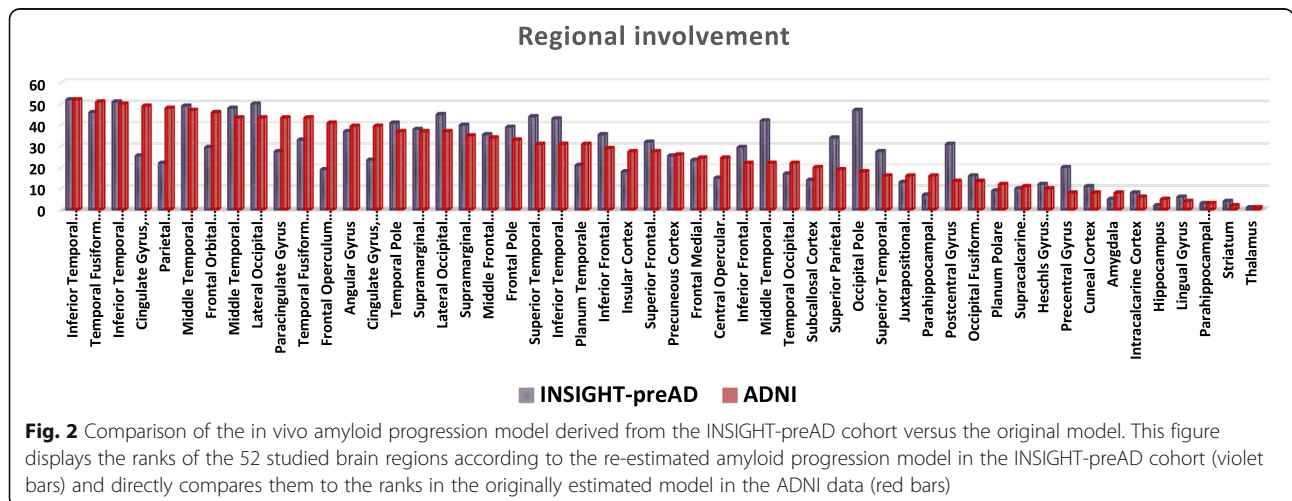
Figure 2 compares the ranks of the 52 studied brain regions between the estimated progression model in the INSIGHT-preAD cohort and the originally estimated model in the ADNI data [7]. Overall, the two models showed a relatively good correspondence with a Spearman correlation between the respective ranks of $R = 0.75$ ($p < 0.001$). Both models generally agreed on a pattern of involvement frequencies that are highest in the inferior temporal lobe and other heteromodal association areas, intermediate in several primary sensory-motor regions (e.g., precentral gyrus and cuneal cortex), and lowest in the medial temporal lobe and sub-cortical areas. However, some discrepancies between both models were also notable. For example, the INSIGHT-preAD cohort showed a relatively higher frequency of involvement in posterior (occipital and parietal) brain regions and the lateral temporal lobe (middle and superior temporal gyri), whereas the anterior and posterior cingulate gyri, fronto-orbital and opercular regions were relatively less frequently involved.

Discussion

Here, we adopted a hierarchical region based in vivo amyloid staging model proposed recently [7] and applied it on a large independent cohort of older individuals at elevated risk for AD [8, 10]. Our findings provide evidence for the applicability of the in vivo amyloid staging model proposed by Grothe and colleagues to different

cohorts. Indeed, 99% of the 156 individuals with detectable amyloid load in the INSIGHT-preAD cohort adhered to the sequential regional pattern of the model. Moreover, it allowed for identifying 49% of clinically normal older individuals as having evidence of regional amyloid deposition in this preclinical cohort opposed to the 21.5% identified as being amyloid-positive using the conventional global measure. Almost all individuals classified as stage I and about 30% of individuals classified as stage II according to the regional staging approach were considered amyloid-negative according to the conventional global measure. Both stages correspond to Thal amyloid phase 1 denoting amyloid deposits confined to the associative neocortex [5]. Thus, in vivo amyloid staging could have crucial implications for clinical trials, as it may allow the identification of individuals at the very early stages of disease pathogenesis.

These findings are consistent with the results of previous studies exploring the correspondence between Thal amyloid staging at autopsy and the ante-mortem depicted PET signal using different radioisotope ligands, namely C^{11} PiB and F^{18} radiolabeled ligands [2, 3, 6]. Some studies concluded that amyloid PET scans are particularly effective in detecting advanced Thal phases and that the early Thal phases (0–2) with amyloid deposition confined to the neocortex were always associated with a negative scan [3, 35, 36]. Analogously, Murray et al. suggested that PET positivity assigned based on global PET



signal and the currently used thresholds fail to recognize initial amyloid phases [2]. They showed that a cutoff point of 1.4 SUVR on ante-mortem PiB PET normalized to whole cerebellar signal corresponded to Thal amyloid phase 2 at autopsy [2, 36]. However, Ikonovic et al. compared the regional CERAD neuritic plaque score at autopsy with ante-mortem PET scans and suggested that 18F-flutemetamol PET may detect amyloid- β plaques early in neocortex even below the level usually associated with clinically significant (moderate) burden [3]. Subsequently, they recommended modifying the amyloid PET scans interpretation method to fit the targeted clinical setting, using a more sensitive method for identifying at risk subjects with still preserved cognitive functions [3]. Consequently, many studies recommended using a lower cutoff than the currently used to assign amyloid positivity based on global PET signal [2, 37]. This approach, however, increases the risk of false positive findings. The solution proposed by the regional staging approach is to consider detailed topographical differences between individuals to identify the early amyloid accumulators who are usually misclassified as negative for amyloid [2], while minimizing misclassification of low unspecific binding.

The second goal of our study was to explore the association between amyloid stage and cognitive performance in this cohort of cognitively intact individuals with subjective memory complaints. We included in our analysis scores of neuropsychological tests that assess the various disease-specific cognitive domains, such as episodic memory and memory binding, executive functions, processing speed and attention [38–42]. Overall, associations between cognitive performance and amyloid load showed only small and non-significant effects, regardless of whether amyloid load was assessed using *in vivo* amyloid stage or conventional binary amyloid status. This could be attributed to the limited variability of the cognitive test scores in a cognitively normal performing cohort. In subsequent follow-up data from the INSIGHT-preAD cohort, we will be able to determine whether regional amyloid stages associate with a stage-proportional risk for longitudinal cognitive decline, thus potentially providing more fine grained risk stratification compared with the binary classification of global amyloid load [43]. The lack of associations between episodic memory and amyloid load in our cohort contradicts previous studies that found that subtle episodic memory changes occur in early, preclinical stages of the disease [39, 44–48]. This contradiction may be attributable to the inclusion criteria of the INSIGHT-preAD cohort requiring normal performance in the FCSRT total recall scores, thus restricting the variability in episodic memory performance in this cohort and possibly masking its cross-sectional association with amyloid burden.

In a secondary analysis, we also assessed the reproducibility of the regional amyloid progression model underlying the hierarchical staging scheme by calculating the regional frequency of amyloid positivity across the 18F-florbetapir PET scans of the INSIGHT-preAD cohort. Overall, the re-estimated model in the INSIGHT-preAD cohort showed a relatively good correspondence with the originally estimated model in the ADNI data. Both models agreed on a general pattern of involvement frequencies that are highest in the inferior temporal lobe and other heteromodal association areas, intermediate in several primary sensory-motor regions and lowest in the medial temporal lobe and subcortical areas. This pattern also largely agrees with regional involvement frequencies observed in a previous study using 18F-florbetaben PET data [6] and is consistent with long-standing neuropathologic estimates of regionally progressing amyloid pathology [5, 49]. However, besides the relatively good overall correspondence, on a regionally more detailed level, some notable discrepancies were also evident between the models derived from the INSIGHT-preAD and ADNI cohorts (Fig. 2), which may relate to differences in the specific characteristics of both cohorts. Thus, the INSIGHT-preAD cohort is a highly selected mono-centric cohort of very old seniors who lack any objective cognitive decline despite presenting with subjective memory complaints. Due to the advanced age, a high prevalence of co-morbid pathologies, particularly cerebrovascular disease and cerebral amyloid angiopathy (CAA), can be expected and these may interact with the regional patterns of amyloid deposition. For example, CAA has been reported in up to 57% of individuals over 70 years and affects primarily the occipital and parietal lobes [50, 51]. Hence, the relatively higher involvement of posterior (occipital and parietal) over frontal brain regions in the INSIGHT-preAD data may potentially be explained by a higher prevalence of CAA in this relatively old cohort. On the other hand, the preserved cognitive performance of these individuals points to a higher brain resilience that may provide a relative resistance to regional pathology progression [52, 53]. Due to these specific cohort characteristics, a regional progression model derived from the INSIGHT-preAD cohort may not generalize well to the broader population of older people. However, it is notable that the regional differences in amyloid distribution in the INSIGHT-preAD data did not translate into an increased number of mismatching individuals in this cohort. Thus, overall amyloid deposition patterns across the four larger anatomical divisions considered in the original staging scheme based on ADNI data also showed a very consistent regional hierarchy across INSIGHT-preAD individuals. This highlights the potential of the proposed staging approach to provide a consistent staging of an overall

amyloid progression pattern across four larger anatomical systems, while accounting for inter-individual differences in amyloid deposition at a higher regional resolution.

It is important to note that the proposed *in vivo* amyloid staging approach relies on a range of methodologic conditions that may affect the final staging outcomes, including for example the employed radiotracer (18F-Florbetapir), the methods used for signal quantification (PVE-corrected SUVR values) and for defining brain regions (Harvard-Oxford atlas), as well as the methods and thresholds used to define amyloid positivity for a region and for an anatomical division. While outside the scope of the present study, it would be important in future methodological studies to analyze in more detail the differential effects that these methodical choices may have on the staging outcomes and which methods may be the most accurate when compared to neuropathologic data as the gold standard.

For example, the described *in vivo* amyloid staging approach relies on PVE-corrected SUVR values for regional PET signal quantification [7]. While SUVR values are by far the most widely used metric for 18F-florbetapir PET scans [33] and for amyloid PET imaging in large-scale cohort studies with high-throughput PET scanning in general [26, 54–57], they are also known to lead to biased estimates when compared to the gold standard estimates derived from tracer kinetic modeling using dynamic PET acquisitions (i.e. BP_{ND} or DVR values) [58–60]. Thus, using DVR values, particularly arterial input-based values, could be an interesting option to further refine the *in vivo* amyloid staging model in future research.

Partial volume effect correction has been shown to enhance the accuracy of regional amyloid PET signal quantification and allows for inter-regional quantitative comparison as it alleviates the differential impact of partial volume effects on different brain regions [61, 62]. In healthy populations, it was described a decline in the global SUVR values following partial volume effect correction due to the predominant spill-in effects from the WM to the GM particularly in case of low brain atrophy and when using 18F-labeled amyloid tracers characterized by high non-specific binding to WM [63–65]. Another advantage of applying partial volume correction on PET data is that it enhances the sensitivity of detecting small changes in follow-up studies as it attenuates the bias induced by the concomitantly progressing cortical atrophy leading to underestimation of the SUVR in non-corrected PET data [29, 62, 63, 66]. This will enable us to further study the amyloid deposition model longitudinally, explore the transition rates between the identified stages of amyloid deposition, and study the correlation between the rates of transition and the rates of cognitive decline in the upcoming follow up data of the INSIGHT-preAD cohort.

For detection of regional amyloid-positivity the *in vivo* staging approach applies a constant threshold to all brain regions. This threshold is based on the mean value of the two most widely used cutoffs for defining amyloid-positivity based on global 18F-florbetapir PET SUVRs ($SUVR_{cereb} = 1.10$ [12, 13, 32] and 1.17 [33, 34], respectively), which is further extrapolated to the PVE-corrected PET data used in the staging approach [7]. Grothe et al. used this relatively high and more conservative threshold owing to a potentially higher signal to noise ratio depicted when exploring the PET signal on a detailed regional level compared to the global PET measure. When estimating the global PET signal, the signal is averaged across all the regions comprising the global mask. Thus, in early amyloid deposition phases, when not all the included regions have already accumulated amyloid, the overall global signal may lie below the conventionally used thresholds, resulting in an amyloid-negative classification although considerable amyloid load may have already deposited in specific regions of the neocortex. However, using a fixed regional threshold for assigning regional amyloid-positivity regardless of differences in gray matter density and surface area between the different brain regions is a potential limitation of the described *in vivo* staging approach and an important methodological aspect to be further investigated. However, Grothe et al. conducted sensitivity analyses across the range of values between the two widely used cutoffs to confirm reproducibility of the amyloid deposition model in normal healthy individuals of the ADNI cohort across the entire range of amyloid cutoffs, suggesting relatively little inter-regional variability in noise levels in the PVE-corrected PET signal [7]. In contrast to the approach used by Grothe et al. [7], Cho et al. in their study determined regional amyloid-positivity using Z scores based on an older, globally negative, control population and a cutoff of Z score > 2.5 [6]. While the use of such region-specific thresholds may potentially account better for regionally differing noise levels, the definition of these thresholds will depend on the specific control cohort used, which limits the transferability of this approach and the generalization of the study results to other cohorts.

Conclusions

In conclusion, our results support the validity and reproducibility of the *in vivo* staging model of regionally progressing amyloidosis in an independent preclinical cohort at elevated risk for AD. Further evaluation of the staging approach in parallel with longitudinal multi-domain cognitive performance will be crucial for assessing its prognostic value for predicting cognitive decline along the course of the disease.

Additional files

Additional file 1: Figure S1. Schematic diagram summarizing the pre-processing pipeline. (PDF 276 kb)

Additional file 2: Figure S2. Regional amyloid positivity cutoff value estimation. The figure shows the linear regression plot of the Global 18F-florbetapir PET SUVRcereb of both non-corrected (X-axis) and PVE-corrected PET (Y-axis) along with the generated equation that was used to transform the regional cutoff value of SUVRcereb = 1.135 to a value of SUVRcereb = 0.98 in the PVE-corrected PET data. (PDF 190 kb)

Additional file 3: Figure S3. Model of the hierarchical in vivo amyloid staging scheme. This figure shows the 52 brain regions merged into four larger anatomical divisions based on equal partitions of frequency range as initially defined in the original model. Then the resulting amyloid progression stage (I-IV) is defined by the involvement of the corresponding anatomical division displayed in red in addition to the affected areas of the previous stage (displayed in blue). The amyloid progression stages are displayed on left, midline sagittal and basal brain views. (PDF 312 kb)

Additional file 4: Table S1. Principal component analysis applied on the neurocognitive test scores. The table shows the three main components that could be identified based on the principal component analysis and subsequently the contributing tests in each component. (PDF 97 kb)

Additional file 5: Table S2. Associations between in vivo amyloid stage and cognitive performance. Analysis of Covariance (ANCOVA) assessing the effect of amyloid stage and conventional binary amyloid status on scores of the main principal components as well as the most representative tests for each of these components. (PDF 240 kb)

Additional file 6: Figure S4. Amyloid progression model in the INSIGHT-preAD data. This figure shows the amyloid progression model in the INSIGHT-preAD data as implied by the frequency of involvement of the 52 studied brain regions. The frequencies were displayed on left, midline sagittal and basal brain views. (PDF 252 kb)

Abbreviations

AD: Alzheimer's disease; ADNI: Alzheimer's Disease Neuroimaging Initiative; ANCOVA: Analysis of covariance; ANOVA: Analysis of variance; ApoE, ApoE-ε4: Apolipoprotein E, ε4 allele; Aβ, Aβ42: β-Amyloid, β amyloid peptide 1–42; C¹¹ PiB: [¹¹C] Pittsburgh Compound B; CAA: Cerebral amyloid angiopathy; CERAD: Consortium to Establish a Registry for Alzheimer's disease; CN: Cognitively normal individuals; CSF: Cerebrospinal fluid; DVR: Distribution volume ratios; FCSRT: Free and Cued Selective Reminding Test; GM: Gray matter; MBT: Memory Binding Test; MCI: Individuals with mild cognitive impairment; MMSE: Mini-mental State Examination; MNI: Montreal Neurological Institute; PCA: Principal component analysis; PET: Positron emission tomography; PVE: Partial volume effects; SMC: Subjective memory complaints; SUVR: Standardized uptake value ratio; SUVRcereb: Standard uptake value ratios scaled by mean uptake value of the whole cerebellum; TMT: Trail Making Test; WM: White matter

Acknowledgements

INSIGHT-preAD study group: Hovagim Bakardjian, Habib Benali, Hugo Bertin, Joel Bonheur, Laurie Boukadida, Nadia Boukerrou, Enrica Cavedo, Patrizia Chiesa, Olivier Colliot, Bruno Dubois, Marion Dubois, Stéphane Epelbaum, Geoffroy Gagliardi, Remy Genthon, Marie-Odile Habert, Harald Hampel, Marion Houot, Aurélie Kas, Foudil Lamari, Marcel Levy, Simone Lista, Christiane Metzinger, Fanny Mochel, Francis Nyasse, Catherine Poisson, Marie-Claude Potier, Marie Revillon, Antonio Santos, Katia Santos Andrade, Marine Sole, Mohamed Surtee, Michel Thiebaud de Schotten, Andrea Vergallo, Nadja Younsi. INSIGHT-preAD Scientific Committee Members: Dubois B, Hampel H, Bakardjian H, Benali H, Colliot O, Habert Marie-O, Lamari F, Mochel F, Potier MC, Thiebaud de Schotten M. Contributors to the Alzheimer Precision Medicine Initiative Working Group (APMI-WG): Lisi Flores AGUILAR (Montréal), Claudio BABILONI (Rome), Filippo BALDACCI (Pisa), Norbert BENDA (Bonn), Keith L. BLACK (Los Angeles), Arun L.W. BOKDE (Dublin), Ubaldo BONUCCELLI (Pisa), Karl BROICH (Bonn), René S.

BUN (Paris), Francesco CACCIOLA (Siena), Juan CASTRILLO† (Derio), Enrica CAVEDO (Paris), Roberto CERAVOLO (Pisa), Patrizia A. CHIESA (Paris), Olivier COLLIOT (Paris), Cristina-Maria COMAN (Paris), Jean-Christophe CORVOL (Paris), Augusto Claudio CUELLO (Montréal), Jeffrey L. CUMMINGS (Las Vegas), Herman DEPYPERE (Gent), Bruno DUBOIS (Paris), Andrea DUGGENTO (Rome), Stanley DURRLEMAN (Paris), Valentina ESCOTT-PRICE (Cardiff), Howard FEDEROFF (Irvine), Maria Teresa FERRETTI (Zürich), Massimo FIANDACA (Irvine), Richard A. FRANK (Malvern), Francesco GARACI (Rome), Remy GENTHON (Paris), Nathalie GEORGE (Paris), Filippo S. GIORGI (Pisa), Manuela GRAZIANI (Roma), Marion HABERKAMP (Bonn), Marie-Odile HABERT (Paris), Harald HAMPPEL (Paris), Karl HERHOLZ (Manchester), Eric KARRAN (Cambridge), Seung H. KIM (Seoul), Yosef KORONYO (Los Angeles), Maya KORONYO-HAMAOUI (Los Angeles), Foudil LAMARI (Paris), Todd LANGEVIN (Minneapolis-Saint Paul), Stéphane LEHÉRICY (Paris), Simone LISTA (Paris), Jean LORENCEAU (Paris), Mark MAPSTONE (Irvine), Christian NERI (Paris), Robert NISTICÒ (Rome), Francis NYASSE-MESSENE (Paris), Sid E. O'BRYANT (Fort Worth), George PERRY (San Antonio), Craig RITCHIE (Edinburgh), Katrine ROJKOVA (Paris), Simone ROSSI (Siena), Amira SAIDI (Rome), Emiliano SANTARNECCHI (Siena), Lon S. SCHNEIDER (Los Angeles), Olaf SPORNS (Bloomington), Nicola TOSCHI (Rome), Steven R. VERDOONER (Sacramento), Andrea VERGALLO (Paris), Nicolas VILLAIN (Paris), Lindsay A. WELIKOVITCH (Montréal), Janet WOODCOCK (Silver Spring), Erfan YOUNESI (Esch-sur-Alzette).

Funding

The study was promoted by INSERM in collaboration with ICM, IHU-A-ICM and Pfizer and has received a support within the "Investissement d'Avenir" (ANR-10-AIHU-06). The study was promoted in collaboration with the "CHU de Bordeaux" (coordination CIC EC7), the promoter of Memento cohort, funded by the Foundation Plan-Alzheimer. The study was further supported by AVID/Lilly. We thank the DNA and Cell Bank from Pitié-Salpêtrière Hospital (Philippe Couarch and Sylvie Forlani).

This research publication benefited from the support of the Program "PHOENIX" led by the Sorbonne University Foundation and sponsored by la Fondation pour la Recherche sur Alzheimer.

HH is supported by the AXA Research Fund, the "Fondation partenariale Sorbonne Université" and the "Fondation pour la Recherche sur Alzheimer", Paris, France. This work was supported within the "Investissements d'avenir" ANR-10-AIHU-06. The research leading to these results has received funding from the program "Investissements d'avenir" ANR-10-AIHU-06 (Agence Nationale de la Recherche-10-IA Agence Institut Hospitalo-Universitaire-6) and 'Infrastructure d'avenir en Biologie Santé - ANR-11-INBS-0006'.

The study was supported by the Marie-Curie Innovative Training Network BBDiag (EU-Horizon2020 Project ID: 721281) as well.

Availability of data and materials

The data analyzed in the present study are not publicly available. However, the use of the INSIGHT-preAD data might be possible after approval of scientific project proposals by the Scientific Committee of INSIGHT-preAD study group.

Authors' contributions

FAS, MJG, and SJT contributed to the study concept, analysis and interpretation of data, and drafting/revising the manuscript for content. EC, BD, and HH contributed to the study concept, acquisition of data, and drafting/revising the manuscript for content. IJ, MD, and GG-E contributed to the analysis of data and contribution of analytic tools. KR, GF, LD, M-CP, HB, and MOH contributed to the acquisition of data and drafting a significant portion of the manuscript. All authors read and approved the final manuscript.

Ethics approval and consent to participate

The ethics committee of the Pitié-Salpêtrière University Hospital approved the study protocol. All participants signed an informed consent form, given and explained to them 2 weeks before enrolment.

Competing interests

The authors declare that they have no competing interests. HH serves as the Senior Associate Editor for the Journal Alzheimer's and Dementia; he received lecture fees from Biogen and Roche, research grants from Pfizer, Avid, and MSD Avenir (paid to the institution), travel funding from Functional Neuromodulation, Axovant, Eli Lilly and company, Takeda and Zinfandel, GE-

Healthcare and Oryzon Genomics, consultancy fees from Jung Diagnostics, Cytox Ltd., Axovant, Anavex, Takeda and Zinfandel, GE Healthcare, Oryzon Genomics, and Functional Neuromodulation, and participated in scientific advisory boards of Functional Neuromodulation, Axovant, Eli Lilly and company, Cytox Ltd., GE Healthcare, Takeda and Zinfandel, Oryzon Genomics and Roche Diagnostics.

HH is a co-inventor in the following patents as a scientific expert and has received no royalties:

- In Vitro Multi-parameter Determination Method for The Diagnosis and Early Diagnosis of Neurodegenerative Disorders Patent Number: 8916388.
- In Vitro Procedure for Diagnosis and Early Diagnosis of Neurodegenerative Diseases Patent Number: 8298784.
- Neurodegenerative Markers for Psychiatric Conditions Publication Number: 20120196300.
- In Vitro Multi-parameter Determination Method for The Diagnosis and Early Diagnosis of Neurodegenerative Disorders Publication Number: 20100062463.
- In Vitro Method for The Diagnosis and Early Diagnosis of Neurodegenerative Disorders Publication Number: 20100035286.
- In Vitro Procedure for Diagnosis and Early Diagnosis of Neurodegenerative Diseases Publication Number: 20090263822.
- In Vitro Method for The Diagnosis of Neurodegenerative Diseases Patent Number: 7547553.
- CSF Diagnostic in Vitro Method for Diagnosis of Dementias and Neuroinflammatory Diseases Publication Number: 20080206797.
- In Vitro Method for The Diagnosis of Neurodegenerative Diseases Publication Number: 20080199966.
- Neurodegenerative Markers for Psychiatric Conditions Publication Number: 20080131921.

Publisher's Note

Springer Nature remains neutral with regard to jurisdictional claims in published maps and institutional affiliations.

Author details

¹Department of Psychosomatic Medicine, Clinical Dementia Research, Faculty of Medicine, Rostock University, Rostock, Germany. ²German Center for Neurodegenerative Diseases (DZNE), Rostock, Germany. ³AXA Research Fund and Sorbonne University Chair, Paris, France. ⁴Sorbonne University, GRC n° 21, Alzheimer Precision Medicine (APM), AP-HP, Pitié-Salpêtrière Hospital, Boulevard de l'hôpital, F-75013 Paris, France. ⁵Brain and Spine Institute (ICM), INSERM U 1127, CNRS UMR 7225, Boulevard de l'hôpital, F-75013 Paris, France. ⁶Department of Neurology, Institute of Memory and Alzheimer's Disease (IM2A), Pitié-Salpêtrière Hospital, AP-HP, Boulevard de l'hôpital, F-75013 Paris, France. ⁷Qynapse, Paris, France. ⁸Sorbonne University, UPMC University Paris 06, CNRS, INSERM, Laboratoire d'Imagerie Biomédicale, F-75013 Paris, France. ⁹Multi-center Neuroimaging Platform <https://www.cati-neuroimaging.com>. ¹⁰Department of Nuclear Medicine, Pitié-Salpêtrière Hospital, AP-HP, F-75013 Paris, France. ¹¹Department of Neurology, University Medical Center of the Johannes-Gutenberg-University Mainz, Langenbeck str, 155131 Mainz, Germany. ¹²Centre de Neuroimagerie de Recherche (CENIR), Institut du Cerveau et de la Moelle Epiniere (ICM), Paris, France. ¹³Department of Neuroradiology, Salpêtrière Hospital, Paris, France.

Received: 21 July 2018 Accepted: 7 January 2019

Published online: 31 January 2019

References

1. Sabri O, Sabbagh MN, Seibyl J, Barthel H, Akatsu H, Ouchi Y, et al. Florbetaben PET imaging to detect amyloid beta plaques in Alzheimer's disease: phase 3 study. *Alzheimers Dement*. 2015;11(8):964–74.
2. Murray ME, Lowe VJ, Graff-Radford NR, Liesinger AM, Cannon A, Przybelski SA, et al. Clinicopathologic and 11C-Pittsburgh compound B implications of Thal amyloid phase across the Alzheimer's disease spectrum. *Brain*. 2015; 138(Pt 5):1370–81.
3. Ikonomic MD, Buckley CJ, Heurling K, Sherwin P, Jones PA, Zanette M, et al. Post-mortem histopathology underlying beta-amyloid PET imaging following flutemetamol F 18 injection. *Acta neuropathol commun*. 2016; 4(1):130.
4. Marcus C, Mena E, Subramaniam RM. Brain PET in the diagnosis of Alzheimer's disease. *Clin Nuclear Med*. 2014;39(10):e413–22 quiz e23–6.
5. Thal DR, Rub U, Orantes M, Braak H. Phases of A beta-deposition in the human brain and its relevance for the development of AD. *Neurology*. 2002;58(12):1791–800.
6. Cho H, Choi JY, Hwang MS, Kim YJ, Lee HM, Lee HS, et al. In vivo cortical spreading pattern of tau and amyloid in the Alzheimer disease spectrum. *Ann Neurol*. 2016;80(2):247–58.
7. Grothe MJ, Barthel H, Sepulcre J, Dyrba M, Sabri O, Teipel SJ. In vivo staging of regional amyloid deposition. *Neurology*. 2017;89(20):2031–8.
8. Mitchell AJ, Beaumont H, Ferguson D, Yagdarfar M, Stubbs B. Risk of dementia and mild cognitive impairment in older people with subjective memory complaints: meta-analysis. *Acta Psychiatr Scand*. 2014;130(6):439–51.
9. Dubois B, Hampel H, Feldman HH, Scheltens P, Aisen P, Andrieu S, et al. Preclinical Alzheimer's disease: definition, natural history, and diagnostic criteria. *Alzheimers Dement*. 2016;12(3):292–323.
10. Kaup AR, Nettiksimmons J, LeBlanc ES, Yaffe K. Memory complaints and risk of cognitive impairment after nearly 2 decades among older women. *Neurology*. 2015;85(21):1852–8.
11. Dubois B, Epelbaum S, Nyasse F, Bakardjian H, Gagliardi G, Uspenskaya O, et al. Cognitive and neuroimaging features and brain beta-amyloidosis in individuals at risk of Alzheimer's disease (INSIGHT-preAD): a longitudinal observational study. *Lancet Neurol*. 2018;17(4):335–46.
12. Clark CM, Pontecorvo MJ, Beach TG, Bedell BJ, Coleman RE, Doraiswamy PM, et al. Cerebral PET with florbetapir compared with neuropathology at autopsy for detection of neuritic amyloid-β plaques: a prospective cohort study. *Lancet Neurol*. 2012;11(8):669–78.
13. Joshi AD, Pontecorvo MJ, Clark CM, Carpenter AP, Jennings DL, Sadowsky CH, et al. Performance characteristics of amyloid PET with florbetapir F 18 in patients with Alzheimer's disease and cognitively normal subjects. *J Nucl Med*. 2012;53(3):378–84.
14. Folstein MF, Folstein SE, McHugh PR. "Mini-mental state". A practical method for grading the cognitive state of patients for the clinician. *J Psychiatr Res*. 1975;12(3):129–18.
15. Amieva H, Carcaillon L, Rouze L, Alzitz-Schuermans P, Millet X, Dartigues JF, Fabrigoule C. Cued and uncued memory tests: norms in elderly adults from the 3 cities epidemiological study. *Rev Neurol*. 2007;163(2):205–21.
16. Buschke H. Cued recall in amnesia. *J Clin Neuropsychol*. 1984;6(4):433–40.
17. Buschke H, Mowrey WB, Ramratan WS, Zimmerman ME, Loewenstein DA, Katz MJ, et al. Memory binding test distinguishes amnesic mild cognitive impairment and dementia from cognitively normal elderly. *Arch Clin Neuropsychol*. 2017;32(1):29–39.
18. Benton AL. Differential behavioral effects in frontal lobe disease. *Neuropsychologia*. 1968;6(1):53–60.
19. Cardebat D, Doyon B, Puel M, Goulet P, Joannet Y. Formal and semantic lexical evocation in normal subjects. Performance and dynamics of production as a function of sex, age and educational level. *Acta Neurol Belg*. 1990;90(4):207–17.
20. Shao Z, Janse E, Visser K, Meyer AS. What do verbal fluency tasks measure? Predictors of verbal fluency performance in older adults. *Front Psychol*. 2014;5:772.
21. Fastenau PS, Denburg NL, Hufford BJ. Adult norms for the Rey-Osterrieth Complex Figure Test and for supplemental recognition and matching trials from the Extended Complex Figure Test. *Clin Neuropsychol*. 1999; 13(1):30–47.
22. Wechsler D. WMS-III Wechsler memory scale-third edition. San Antonio: The Psychological Corporation; 1997.
23. Kessels RP, van den Berg E, Ruis C, Brands AM. The backward span of the Corsi Block-Tapping Task and its association with the WAIS-III Digit Span. *Assessment*. 2008;15(4):426–34.
24. Tombaugh TN. Trail Making Test A and B: normative data stratified by age and education. *Arch Clin Neuropsychol*. 2004;19(2):203–14.
25. Dubois B, Slachevsky A, Litvan I, Pillon B. The FAB: a Frontal Assessment Battery at bedside. *Neurology*. 2000;55(11):1621–6.
26. Habert M-O, Bertin H, Labit M, Diallo M, Marie S, Martineau K, et al. Evaluation of amyloid status in a cohort of elderly individuals with memory complaints: validation of the method of quantification and determination of positivity thresholds. *Ann Nucl Med*. 2018;32(2):75–86. <https://doi.org/10.1007/s12149-017-1221-0>.
27. Muller-Gartner HW, Links JM, Prince JL, Bryan RN, McVeigh E, Leal JP, et al. Measurement of radiotracer concentration in brain gray matter using positron emission tomography: MRI-based correction for partial volume effects. *J Cereb Blood Flow Metab*. 1992;12(4):571–83.

28. Desikan RS, Segonne F, Fischl B, Quinn BT, Dickerson BC, Blacker D, et al. An automated labeling system for subdividing the human cerebral cortex on MRI scans into gyral based regions of interest. *NeuroImage*. 2006;31(3):968–80.
29. Gonzalez-Escamilla G, Lange C, Teipel S, et al. PETPVE12: an SPM toolbox for partial volume effects correction in brain PET - application to amyloid imaging with AV45-PET. *NeuroImage*. 2017;147:8.
30. Klunk WE, Koeppe RA, Price JC, Benzinger TL, Devous MD Sr, Jagust WJ, et al. The Centiloid Project: standardizing quantitative amyloid plaque estimation by PET. *Alzheimers Dement*. 2015;11(1):1–15 e1–4.
31. Catafau AM, Bullich S, Seibyl JP, Barthel H, Ghetti B, Leverenz J, et al. Cerebellar amyloid-beta plaques: how frequent are they, and do they influence 18F-Florbetaben SUV ratios? *J Nucl Med*. 2016;57(11):1740–5.
32. Landau SM, Breault C, Joshi AD, Pontecorvo M, Mathis CA, Jagust WJ, et al. Amyloid- β imaging with Pittsburgh compound B and florbetapir: comparing radiotracers and quantification methods. *J Nuclear Med*. 2013;54(1):70–7.
33. Clark CM, Schneider JA, Bedell BJ, Beach TG, Bilker WB, Mintun MA, et al. Use of florbetapir-PET for imaging beta-amyloid pathology. *JAMA*. 2011;305(3):275–83.
34. Fleisher AS, Chen K, Liu X, Roontiva A, Thiyyagura P, Ayutyanont N, et al. Using positron emission tomography and florbetapir F18 to image cortical amyloid in patients with mild cognitive impairment or dementia due to Alzheimer disease. *Arch Neurol*. 2011;68(11):1404–11.
35. Thal DR, Beach TG, Zanette M, Heurling K, Chakrabarty A, Ismail A, et al. [18F]flutemetamol amyloid positron emission tomography in preclinical and symptomatic Alzheimer's disease: specific detection of advanced phases of amyloid- β pathology. *Alzheimers Dement*. 2015;11(8):975–85.
36. Salloway S, Gamez JE, Singh U, Sadowsky CH, Villena T, Sabbagh MN, et al. Performance of [(18F)flutemetamol amyloid imaging against the neuritic plaque component of CERAD and the current (2012) NIA-AA recommendations for the neuropathologic diagnosis of Alzheimer's disease. *Alzheimer's Dementia*. 2017;9:25–34.
37. Villeneuve S, Rabinovici GD, Cohn-Sheehy BI, Madison C, Ayakta N, Ghosh PM, et al. Existing Pittsburgh compound-B positron emission tomography thresholds are too high: statistical and pathological evaluation. *Brain*. 2015;138(Pt 7):2020–33.
38. Lemos R, Cunha C, Maroco J, Afonso A, Simoes MR, Santana I. Free and Cued Selective Reminding Test is superior to the Wechsler Memory Scale in discriminating mild cognitive impairment from Alzheimer's disease. *Geriatr Gerontol Int*. 2015;15(8):961–8.
39. Mowrey WB, Lipton RB, Katz MJ, Ramratan WS, Loewenstein DA, Zimmerman ME, et al. Memory binding test predicts incident amnesic mild cognitive impairment. *J Alzheimers Dis*. 2016;53(4):1585–95.
40. Papp KV, Rentz DM, Orlovsky I, Sperling RA, Mormino EC. Optimizing the preclinical Alzheimer's cognitive composite with semantic processing: the PACC5. *Alzheimers Dementia*. 2017;3(4):668–77.
41. Rentz DM, Parra Rodriguez MA, Amariglio R, Stern Y, Sperling R, Ferris S. Promising developments in neuropsychological approaches for the detection of preclinical Alzheimer's disease: a selective review. *Alzheimers Res Ther*. 2013;5(6):58.
42. Schindler SE, Jasielc MS, Weng H, Hassenstab JJ, Grober E, McCue LM, et al. Neuropsychological measures that detect early impairment and decline in preclinical Alzheimer disease. *Neurobiol Aging*. 2017;56:25–32.
43. Donohue MC, Sperling RA, Petersen R, Sun CK, Weiner MW, Aisen PS. Association between elevated brain amyloid and subsequent cognitive decline among cognitively normal persons. *JAMA*. 2017;317(22):2305–16.
44. Duke Han S, Nguyen CP, Stricker NH, Nation DA. Detectable neuropsychological differences in early preclinical Alzheimer's disease: a meta-analysis. *Neuropsychol Rev*. 2017;27(4):305–25.
45. Bilgel M, An Y, Lang A, Prince J, Ferrucci L, Jedynek B, et al. Trajectories of Alzheimer disease-related cognitive measures in a longitudinal sample. *Alzheimers Dementia*. 2014;10(6):735–42.e4.
46. Grober E, Hall CB, Lipton RB, Zonderman AB, Resnick SM, Kawas C. Memory impairment, executive dysfunction, and intellectual decline in preclinical Alzheimer's disease. *J Int Neuropsychol Soc*. 2008;14(2):266–78.
47. Langbaum JB, Hendrix S, Ayutyanont N, Bennett DA, Shah RC, Barnes LL, et al. Establishing composite cognitive endpoints for use in preclinical Alzheimer's disease trials. *J Prev Alzheimer's Dis*. 2015;2(1):2–3.
48. Amariglio RE, Becker JA, Carmasin J, Wadsworth LP, Lorus N, Sullivan C, et al. Subjective cognitive complaints and amyloid burden in cognitively normal older individuals. *Neuropsychologia*. 2012;50(12):2880–6.
49. Braak H, Braak E. Neuropathological staging of Alzheimer-related changes. *Acta Neuropathol*. 1991;82(4):239–59.
50. Charidimou A, Farid K, Tsai HH, Tsai LK, Yen RF, Baron JC. Amyloid-PET burden and regional distribution in cerebral amyloid angiopathy: a systematic review and meta-analysis of biomarker performance. *J Neurol Neurosurg Psychiatry*. 2018;89(4):410–7.
51. Tanskanen M, Makela M, Myllykangas L, Notkola IL, Polvikoski T, Sulkava R, et al. Prevalence and severity of cerebral amyloid angiopathy: a population-based study on very elderly Finns (Vantaa 85+). *Neuropathol Appl Neurobiol*. 2012;38(4):329–36.
52. Arenaza-Urquijo EM, Vemuri P. Resistance vs resilience to Alzheimer disease. *Clarifying Terminol Preclin Stud*. 2018;90(15):695–703.
53. Rogalski EJ, Gefen T, Shi J, Samimi M, Bigio E, Weintraub S, et al. Youthful memory capacity in old brains: anatomic and genetic clues from the Northwestern SuperAging Project. *J Cogn Neurosci*. 2013;25(1):29–36.
54. Donohue MC, Sperling RA, Petersen R, et al. Association between elevated brain amyloid and subsequent cognitive decline among cognitively normal persons. *JAMA*. 2017;317(22):2305–16.
55. Jagust WJ, Landau SM, Koeppe RA, Reiman EM, Chen K, Mathis CA, et al. The Alzheimer's Disease Neuroimaging Initiative 2 PET Core: 2015. *Alzheimer's Dementia*. 2015;11(7):757–71.
56. Rodrigue KM, Kennedy KM, Devous MD Sr, Rieck JR, Hebrank AC, Diaz-Arrastia R, et al. β -Amyloid burden in healthy aging: regional distribution and cognitive consequences. *Neurology*. 2012;78(6):387–95.
57. Mielke MM, Wiste HJ, Weigand SD, Knopman DS, Lowe VJ, Roberts RO, et al. Indicators of amyloid burden in a population-based study of cognitively normal elderly. *Neurology*. 2012;79(15):1570–7.
58. McNamee RL, Yee SH, Price JC, Klunk WE, Rosario B, Weissfeld L, et al. Consideration of optimal time window for Pittsburgh compound B PET summed uptake measurements. *J Nucl Med*. 2009;50(3):348–55.
59. Golla SS, Verfaillie SC, Boellaard R, Adriaanse SM, Zwan MD, Schuit RC, et al. Quantification of [18F]florbetapir: a test-retest tracer kinetic modelling study. *J Cereb Blood Flow Metab*. 2018;27:1678X18783628. <https://doi.org/10.1177/0271678X18783628>.
60. Ottoy J, Verhaeghe J, Niemantsverdriet E, Wyffels L, Somers C, De Roeck E, et al. Validation of the semiquantitative static SUVR method for (18F)-AV45 PET by pharmacokinetic modeling with an arterial input function. *J Nucl Med*. 2017;58(9):1483–9.
61. Thomas BA, Erlandsson K, Modat M, Thurfjell L, Vandenberghe R, Ourselin S, et al. The importance of appropriate partial volume correction for PET quantification in Alzheimer's disease. *Eur J Nucl Med Mol Imaging*. 2011;38(6):1104–19.
62. Su Y, Blazey TM, Snyder AZ, Raichle ME, Marcus DS, Ances BM, et al. Partial volume correction in quantitative amyloid imaging. *NeuroImage*. 2015;107:55–64.
63. Brendel M, Hogenauer M, Delker A, Sauerbeck J, Bartenstein P, Seibyl J, et al. Improved longitudinal [(18F)-AV45 amyloid PET by white matter reference and VOI-based partial volume effect correction. *NeuroImage*. 2015;108:450–9.
64. Matsubara K, Ibaraki M, Shimada H, Ikoma Y, Suhara T, Kinoshita T, et al. Impact of spillover from white matter by partial volume effect on quantification of amyloid deposition with [(11)C]PIB PET. *NeuroImage*. 2016;143:316–24.
65. Gonzalez-Escamilla G, Lange C, Teipel S, Buchert R, Grothe MJ. Alzheimer's disease neuroimaging I. PETPVE12: an SPM toolbox for partial volume effects correction in brain PET - application to amyloid imaging with AV45-PET. *NeuroImage*. 2017;147:669–77.
66. Rullmann M, Dukart J, Hoffmann KT, Luthardt J, Tiepolt S, Patt M, et al. Partial-volume effect correction improves quantitative analysis of 18F-Florbetaben beta-amyloid PET scans. *J Nucl Med*. 2016;57(2):198–203.

Ready to submit your research? Choose BMC and benefit from:

- fast, convenient online submission
- thorough peer review by experienced researchers in your field
- rapid publication on acceptance
- support for research data, including large and complex data types
- gold Open Access which fosters wider collaboration and increased citations
- maximum visibility for your research: over 100M website views per year

At BMC, research is always in progress.

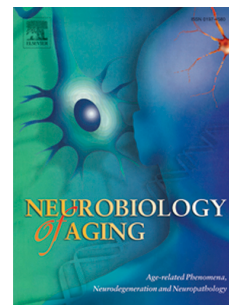
Learn more [biomedcentral.com/submissions](https://www.biomedcentral.com/submissions)



Journal Pre-proof

In-vivo staging of regional amyloid deposition predicts functional conversion in the preclinical and prodromal phases of Alzheimer's disease

Stefan J. Teipel, Martin Dyrba, Patrizia A. Chiesa, Fatemah Sakr, Irina Jelistratova, Simone Lista, Andrea Vergallo, Pablo Lemercier, Enrica Cavedo, Marie Odile Habert, Bruno Dubois, Harald Hampel, Michel J. Grothe, the INSIGHT-preAD study group and for the Alzheimer's Disease Neuroimaging Initiative



PII: S0197-4580(20)30090-7

DOI: <https://doi.org/10.1016/j.neurobiolaging.2020.03.011>

Reference: NBA 10804

To appear in: *Neurobiology of Aging*

Received Date: 13 September 2019

Revised Date: 10 March 2020

Accepted Date: 12 March 2020

Please cite this article as: Teipel, S.J., Dyrba, M., Chiesa, P.A., Sakr, F., Jelistratova, I., Lista, S., Vergallo, A., Lemercier, P., Cavedo, E., Habert, M.O., Dubois, B., Hampel, H., Grothe, M.J., the INSIGHT-preAD study group and for the Alzheimer's Disease Neuroimaging Initiative, In-vivo staging of regional amyloid deposition predicts functional conversion in the preclinical and prodromal phases of Alzheimer's disease, *Neurobiology of Aging* (2020), doi: <https://doi.org/10.1016/j.neurobiolaging.2020.03.011>.

This is a PDF file of an article that has undergone enhancements after acceptance, such as the addition of a cover page and metadata, and formatting for readability, but it is not yet the definitive version of record. This version will undergo additional copyediting, typesetting and review before it is published in its final form, but we are providing this version to give early visibility of the article. Please note that, during the production process, errors may be discovered which could affect the content, and all legal disclaimers that apply to the journal pertain.

© 2020 Published by Elsevier Inc.

CRedit author statement

Stefan Teipel: Conceptualization, Formal Analysis, Writing - Original Draft, Writing - Review & Editing

Martin Dyrba: Software, Formal Analysis, Data Curation, Visualization

Patrizia A. Chiesa: Resources, Data Curation, Writing - Original Draft

Fatemah Sakr: Writing - Original Draft, Writing - Review & Editing

Irina Jelistratova: Formal Analysis, Writing - Original Draft

Simone Lista: Resources, Writing - Original Draft, Investigation

Andrea Vergallo: Resources, Writing - Original Draft, Investigation

Pablo Lemercier: Formal Analysis, Software

Enrica Cavedo: Resources, Data Curation, Writing - Original Draft

Marie Odile Habert: Resources, Investigation, Writing - Original Draft

Bruno Dubois: Supervision, Investigation, Editing

Harald Hampel: Supervision, Editing

Michel J. Grothe: Conceptualization, Writing - Original Draft, Writing - Review & Editing

In-vivo staging of regional amyloid deposition predicts functional conversion in the preclinical and prodromal phases of Alzheimer's disease

Stefan J. Teipel^{1,2}, Martin Dyrba¹, Patrizia A. Chiesa^{3,4,5}, Fatemah Sakr², Irina Jelistratova¹, Simone Lista^{3,4,5}, Andrea Vergallo^{3,4,5}, Pablo Lemercier^{3,4,5}, Enrica Cavedo^{3,4,5,6}, Marie Odile Habert^{7,8,9}, Bruno Dubois⁵, Harald Hampel³, Michel J. Grothe¹; and the INSIGHT-preAD study group and for the Alzheimer's Disease Neuroimaging Initiative*

¹German Center for Neurodegenerative Diseases (DZNE), Rostock, Germany

²Department of Psychosomatic Medicine, University Medicine Rostock, Rostock, Germany

³ Sorbonne University, GRC n° 21, Alzheimer Precision Medicine (APM), AP-HP, Pitié-Salpêtrière Hospital, Boulevard de l'hôpital, F-75013, Paris, France; <https://www.apmiscience.com/>

⁴ Brain & Spine Institute (ICM), INSERM U 1127, CNRS UMR 7225, Boulevard de l'hôpital, F-75013, Paris, France

⁵ Institute of Memory and Alzheimer's Disease (IM2A), Department of Neurology, Pitié-Salpêtrière Hospital, AP-HP, Boulevard de l'hôpital, F-75013, Paris, France

⁶ Qynapse, Paris, France

⁷ Sorbonne University, CNRS, INSERM, Laboratoire d'Imagerie Biomédicale, LIB, F-75006, Paris, France

⁸ AP-HP, Pitié-Salpêtrière Hospital, Department of Nuclear Medicine, F-75013, Paris, France

⁹ Centre d'Acquisition et Traitement des Images (CATI platform), www.cati-neuroimaging.com

*Data used in preparation of this article were obtained from the Alzheimer's Disease Neuroimaging Initiative (ADNI) database (adni.loni.usc.edu/). As such, the investigators within the ADNI contributed to the design and implementation of ADNI and/or provided data but did not participate in analysis or writing of this report. A complete listing of ADNI investigators can be found at: http://adni.loni.usc.edu/wp-content/uploads/how_to_apply/ADNI_Acknowledgement_List.pdf

Running Title: Regional amyloid stages and conversion to MCI or dementia

Manuscript requirements:

Title:	140 spaces
Abstract:	164
Text:	4,277
References:	40
Tables:	2
Figures	4
Supplementary Figures	3

Corresponding Author:

Stefan J. Teipel, M.D.
Department of Psychosomatic Medicine
University Medicine Rostock,
and DZNE Rostock,
Gehlsheimer Str. 20,
18147 Rostock, Germany
Tel.: 01149-381-494-9470
Fax: 01149-381-494-9682
E-mail: stefan.teipel@med.uni-rostock.de

Journal Pre-proof

Abstract

We tested the usefulness of a regional amyloid staging based on amyloid sensitive Positron Emission Tomography (PET) to predict conversion to cognitive impairment and dementia in preclinical and prodromal Alzheimer's disease (AD). We analyzed 884 cases, including normal controls, and people with subjective cognitive decline or mild cognitive impairment (MCI), from the Alzheimer's Disease Neuroimaging Initiative (ADNI) with a maximum follow-up of 6 years and 318 cases with subjective memory complaints with a maximum follow-up time of three years from the INveStIGATION of AlzHeimer's PredicTors cohort (INSIGHT-preAD study). Cox regression showed a significant association of regional amyloid stages with time to conversion from a cognitively normal to a MCI, and from a MCI to a dementia status. The most advanced amyloid stages identified very high-risk groups of conversion. All results were robustly replicated across the independent samples. These findings indicate the usefulness of regional amyloid staging for identifying preclinical and prodromal AD cases at very high risk of conversion for future amyloid targeted trials.

Key words: amyloid; longitudinal study; dementia; MCI; subjective cognitive decline

Introduction

Cerebral amyloid deposition is considered an upstream event in the pathogenesis of Alzheimer's disease (AD) (Thal et al., 2006). In-vivo imaging using amyloid sensitive Positron Emission Tomography (PET) detected increased levels of amyloid in 15-30% of cognitively normal people older than 70 years, and in at least 50% of people with a clinical phenotype of amnesic mild cognitive impairment (MCI) (Quigley et al., 2010). However, the positive predictive value of increased amyloid signal in PET for subsequent cognitive decline in preclinical or prodromal AD cases is limited. In cognitively normal people, the positive predictive value of a positive amyloid PET status for subsequent conversion to MCI or dementia is only about 25% over 3 to 5 years of follow-up (Baker et al., 2017; Morris et al., 2009; Villemagne et al., 2011). In people with MCI, the positive predictive value of positive amyloid status for subsequent conversion to AD dementia is about 65% to 84% for a follow-up period of 3 to 5 years (Martinez et al., 2017; Zhang et al., 2014).

The current standard of amyloid PET imaging data analysis is a dichotomous classification in amyloid positive or amyloid negative cases (Klunk et al., 2015). Recently, we have developed a more fine grained (Grothe et al., 2017) and replicable (Sakr et al., 2019) PET-based in-vivo amyloid staging scheme that considers five regional stages of progressive cerebral amyloid deposition. The staging identified neurobiologically meaningful regional variation of amyloid deposition even in people with an amyloid negative status, as shown by associations of amyloid stages with cerebrospinal fluid (CSF) A β 1-42 concentrations and cognitive performance. An alternative tripartite staging approach has been based on differential involvement of cortical vs subcortical structures (amygdala, putamen, and caudate nucleus) (Cho et al., 2018). This previous study showed promising results for the predictive utility of amyloid staging but lacked a differentiation of cortical stages and a comparison with the standard binary classification.

Here, we evaluated the usefulness of regional amyloid staging to predict conversion of cognitively normal people with and without subjective cognitive decline (SCD) or subjective

memory complaints (SMC) to MCI or AD dementia and of MCI cases to AD dementia, respectively. We compared our results with classical binary amyloid classification. We studied replicability of effects in three different longitudinal samples: a sample from the Alzheimer's Disease Neuroimaging Initiative (ADNI) that had previously been used for establishing the regional amyloid staging approach (Grothe et al., 2017), a second sample from ADNI that was not part of the development of the staging scheme, and an independent cohort of SMC cases from the monocentric INveStIGation of AlzHeimer's PredicTors in subjective memory complainers (INSIGHT-preAD cohort) (Dubois et al., 2018). As endpoint we assessed functional conversion as defined by transition in clinical dementia rating scale (CDR) scores (Berg, 1988).

Material and Methods

Data source

Data used in the preparation of this article were obtained from two independent cohorts. The first cohort contained data from the ADNI database (<http://adni.loni.usc.edu/>). The ADNI was launched in 2003 by the National Institute on Aging, the National Institute of Biomedical Imaging and Bioengineering, the Food and Drug Administration, private pharmaceutical companies and non-profit organizations, with the primary goal of testing whether neuroimaging, neuropsychologic, and other biologic measurements can be used as reliable in-vivo markers of AD pathogenesis. A fuller description of ADNI and up-to-date information is available at www.adni-info.org. The second cohort was taken from the INSIGHT-preAD study (Dubois et al., 2018). The INSIGHT-preAD study is a monocentric university based cohort derived from the Institute for Memory and Alzheimer's Disease (IM2A) at the Pitié-Salpêtrière University Hospital in Paris, France, that aims to investigate the earliest preclinical stages of AD and its development including influencing factors and markers of progression.

Study participants

From the ADNI cohort, we retrieved two different samples: first, a sample of 582 cases that was previously used to establish the regional amyloid staging approach (Grothe et al., 2017), henceforth termed ADNI-A sample, and second an independent sample of 302 cases that had not been part of the previous analysis, henceforth termed ADNI-B sample. Both samples provided amyloid PET data at baseline as well as longitudinal clinical follow-up using cognitive testing over a maximum interval of 6 years. ADNI-A included data of 179 cognitively normal elderly subjects, and 403 subjects with MCI. Mean follow-up time was 3.3 (SD 1.8) years. ADNI-B included data of 75 cognitively normal older subjects, 103 subjects with SCD, and 124 subjects with MCI. Mean follow-up time was 3.2 (SD 1.8) years. Detailed inclusion criteria for the diagnostic categories can be found at the ADNI web site (<http://adni.loni.usc.edu/methods/>).

The INSIGHT-preAD study included 318 cognitively normal Caucasian individuals from the Paris area at baseline, between 70-85 years old, with subjective memory complaints and with defined brain amyloid status.(Dubois et al., 2018) The study aims at a total of 7-years of annual follow-up, with the first three years follow-up being available for the current analysis; the mean follow-up time was 2.7 (SD 0.8) years. Details on participants' demographics for the three samples are shown in Table 1.

All procedures performed in the ADNI studies and The INSIGHT-preAD study involving human participants were in accordance with the ethical standards of the institutional research committees and with the 1975 Helsinki declaration and its later amendments. Written informed consent was obtained from all participants and/or authorized representatives and the study partners before any protocol-specific procedures were carried out in the ADNI or INSIGHT-preAD studies, respectively.

Cognitive tests

Both ADNI and INSIGHT-preAD cohorts underwent comprehensive neuropsychological examinations at least every 12 months. The MMSE (Folstein et al., 1975) was available for both cohorts to assess global cognition. We used the CDR score (Berg, 1988) as primary endpoint to assess change in functional status.

Imaging data acquisition

Detailed acquisition and standardized pre-processing steps of ADNI imaging data are available at the ADNI website (<https://adni.loni.usc.edu/methods/>). Amyloid-PET data was collected during a 50- to 70-minute interval following a 370 MBq bolus injection of 18F-Florbetapir. To account for the multicentric acquisition of the data across different scanners and sites, all PET scans undergo standardized pre-processing steps within ADNI.

The methods and results for the PET data acquisition in the INSIGHT-preAD cohort have been detailed in a previous paper (Habert et al., 2017). All amyloid PET scans were acquired in a single session on a Philips Gemini GXL CT-PET scanner 50 (\pm 5) minutes after

the injection of approximately 370 MBq (333-407 MBq) of 18F-Florbetapir (AVID radiopharmaceuticals).

For anatomical reference and pre-processing of the PET scans we used the corresponding structural MRI scan that was closest in time to the Florbetapir PET scan. In the ADNI-A sample MRI data were acquired on multiple 3T MRI scanners using scanner-specific T1-weighted sagittal 3D MPRAGE sequences. The ADNI-B sample additionally included 1.5 T MRI scans from 155 cases. Similar to the PET data, MRI scans undergo standardized preprocessing steps aimed at increasing data uniformity across the multicenter scanner platforms (see <https://adni.loni.usc.edu/methods/> for detailed information on multicentric MRI acquisition and preprocessing in ADNI). MRI scans for INSIGHT-preAD were acquired on a Siemens Verio 3T scanner at Pitié-Salpêtrière Hospital, Paris. A T1 weighted image was acquired using a fast three dimensional gradient echo pulse sequence using a magnetization preparation pulse (Turbo FLASH) (Habert et al., 2017).

Imaging data pre-processing

Images were preprocessed using Statistical Parametric Mapping software version 8 (SPM8) (The Wellcome Trust Centre for Neuroimaging, Institute of Neurology, University College London) implemented in Matlab 2013. The pre-processing pipeline followed the routine previously described in (Grothe et al., 2017). First, each subject's averaged PET frames were co-registered to their corresponding T1-weighted MRI scan. Then, partial volume effects (PVE) were corrected in native space using the 3-compartmental voxel-based post-reconstruction method as described by Müller-Gärtner and colleagues (Gonzalez-Escamilla et al., 2017; Müller-Gärtner et al., 1992). The corrected PET images were spatially normalized to an aging/AD-specific reference template using the deformation parameters derived from the normalization of their corresponding MRI.

The regional 18F-Florbetapir-PET mean uptake values were estimated for 52 brain regions defined by the Harvard–Oxford structural atlas (Desikan et al., 2006), including both cortical and subcortical regions (<https://fsl.fmrib.ox.ac.uk/fsl/fslwiki/Atlases>). Standard uptake

value ratios ($SUVR_{Cer}$) were computed for the 52 brain regions by dividing the mean uptake values by the mean uptake value of the whole cerebellum as estimated in non-PVE-corrected PET data (Catafau et al., 2016; Gonzalez-Escamilla et al., 2017; Grothe et al., 2017; Klunk et al., 2015).

In accordance with the methods used for the published PET-based amyloid staging approach, we based the cutoff used for determining regional amyloid positivity on a cutoff value of $SUVR_{Cer} = 1.135$ (Grothe et al., 2017), which lies in between the two most widely used global signal cutoffs for non-PVE-corrected 18F-Florbetapir-PET SUVRs, i.e. $SUVR_{Cer} = 1.10$ (Clark et al., 2012; Joshi et al., 2012; Landau et al., 2013) and $SUVR_{Cer} = 1.17$ (Clark et al., 2011a; Clark et al., 2011b; Fleisher et al., 2011). This threshold was converted to the PVE-corrected PET data used for the regional staging approach using linear regression between PVE-corrected and non-corrected global $SUVR_{Cer}$ values, which resulted in a value of $SUVR_{Cer} = 0.92$ in the ADNI cohort (Grothe et al., 2017) and of $SUVR_{Cer} = 0.98$ in the INSIGHT-preAD cohort (Sakr et al., 2019).

PET data analysis

Staging of regional amyloid deposition followed the previously developed 4-stage model of amyloid pathology progression derived from 18F-Florbetapir-PET data of cognitively normal older individuals enrolled in the ADNI study (Grothe et al., 2017). This 4-stage model was estimated by counting the frequency of amyloid positivity across the 52 brain regions defined in the Harvard–Oxford structural atlas and then merging the regions into four broader anatomical divisions based on equal proportions of the observed range of involvement frequencies. The four anatomical divisions defining the staging scheme are illustrated in Figure 1.

According to this staging approach (Grothe et al., 2017), an anatomical division was considered positive for amyloid pathology if at least 50% of the regions included in this division exceeded the cutoff value in the respective participant. Subsequently, participants were classified as stage I if only the first division was considered positive. Then, the

successive stages II-IV were defined by the additional involvement of their corresponding divisions II, III, and IV, respectively. Participants who exhibited amyloid positivity in any division without concurrent amyloid positivity in the preceding divisions were classified as non-stageable (mismatch).

For comparison, we also studied conventional classifications of 18F-Florbetapir-PET scans into global amyloid-positive or amyloid-negative categories. For the ADNI data this classification was derived using centrally calculated global composite $SUVR_{Cer}$ values that are made available on the ADNI server (Jagust Lab, UC Berkley; adni.loni.usc.edu/methods/pet-analysis). Originally, amyloid-positivity was defined using a cutoff of $SUVR_{Cer} > 1.17$ (Clark et al., 2011b; Fleisher et al., 2011). The even more widely recommended cutoff of $SUVR_{Cer} > 1.1$ (Clark et al., 2012; Joshi et al., 2012; Landau et al., 2013) yielded inferior results for the prediction accuracy so that we decided to use the better performing cutoff for the reference test of global amyloid status. For the INSIGHT-preAD data the classification was based on centrally calculated global composite values published by the INSIGHT-preAD PET core, and amyloid-positivity was defined using a recommended cutoff of 0.88 for this data, which resulted from a conversion of the above mentioned cutoff of $SUVR_{Cer} > 1.1$ to the specific processing pipeline used by the INSIGHT-preAD PET core (Habert et al., 2018). A lower cut-off of $SUVR > 0.79$ that was also published by the INSIGHT-preAD PET core yielded lower prediction performance in our analyses so that again we decided to use the better performing cutoff for the reference test.

Statistical analysis

We predicted time to conversion in CDR status (from 0 to 0.5 or higher, and from 0.5 to 1 or higher, respectively) using Cox regression with regional amyloid stages, age, and sex as predictors taking censoring into account. For comparison, we replaced regional amyloid stages by binary amyloid status in the model. This analysis was conducted using the R library “survival” with the command “coxph” for Cox regression. We compared overall model fit as estimated from Akaike information criterion (AIC) between Cox regression models based on staging vs. models based on global amyloid load. We selected the AIC as fit index as it penalizes the use of a higher number of parameters, hence discourages overfitting (Burnham and Anderson, 2004). In addition, we conducted survival curve analysis with regional amyloid stages as predictor, adjusted for average age and sex distribution within each stratum. For comparison, we replaced regional amyloid stages by binary amyloid status in the curve fitting. This analysis used the R library “survminer” with the command “survfit” for survival curve plotting. Analyses were performed with RStudio, version 1.1.463, a user interface of R Project for Statistical Computing Analyses. The libraries used are available at <http://cran.r-project.org/web/packages>.

Results

Staging

Across the 1,202 cases we found 17 cases (1.4%) that were non-stageable, i.e. whose regional amyloid distribution violated the regional staging scheme depicted in Figure 1. The distribution of non-stageable cases across cohorts and diagnoses is shown in Table 1. The subsequent analyses exclude these non-stageable cases.

The following results report hazard ratios (HR) and 95% confidence intervals relative to stage 0 for the amyloid stages and relative to the amyloid negative cases for the binary classification based on global amyloid.

ADNI-A sample

For prediction of CDR conversion in the cognitively normal controls, HR relative to stage 0 was 4.4 (95% confidence interval 1.7 to 11.6) for stage II and 4.8 (1.7 – 13.8) for stage IV, but there was no significant effect for stages I and III. For binary amyloid the hazard ratio was 3.1 (1.4 – 6.6) relative to amyloid negative cases (see Table 2 for details). Correspondingly, the stage IV cases had 50% conversion compared with 35% conversion for global amyloid increase.

For prediction of CDR conversion in the MCI cases, we found significant effects for amyloid stage III with a HR of 7.0 (3.3 – 14.7), and stage IV with a HR of 9.6 (4.7 – 19.5). The prediction by global amyloid ($SUVR_{Cer} > 1.17$) was significant as well with a HR of 7.7 (4.1 – 14.4) (see Table 2 for details). Risk enrichment was strongest in the stage IV cases with 47% conversion compared with 38% for global amyloid increase (Figure 2). Both for controls and MCI cases, the lower cutoff for global amyloid of $SUVR_{Cer} > 1.1$ yielded inferior results.

ADNI-B sample

For prediction of CDR conversion results were similar to those in the ADNI-A sample. In the MCI cases, hazard ratio was 18.0 (2.3 – 142.4) for stage III, and 27.1 (3.4- 216.2) for stage IV, but there was no significant effect for stages I and II. For binary amyloid the hazard

ratio was 23.5 (3.1 – 175.3) (see Table 2 for details). The stage III cases had 55% conversion and the stage IV cases 52% conversion, compared with 45% conversion for global amyloid increase (Figure 3).

Only two cases of the cognitively normal controls were amyloid stage IV, so that we pooled amyloid stages III and IV (henceforth stage III/IV). For the cognitively normal controls, the hazard ratio was 4.1 (1.3 – 13.3) for stage II, and 8.7 (2.9 – 26.2) for stage III/IV. For binary amyloid the hazard ratio was 6.2 (2.5 -15.6) (see Table 2 for details). The stage II cases had 55% conversion, and the stage III/IV cases 77%, compared with 65% conversion for global amyloid increase.

For the cases with SCD, the hazard ratio was 4.9 (1.4 – 17.3) for stage IV, but there was no significant effect for stages I through III. For binary amyloid the hazard ratio was not significant (see Table 2 for details). The stage IV cases had 56% conversion, compared with 32% conversion for global amyloid increase.

Insight-preAD sample

For the INSIGHT-preAD SMC cases only four cases were amyloid stage IV at baseline, so that we pooled amyloid stages III and IV (henceforth stage III/IV).

For prediction of CDR conversion in the INSIGHT-preAD SMC cases, we found significant effects for amyloid stage III/IV with a HR of 5.5 (1.8 – 15.2). The prediction by global amyloid ($SUVR_{Cer} > 0.88$) was significant as well with a HR of 3.2 (1.2 – 7.7) (see Table 2 for details). The lower cut-off for global amyloid of $SUVR_{Cer} > 0.79$ yielded inferior results. Risk enrichment was strongest in the stage III/IV cases with 22% conversion compared with 14% for global amyloid increase (Figure 4).

Model fit

As reported in Table 2, for all except one comparison the staging based models had lower AIC than the global amyloid load based model so that the staging based models would be preferred. The probability for the global amyloid model to provide a better fit than the

staging model was below 0.002 for the ADNI-A controls and the ADNI-B MCI and SCD cases, and below 0.3 for the ADNI-A MCI cases and the INSIGHT-preAD SMC cases. Only for the ADNI-B controls was the fit as measured by AIC better for the binary than the stage model.

Journal Pre-proof

Discussion

We found a significant association of regional amyloid stages and global amyloid status with time to conversion from a functionally healthy status to mild functional impairment and from mild functional impairment to dementia, respectively. These findings were widely consistent across the three independent samples.

The association of global amyloid status with change in functional status agrees with previous studies using amyloid sensitive PiB-PET as summarized in a meta-analysis covering controls and MCI cases (Chen et al., 2014) and replicated in subsequent studies on MCI cases (Frings et al., 2018; Iaccarino et al., 2017). Similar results were reported for amyloid sensitive ^{18}F tracers in MCI (Schreiber et al., 2015), with limited evidence for predicting conversion of healthy controls to MCI using ^{18}F tracers. Here, we used change in functional status as outcome, i.e. from CDR score 0 to CDR score ≥ 0.5 , and from CDR score 0.5 to CDR score ≥ 1 . The global CDR score provides a commonly defined operationalized standard for functional assessment with high reliability across different cohorts (Schafer et al., 2004) and raters (Burke et al., 1988). Also, the CDR is being used as primary or secondary outcome in ongoing clinical trials on AD. Diagnosis of MCI and dementia is closely linked with functional assessment using the CDR score (Woolf et al., 2016).

From a clinical perspective, the most interesting finding is the added value of regional amyloid stages over global amyloid status to identify a subsample of people with a very high risk of conversion. Thus, amyloid stage IV MCI cases had a 47% rate of conversion to dementia compared with 38% of the global amyloid-positive MCI cases in the ADNI-A sample, and in the INSIGHT-preAD cohort, 22% of the stage III/IV individuals with SMC converted to CDR 0.5 or higher compared with only 14% in the global amyloid-positive cases. The effects were similar in the ADNI-B MCI sample. Assessment of the model fit using AIC as fit criterion that penalizes for the higher number of parameters (Burnham and Anderson, 2004) with the amyloid staging compared to the binary global amyloid status supports the notion that the staging model would be preferred over the binary model in

almost all cohorts and diagnostic subgroups except for the ADNI-B controls. In consequence, regional amyloid staging would allow identifying a high risk group of preclinical or prodromal cases for future amyloid targeted treatment studies. This would require a larger screening effort as for example only 7% of controls and 23% of MCI cases in the ADNI-A sample were in amyloid stage IV, compared with 23% global amyloid-positive controls and 49% global amyloid-positive MCI cases. However, a larger effort in screening is less costly than including people with a low risk of conversion. For example, at an initial conversion rate of 47% for stage IV MCI cases, one would need 429 cases to detect a 20% reduction of conversion rate at a level of significance of 5% with 80% power. However, at an initial conversion rate of 38% for global amyloid-positive MCI, this number would increase to 607 cases.¹

In an alternative approach, global amyloid SUVR has been classified according to tertiles, where MCI cases in the highest tertile of global SUVR values had the highest hazard ratio for conversion (HR 9.4) (Jun et al., 2019), similar to the hazard ratios of the regional stage III and IV MCI cases in our ADNI-A and ADNI-B samples. Both approaches are similarly easy to apply. However, the usefulness of the tertile staging scheme for predicting functional decline in cognitively healthy people and SMC cases has not been assessed so far. Another approach used an a priori distinction between neocortical and striatal amyloid deposition to define three stages based on (i) overall low amyloid, (ii) high cortical but low striatal amyloid, and (iii) high cortical and high striatal amyloid load (Hanseeuw et al., 2018). They found a significant association of these stages with rates of cognitive decline, with striatum amyloid load adding to the cortical amyloid load alone. We further extend this previous evidence for significant risk enrichment in advanced stages of amyloid progression by assessing the stage-specific risk of functional conversion and comparing it to more fine-grained stages of differential cortical involvement as well as to standard global amyloid status. Also a recent staging scheme based on frequency of longitudinal regional

¹ Using the formula from Chow, S., Shao, J., Wang, H., 2008. *Sample Size Calculations in Clinical Research*, 2nd ed. Chapman & Hall/., page 89, implemented in <http://powerandsamplesize.com/Calculators/Compare-2-Proportions/2-Sample-Equality> (last access 8/2019)

involvement showed higher rates of cognitive decline with more advanced amyloid stages (Mattsson et al., 2019), but did not assess prediction of functional conversion. One can assume that stratification of global amyloid not only in two but in a higher number of classes will lead to more precise prediction of functional conversion as well. This is comparable to a top down approach, where driven by the precision of prediction, a range of global thresholds would be defined. Here, we used a bottom-up approach with regional staging that was motivated by the notion of a consistent distribution of amyloid across cortical regions and compared its ability to predict functional conversion with the current standard of binarized global amyloid levels. For both ADNI and INSIGHT-.preAD the more lenient cut-off yielded consistently lower performance so that we only reported the analysis results for the higher cut-off. In clinical practice, however, often not binarized amyloid levels are being used but expert visual reads of PET scans. A comparison with this clinical standard, however, was beyond the scope of the current study. One potential disadvantage of the method is the occurrence of mismatch cases that do not fit with the staging scheme. In the current analysis only 17 of 1,202 cases did not match the regional staging scheme.

Our study presents some caveats. First, even when using regional amyloid stages, prediction accuracy falls short of a useful biomarker for individual counselling. Rather, regional amyloid stages seem useful as marker for risk enrichment of study samples at a group level. The use of regional amyloid stages to predict an individual's cognitive decline will likely need combination with markers of tau pathology, such as CSF p-tau concentration or Tau PET, or markers of neuronal degeneration, such as FDG PET or MRI volumetry. Secondly, the numbers of MCI and SMC cases in stages III and IV are substantial across the three cohorts, but for controls numbers are small so that inference for the controls is based on a small number of conversion events. However, the consistency of findings across the independent cohorts lends some credibility to the results. Thirdly, we want to point out that we want to avoid the impression that the current data on the amyloid stages somehow prove a regional spread of amyloid through the brain. It is an intriguing observation that the large majority of cases with higher stage positive regions have also lower stages positive regions,

but not the other way round, with only 17 of 1,202 cases deviating from this pattern. This does, however, not prove a longitudinal spread of amyloid through the brain but would only conceptually fit to such assumption. Fourthly, on a methodological note, here we used a constant threshold for determining regional amyloid positivity as previously defined (Grothe et al., 2017). As an alternative approach, one could define region-specific cutoffs that may better account for regionally differing noise levels and signal confounds in the amyloid-PET data. For example, subcortical nuclei such as the striatum that are entirely embedded in the white matter may be differentially affected by spill-in effects from the typically high non-specific white matter signal compared with neocortical areas (Matsubara et al., 2016). We partially addressed this confound by using a 3-compartmental PVE correction method (Gonzalez-Escamilla et al., 2017), but this technique would not account for intrinsic differences in regional noise levels, such as signal confounds from traversing white matter bundles within the striatum itself. We work in parallel on a region-specific threshold approach but decided to use the constant threshold approach here, as it provided robust findings across two different cohorts in our previous analyses (Grothe et al., 2017; Sakr et al., 2019) and may be more easily applicable in future routine use. Still, a comparison of predictive accuracy of regional staging using constant vs. region-specific thresholds is currently lacking.

In summary, we found that regional amyloid stages led to identify a high-risk group of controls, SMC and MCI cases for subsequent functional decline. This finding may be useful for future clinical trials on amyloid targeted interventions to enrich the risk of conversion. Future studies are needed to explicitly model a direct vs. an indirect effect of amyloid stages on cognitive decline via supposedly downstream markers such as regional hypometabolism or atrophy.

Acknowledgment

ADNI cohort

Data collection and sharing for this project was funded by the Alzheimer's Disease Neuroimaging Initiative (ADNI) (National Institutes of Health Grant U01 AG024904) and DOD ADNI (Department of Defense award number W81XWH-12-2-0012). ADNI is funded by the National Institute on Aging, the National Institute of Biomedical Imaging and Bioengineering, and through generous contributions from the following: Alzheimer's Association; Alzheimer's Drug Discovery Foundation; Araclon Biotech; BioClinica, Inc.; Biogen Idec Inc.; Bristol-Myers Squibb Company; Eisai Inc.; Elan Pharmaceuticals, Inc.; Eli Lilly and Company; EuroImmun; F. Hoffmann-La Roche Ltd and its affiliated company Genentech, Inc.; Fujirebio; GE Healthcare; IXICO Ltd.; Janssen Alzheimer Immunotherapy Research & Development, LLC.; Johnson & Johnson Pharmaceutical Research & Development LLC.; Medpace, Inc.; Merck & Co., Inc.; Meso Scale Diagnostics, LLC.; NeuroRx Research; Neurotrack Technologies; Novartis Pharmaceuticals Corporation; Pfizer Inc.; Piramal Imaging; Servier; Synarc Inc.; and Takeda Pharmaceutical Company. The Canadian Institutes of Health Research is providing funds to support ADNI clinical sites in Canada. Private sector contributions are facilitated by the Foundation for the National Institutes of Health (www.fnih.org). The grantee organization is the Northern California Institute for Research and Education, and the study is coordinated by the Alzheimer's Disease Cooperative Study at the University of California, San Diego. ADNI data are disseminated by the Laboratory for Neuro Imaging at the University of Southern California.

INSIGHT-preAD cohort

This research benefited from the support of the Program "**PHOENIX**" led by the Sorbonne University Foundation and sponsored by la *Fondation pour la Recherche sur Alzheimer*.

The study was promoted by INSERM in collaboration with ICM, IHU-A-ICM and Pfizer and has received support within the "Investissement d'Avenir" (ANR-10-AIHU-06) French program. The study was promoted in collaboration with the "CHU de Bordeaux" (coordination

CIC EC7), the promoter of Memento cohort, funded by the Foundation Plan-Alzheimer. The study was further supported by AVID/Lilly.

CATI is a French neuroimaging platform funded by the French Plan Alzheimer (available at <http://cati-neuroimaging.com>).

INSIGHT-preAD Study Group:

Hovagim Bakardjian, Habib Benali, Hugo Bertin, Joel Bonheur, Laurie Boukadida, Nadia Boukerrou, Enrica Cavedo, Patrizia A. Chiesa, Olivier Colliot, Bruno Dubois, Marion Dubois, Stéphane Epelbaum, Geoffroy Gagliardi, Remy Genthon, Marie-Odile Habert, Harald Hampel, Marion Houot, Aurélie Kas, Foudil Lamari, Marcel Levy, Simone Lista, Christiane Metzinger, Fanny Mochel, Francis Nyasse, Catherine Poisson, Marie-Claude Potier, Marie Revillon, Antonio Santos, Katia Santos Andrade, Marine Sole, Mohmed Surtee, Michel Thiebaut de Schotten, Andrea Vergallo, Nadjia Younsi.

DISCLOSURES

SJT participated in scientific advisory boards of Roche Pharma AG and MSD, and received lecture fees from Roche and MSD.

HH is an employee of Eisai Inc. and serves as Senior Associate Editor for the Journal Alzheimer's & Dementia; he received lecture fees from Servier, Biogen and Roche, research grants from Pfizer, Avid, and MSD Avenir (paid to the institution), travel funding from Functional Neuromodulation, Axovant, Eli Lilly and company, Takeda and Zinfandel, GE-Healthcare and Oryzon Genomics, consultancy fees from Qynapse, Jung Diagnostics, Cytox Ltd., Axovant, Anavex, Takeda and Zinfandel, GE Healthcare and Oryzon Genomics, and Functional Neuromodulation, and participated in scientific advisory boards of Functional Neuromodulation, Axovant, Eisai, Eli Lilly and company, Cytox Ltd., GE Healthcare, Takeda and Zinfandel, Oryzon Genomics and Roche Diagnostics.

HH is co-inventor in the following patents as a scientific expert and has received no royalties:

- *In Vitro* Multiparameter Determination Method for The Diagnosis and Early Diagnosis of Neurodegenerative Disorders Patent Number: 8916388
- *In Vitro* Procedure for Diagnosis and Early Diagnosis of Neurodegenerative Diseases Patent Number: 8298784
- Neurodegenerative Markers for Psychiatric Conditions Publication Number: 20120196300
- *In Vitro* Multiparameter Determination Method for The Diagnosis and Early Diagnosis of Neurodegenerative Disorders Publication Number: 20100062463
- *In Vitro* Method for The Diagnosis and Early Diagnosis of Neurodegenerative Disorders Publication Number: 20100035286
- *In Vitro* Procedure for Diagnosis and Early Diagnosis of Neurodegenerative Diseases Publication Number: 20090263822
- *In Vitro* Method for The Diagnosis of Neurodegenerative Diseases Patent Number: 7547553
- CSF Diagnostic *In Vitro* Method for Diagnosis of Dementias and Neuroinflammatory Diseases Publication Number: 20080206797

- *In Vitro* Method for The Diagnosis of Neurodegenerative Diseases Publication Number: 20080199966

- Neurodegenerative Markers for Psychiatric Conditions Publication Number: 20080131921

MJG, FS, EC, PAC, IJ and **PL** declare no conflict of interest

MOH received consultant fees from Blue Earth, and honoraria from Lilly, PIRAMAL and GE as a speaker.

SL received lecture honoraria from Roche and Servier.

AV received lecture honoraria from Meg-Q, Roche, and Servier.

BD received consultant fees from Lilly, Boehringer Ingelheim and has received grants from Roche for his institution.

References:

- Baker, J.E., Lim, Y.Y., Pietrzak, R.H., Hassenstab, J., Snyder, P.J., Masters, C.L., Maruff, P., 2017. Cognitive impairment and decline in cognitively normal older adults with high amyloid-beta: A meta-analysis. *Alzheimer's & dementia : diagnosis, assessment & disease monitoring* 6, 108-121.
- Berg, L., 1988. Clinical Dementia Rating (CDR). *Psychopharmacol. Bull.* 24(4), 637-639.
- Burke, W.J., Miller, J.P., Rubin, E.H., Morris, J.C., Coben, L.A., Duchek, J., Wittels, I.G., Berg, L., 1988. Reliability of the Washington University Clinical Dementia Rating. *Arch Neurol* 45(1), 31-32.
- Burnham, K.P., Anderson, D.R., 2004. Multimodel inference - understanding AIC and BIC in model selection. *Sociol Method Res* 33(2), 261-304.
- Catafau, A.M., Bullich, S., Seibyl, J.P., Barthel, H., Ghetti, B., Leverenz, J., Ironside, J.W., Schulz-Schaeffer, W.J., Hoffmann, A., Sabri, O., 2016. Cerebellar Amyloid-beta Plaques: How Frequent Are They, and Do They Influence 18F-Florbetaben SUV Ratios? *J Nucl Med* 57(11), 1740-1745.
- Chen, X., Li, M., Wang, S., Zhu, H., Xiong, Y., Liu, X., 2014. Pittsburgh compound B retention and progression of cognitive status--a meta-analysis. *Eur J Neurol* 21(8), 1060-1067.
- Cho, S.H., Shin, J.H., Jang, H., Park, S., Kim, H.J., Kim, S.E., Kim, S.J., Kim, Y., Lee, J.S., Na, D.L., Lockhart, S.N., Rabinovici, G.D., Seong, J.K., Seo, S.W., 2018. Amyloid involvement in subcortical regions predicts cognitive decline. *European journal of nuclear medicine and molecular imaging* 45(13), 2368-2376.
- Chow, S., Shao, J., Wang, H., 2008. *Sample Size Calculations in Clinical Research*, 2nd ed. Chapman & Hall/.
- Clark, C.M., Pontecorvo, M.J., Beach, T.G., Bedell, B.J., Coleman, R.E., Doraiswamy, P.M., Fleisher, A.S., Reiman, E.M., Sabbagh, M.N., Sadowsky, C.H., Schneider, J.A., Arora, A., Carpenter, A.P., Flitter, M.L., Joshi, A.D., Krautkramer, M.J., Lu, M., Mintun, M.A.,

Skovronsky, D.M., Group, A.-A.S., 2012. Cerebral PET with florbetapir compared with neuropathology at autopsy for detection of neuritic amyloid-beta plaques: a prospective cohort study. *Lancet neurology* 11(8), 669-678.

Clark, C.M., Schneider, J.A., Bedell, B.J., Beach, T.G., Bilker, W.B., Mintun, M.A., Pontecorvo, M.J., Hefti, F., Carpenter, A.P., Flitter, M.L., Krautkramer, M.J., Kung, H.F., Coleman, R.E., Doraiswamy, P.M., Fleisher, A.S., Sabbagh, M.N., Sadowsky, C.H., Reiman, E.P., Zehntner, S.P., Skovronsky, D.M., 2011a. Use of florbetapir-PET for imaging beta-amyloid pathology. *Jama* 305(3), 275-283.

Clark, C.M., Schneider, J.A., Bedell, B.J., Beach, T.G., Bilker, W.B., Mintun, M.A., Pontecorvo, M.J., Hefti, F., Carpenter, A.P., Flitter, M.L., Krautkramer, M.J., Kung, H.F., Coleman, R.E., Doraiswamy, P.M., Fleisher, A.S., Sabbagh, M.N., Sadowsky, C.H., Reiman, E.P., Zehntner, S.P., Skovronsky, D.M., Group, A.A.S., 2011b. Use of florbetapir-PET for imaging beta-amyloid pathology. *JAMA* 305(3), 275-283.

Desikan, R.S., Segonne, F., Fischl, B., Quinn, B.T., Dickerson, B.C., Blacker, D., Buckner, R.L., Dale, A.M., Maguire, R.P., Hyman, B.T., Albert, M.S., Killiany, R.J., 2006. An automated labeling system for subdividing the human cerebral cortex on MRI scans into gyral based regions of interest. *NeuroImage* 31(3), 968-980.

Dubois, B., Epelbaum, S., Nyasse, F., Bakardjian, H., Gagliardi, G., Uspenskaya, O., Houot, M., Lista, S., Cacciamani, F., Potier, M.C., Bertrand, A., Lamari, F., Benali, H., Mangin, J.F., Colliot, O., Genthon, R., Habert, M.O., Hampel, H., group, I.N.-p.s., 2018. Cognitive and neuroimaging features and brain beta-amyloidosis in individuals at risk of Alzheimer's disease (INSIGHT-preAD): a longitudinal observational study. *Lancet neurology* 17(4), 335-346.

Fleisher, A.S., Chen, K., Liu, X., Roontiva, A., Thiyyagura, P., Ayutyanont, N., Joshi, A.D., Clark, C.M., Mintun, M.A., Pontecorvo, M.J., Doraiswamy, P.M., Johnson, K.A., Skovronsky, D.M., Reiman, E.M., 2011. Using positron emission tomography and florbetapir F18 to image cortical amyloid in patients with mild cognitive impairment or dementia due to Alzheimer disease. *Arch Neurol* 68(11), 1404-1411.

Folstein, M.F., Folstein, S.E., McHugh, P.R., 1975. Mini-mental-state: a practical method for grading the cognitive state of patients for the clinician. *J. Psychiatr. Res.* 12, 189-198.

Frings, L., Hellwig, S., Bormann, T., Spehl, T.S., Buchert, R., Meyer, P.T., 2018. Amyloid load but not regional glucose metabolism predicts conversion to Alzheimer's dementia in a memory clinic population. *European journal of nuclear medicine and molecular imaging* 45(8), 1442-1448.

Gonzalez-Escamilla, G., Lange, C., Teipel, S., Buchert, R., Grothe, M.J., Alzheimer's Disease Neuroimaging, I., 2017. PETPVE12: an SPM toolbox for Partial Volume Effects correction in brain PET - Application to amyloid imaging with AV45-PET. *NeuroImage* 147, 669-677.

Grothe, M.J., Barthel, H., Sepulcre, J., Dyrba, M., Sabri, O., Teipel, S.J., Alzheimer's Disease Neuroimaging, I., 2017. In vivo staging of regional amyloid deposition. *Neurology* 89(20), 2031-2038.

Habert, M.O., Bertin, H., Labit, M., Diallo, M., Marie, S., Martineau, K., Kas, A., Causse-Lemercier, V., Bakardjian, H., Epelbaum, S., Chetelat, G., Houot, M., Hampel, H., Dubois, B., Mangin, J.F., group, I.-A.s., 2017. Evaluation of amyloid status in a cohort of elderly individuals with memory complaints: validation of the method of quantification and determination of positivity thresholds. *Ann Nucl Med*.

Habert, M.O., Bertin, H., Labit, M., Diallo, M., Marie, S., Martineau, K., Kas, A., Causse-Lemercier, V., Bakardjian, H., Epelbaum, S., Chetelat, G., Houot, M., Hampel, H., Dubois, B., Mangin, J.F., group, I.-A.s., 2018. Evaluation of amyloid status in a cohort of elderly individuals with memory complaints: validation of the method of quantification and determination of positivity thresholds. *Ann Nucl Med* 32(2), 75-86.

Hanseeuw, B.J., Betensky, R.A., Mormino, E.C., Schultz, A.P., Sepulcre, J., Becker, J.A., Jacobs, H.I.L., Buckley, R.F., LaPoint, M.R., Vannini, P., Donovan, N.J., Chhatwal, J.P., Marshall, G.A., Papp, K.V., Amariglio, R.E., Rentz, D.M., Sperling, R.A., Johnson, K.A.,

Alzheimer's Disease Neuroimaging, I., Harvard Aging Brain, S., 2018. PET staging of amyloidosis using striatum. *Alzheimers Dement* 14(10), 1281-1292.

Iaccarino, L., Chiotis, K., Alongi, P., Almkvist, O., Wall, A., Cerami, C., Bettinardi, V., Gianolli, L., Nordberg, A., Perani, D., 2017. A Cross-Validation of FDG- and Amyloid-PET Biomarkers in Mild Cognitive Impairment for the Risk Prediction to Dementia due to Alzheimer's Disease in a Clinical Setting. *J Alzheimers Dis* 59(2), 603-614.

Joshi, A.D., Pontecorvo, M.J., Clark, C.M., Carpenter, A.P., Jennings, D.L., Sadowsky, C.H., Adler, L.P., Kovnat, K.D., Seibyl, J.P., Arora, A., Saha, K., Burns, J.D., Lowrey, M.J., Mintun, M.A., Skovronsky, D.M., Florbetapir, F.S.I., 2012. Performance characteristics of amyloid PET with florbetapir F 18 in patients with alzheimer's disease and cognitively normal subjects. *J Nucl Med* 53(3), 378-384.

Jun, S., Kim, H., Kim, B.S., Yoo, B.G., Lee, W.G., Alzheimer's Disease Neuroimaging, I., 2019. Quantitative Brain Amyloid Measures Predict Time-to-Progression from Amnesic Mild Cognitive Impairment to Alzheimer's Disease. *J Alzheimers Dis*.

Klunk, W.E., Koeppe, R.A., Price, J.C., Benzinger, T.L., Devous, M.D., Sr., Jagust, W.J., Johnson, K.A., Mathis, C.A., Minhas, D., Pontecorvo, M.J., Rowe, C.C., Skovronsky, D.M., Mintun, M.A., 2015. The Centiloid Project: standardizing quantitative amyloid plaque estimation by PET. *Alzheimers Dement* 11(1), 1-15 e11-14.

Landau, S.M., Breault, C., Joshi, A.D., Pontecorvo, M., Mathis, C.A., Jagust, W.J., Mintun, M.A., Alzheimer's Disease Neuroimaging, I., 2013. Amyloid-beta imaging with Pittsburgh compound B and florbetapir: comparing radiotracers and quantification methods. *J Nucl Med* 54(1), 70-77.

Martinez, G., Vernooij, R.W., Fuentes Padilla, P., Zamora, J., Flicker, L., Bonfill Cosp, X., 2017. 18F PET with florbetaben for the early diagnosis of Alzheimer's disease dementia and other dementias in people with mild cognitive impairment (MCI). *Cochrane Database Syst Rev* 11, CD012883.

Matsubara, K., Ibaraki, M., Shimada, H., Ikoma, Y., Suhara, T., Kinoshita, T., Ito, H., 2016. Impact of spillover from white matter by partial volume effect on quantification of amyloid deposition with [(11)C]PiB PET. *NeuroImage* 143, 316-324.

Mattsson, N., Palmqvist, S., Stomrud, E., Vogel, J., Hansson, O., 2019. Staging beta-Amyloid Pathology With Amyloid Positron Emission Tomography. *JAMA Neurol.*

Morris, J.C., Roe, C.M., Grant, E.A., Head, D., Storandt, M., Goate, A.M., Fagan, A.M., Holtzman, D.M., Mintun, M.A., 2009. Pittsburgh compound B imaging and prediction of progression from cognitive normality to symptomatic Alzheimer disease. *Arch Neurol* 66(12), 1469-1475.

Müller-Gärtner, H.W., Links, J.M., Prince, J.L., Bryan, R.N., McVeigh, E., Leal, J.P., Davatzikos, C., Frost, J.J., 1992. Measurement of radiotracer concentration in brain gray matter using positron emission tomography: MRI-based correction for partial volume effects. *Journal of Cerebral Blood Flow and Metabolism* 12, 571-583.

Quigley, H., Colloby, S.J., O'Brien, J.T., 2010. PET imaging of brain amyloid in dementia: a review. *Int J Geriatr Psychiatry.*

Risacher, S.L., Kim, S., Nho, K., Foroud, T., Shen, L., Petersen, R.C., Jack, C.R., Jr., Beckett, L.A., Aisen, P.S., Koeppe, R.A., Jagust, W.J., Shaw, L.M., Trojanowski, J.Q., Weiner, M.W., Saykin, A.J., Alzheimer's Disease Neuroimaging, I., 2015. APOE effect on Alzheimer's disease biomarkers in older adults with significant memory concern. *Alzheimers Dement* 11(12), 1417-1429.

Sakr, F.A., Grothe, M.J., Cavado, E., Jelistratova, I., Habert, M.O., Dyrba, M., Gonzalez-Escamilla, G., Bertin, H., Locatelli, M., Lehericy, S., Teipel, S., Dubois, B., Hampel, H., for the, I.-p.s.g., Alzheimer Precision Medicine, I., 2019. Applicability of in vivo staging of regional amyloid burden in a cognitively normal cohort with subjective memory complaints: the INSIGHT-preAD study. *Alzheimers Res Ther* 11(1), 15.

Schafer, K.A., Tractenberg, R.E., Sano, M., Mackell, J.A., Thomas, R.G., Gamst, A., Thal, L.J., Morris, J.C., Alzheimer's Disease Cooperative, S., 2004. Reliability of monitoring

the clinical dementia rating in multicenter clinical trials. *Alzheimer disease and associated disorders* 18(4), 219-222.

Schreiber, S., Landau, S.M., Fero, A., Schreiber, F., Jagust, W.J., Alzheimer's Disease Neuroimaging, I., 2015. Comparison of Visual and Quantitative Florbetapir F 18 Positron Emission Tomography Analysis in Predicting Mild Cognitive Impairment Outcomes. *JAMA Neurol* 72(10), 1183-1190.

Thal, D.R., Capetillo-Zarate, E., Del Tredici, K., Braak, H., 2006. The development of amyloid beta protein deposits in the aged brain. *Sci Aging Knowledge Environ* 2006(6), re1.

Villemagne, V.L., Pike, K.E., Chetelat, G., Ellis, K.A., Mulligan, R.S., Bourgeat, P., Ackermann, U., Jones, G., Szoeki, C., Salvado, O., Martins, R., O'Keefe, G., Mathis, C.A., Klunk, W.E., Ames, D., Masters, C.L., Rowe, C.C., 2011. Longitudinal assessment of Abeta and cognition in aging and Alzheimer disease. *Annals of neurology* 69(1), 181-192.

Wolf, C., Slavin, M.J., Draper, B., Thomassen, F., Kochan, N.A., Reppermund, S., Crawford, J.D., Trollor, J.N., Brodaty, H., Sachdev, P.S., 2016. Can the Clinical Dementia Rating Scale Identify Mild Cognitive Impairment and Predict Cognitive and Functional Decline? *Dementia and geriatric cognitive disorders* 41(5-6), 292-302.

Zhang, S., Smailagic, N., Hyde, C., Noel-Storr, A.H., Takwoingi, Y., McShane, R., Feng, J., 2014. (11)C-PIB-PET for the early diagnosis of Alzheimer's disease dementia and other dementias in people with mild cognitive impairment (MCI). *Cochrane Database Syst Rev*(7), CD010386.

Table 1: Participant's demographics

	m/f	Age (SD) [years]	MMSE (SD)	non stage- able	Median follow- up [months] (interquartile range)
<i>ADNI-A</i>					
Controls	88/91	73.8 (6.5)	29.1 (1.2)	3 (1.7%)	65 (54; 68)
MCI	220/183	71.8 (7.6)	28.1 (1.7)	4 (0.7%)	47 (43; 51)
<i>ADNI-B</i>					
Controls	36/39	79.2 (5.2)	29.2 (1.3)	1 (1.3%)	64 (60; 71)
MCI	79/45	75.4 (8.1)	27.8 (1.8)	3 (2.4%)	52 (49; 56)
SCD	42/61	72.4 (5.6)	29.0 (1.2)	4 (3.9%)	51 (38; 59)
<i>INSIGHT-preAD</i>					
SMC	114/204	76.5 (3.5)	28.7 (1.0)	2 (0.6%)	Non estimable ¹

SCD – subjective cognitive decline according to the definition in the ADNI cohort (Risacher et al., 2015)

SMC - subjective memory complaints as defined in the INSIGHT-preAD cohort (Dubois et al., 2018)

¹The proportion of censoring in the reversed survival plot with censored data assigned as events did not reach the median value during the available observation time

Table 2: Results of Cox regression models

Cohort	Group	Amyloid-Status	Number of cases	HR (SE)	p	AIC	median time to conversion [months]
ADNI-A	Controls	0	95	-	-	237	n.r.
		I	27	< 0.1	n.s.		n.r.
		II	15	4.4 (0.49)	< 0.003		70
		III	20	1.8 (0.60)	n.s.		n.r.
		IV	12	4.8 (0.54)	< 0.004		66
		A-	132	-	-		n.r.
	MCI	A+	40	3.1 (0.40)	< 0.004	260**	70
			0	136			n.r.
		I	34	0.7 (1.1)	n.s.	70	
		II	44	1.6 (0.59)	n.s.	n.r.	
		III	75	7.0 (0.38)	< 0.0001	66	
		IV	85	9.6 (0.36)	<0.0001	790	55
		A-	194	-	-	n.r.	
		A+	183	7.7 (0.32)	< 0.0001	794 [§]	63
ADNI-B	Controls	0	37	-	-	173	n.r.
		I	9	1.3 (0.82)	n.s.		n.r.
		II	11	4.1 (0.60)	< 0.02		37
		III/IV	13	8.7 (0.56)	< 0.0002		35
	MCI	A-	48	-	-	170	n.r.
			A+	23	6.2 (0.47)		< 0.0001
		0	39	-	-	n.r.	
		I	11	< 0.1	n.s.	n.r.	

Cohort	Group	Amyloid-Status	Number of cases	HR (SE)	p	AIC	median time to conversion [months]
		II	14	6.0 (1.2)	n.s.	173	63
		III	20	18.0 (1.06)	< 0.007		36
		IV	21	27.1 (1.06)	< 0.002		36
		A-	50	-	-	186*	n.r.
		A+	58	23.5 (1.03)	< 0.003		63
	SCD	0	49	-	-	176	n.r.
		I	14	0.9 (0.81)	n.s.		n.r.
		II	11	1.1 (0.86)	n.s.		n.r.
		III	13	3.2 (0.62)	n.s.		n.r.
		IV	9	4.9 (0.64)	< 0.02		50
		A-	62	-	-		n.r.
		A+	37	1.9 (0.43)	n.s.	193*	n.r.
INSIGHT-preAD	SMC	0	162	-	-	211	n.r.
		I	78	1.0 (0.64)	n.s.		n.r.
		II	40	0.48 (1.1)	n.s.		n.r.
		III/IV	36	5.5 (0.52)	< 0.002		n.r.
		A-	255	-	-	214 ^{\$\$}	n.r.
		A+	63	3.2 (0.45)	< 0.02		n.r.

- HR - Hazard ratio with standard error (SE) from cox regression models, including age and sex as covariates
- SCD - subjective cognitive decline according to the definition in the ADNI cohort (Risacher et al., 2015)
- SMC - subjective memory complaints as defined in the INSIGHT-preAD cohort (Dubois et al., 2018)
- I – IV - amyloid stages
- A+ - amyloid positive according to global threshold
- * - Probability $p < 0.002$ that the binary model minimizes AIC compared with the staging model
- ** - Probability $p < 0.0001$ that the binary model minimizes AIC compared with the staging model
- \$ - Probability $p = 0.13$ that the binary model minimizes AIC compared with the staging model
- \$\$ - Probability $p = 0.22$ that the binary model minimizes AIC compared with the staging model
- n.r. - not reached

Figure legends**Figure 1: Regional amyloid stages**

Stages I to IV of nested regional amyloid accumulation, according to the previously established staging approach (Grothe et al., 2017). Adapted with permission from the previous publication (Grothe et al., 2017).

Figure 2: Survival curves for amyloid in the ADNI-A sample, adjusted for age and sex

Survival curves comparing time-to-conversion of amyloid stages strata (Figure 2a) vs. global amyloid load (Figure 2b) in the ADNI-A MCI sample. Curves were adjusted for the average age and sex distribution within each amyloid stratum.

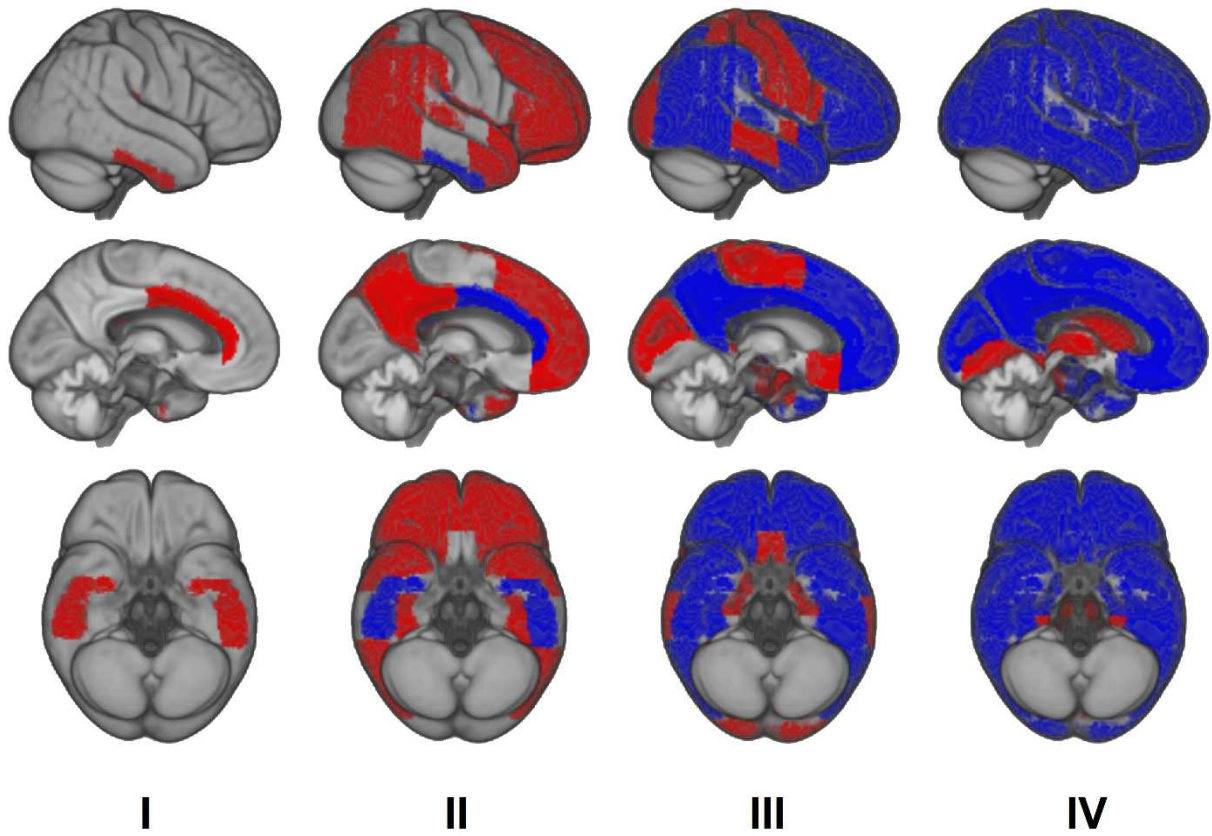
Figure 3: Survival curves for amyloid in the ADNI-B sample, adjusted for age and sex

Cumulative survival of CDR conversion endpoint vs. censoring comparing amyloid stages (Figure 3a) vs. global amyloid load (Figure 3b) in the ADNI-B MCI sample. Curves were adjusted for the average age and sex distribution within each amyloid stratum.

Figure 4: Survival curves for amyloid in the INSIGHT-preAD sample, adjusted for age and sex

Cumulative survival of CDR conversion endpoint vs. censoring comparing amyloid stages (Figure 4a) vs. global amyloid load (Figure 4b) in the INSIGHT-preAD sample. Curves were adjusted for the average age and sex distribution within each amyloid stratum.

Figure 1: Regional Amyloid Stages



Journal

Figure 2: Survival curves for amyloid in the ADNI-A sample, adjusted for age and sex

Figure 2a) Amyloid stages – ADNI-A MCI sample

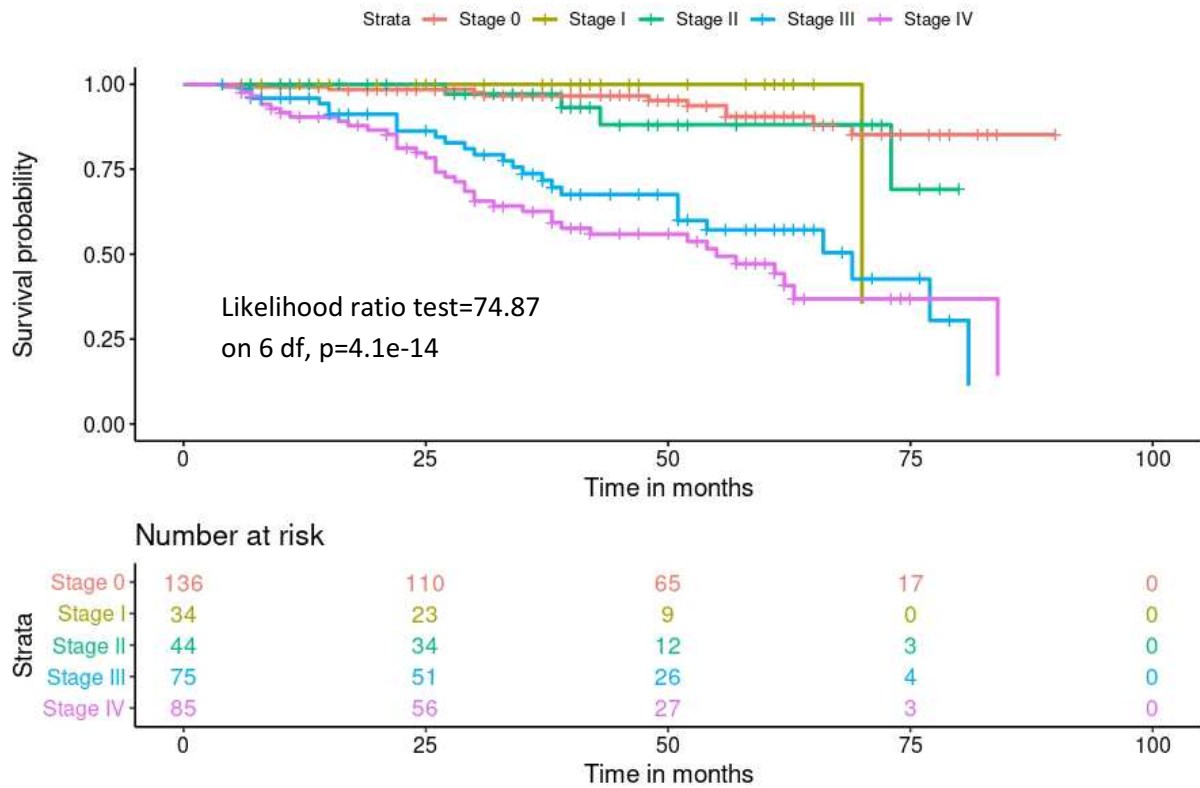


Figure 2b) SUVR binary – ADNI-A MCI sample

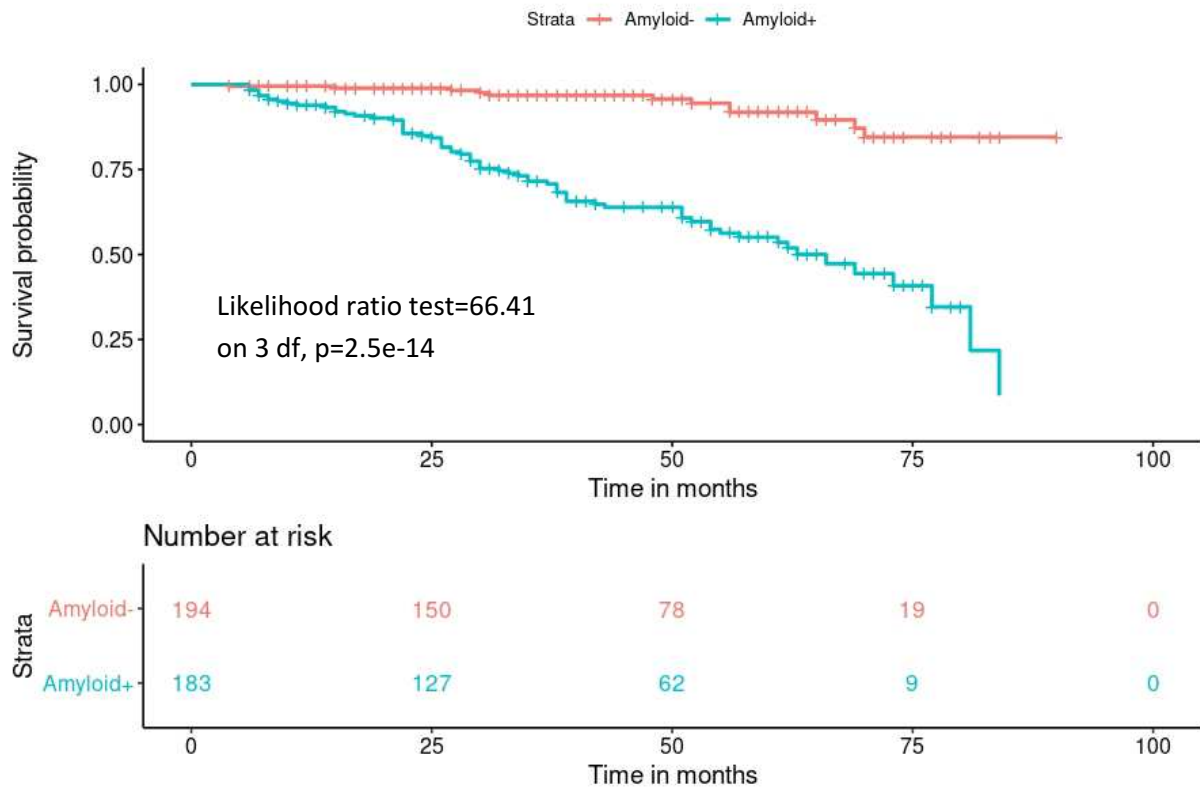


Figure 3: Survival curves for amyloid in the ADNI-B sample, adjusted for age and sex

Figure 3a) Amyloid stages – ADNI-B MCI sample

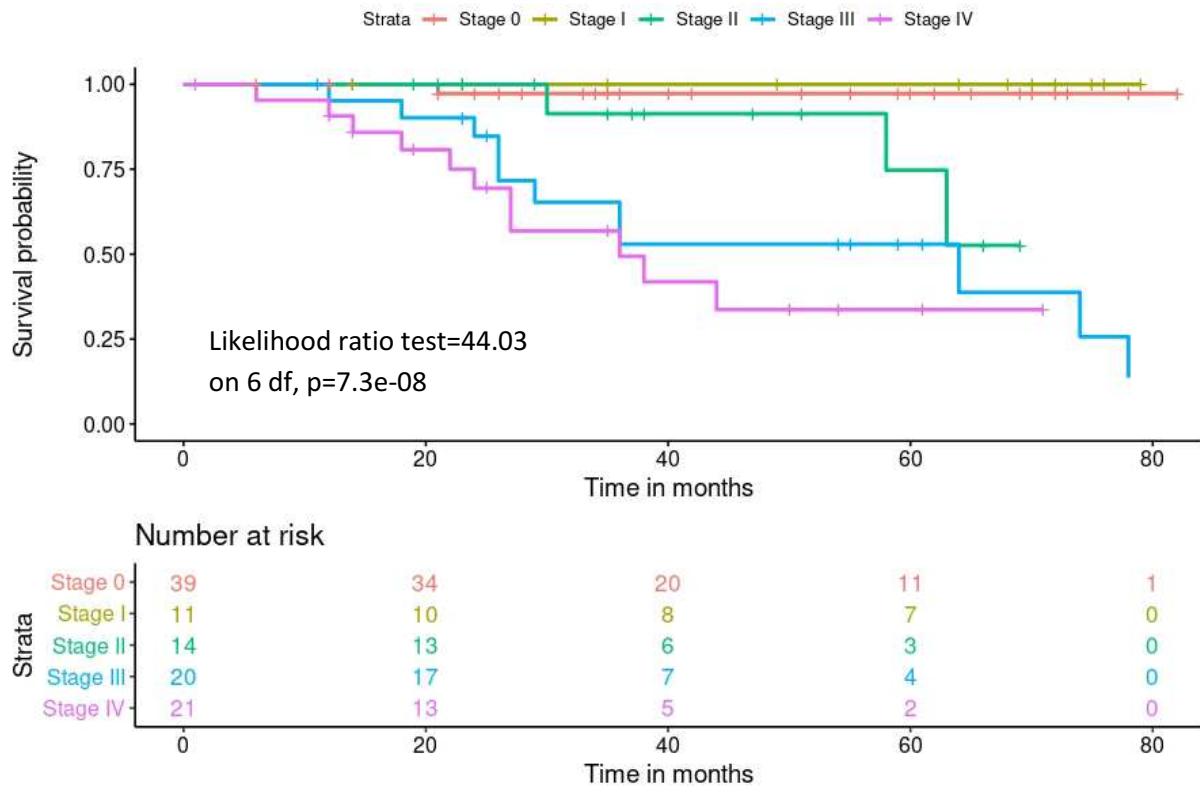


Figure 3b) SUVR binary – ADNI-B MCI sample

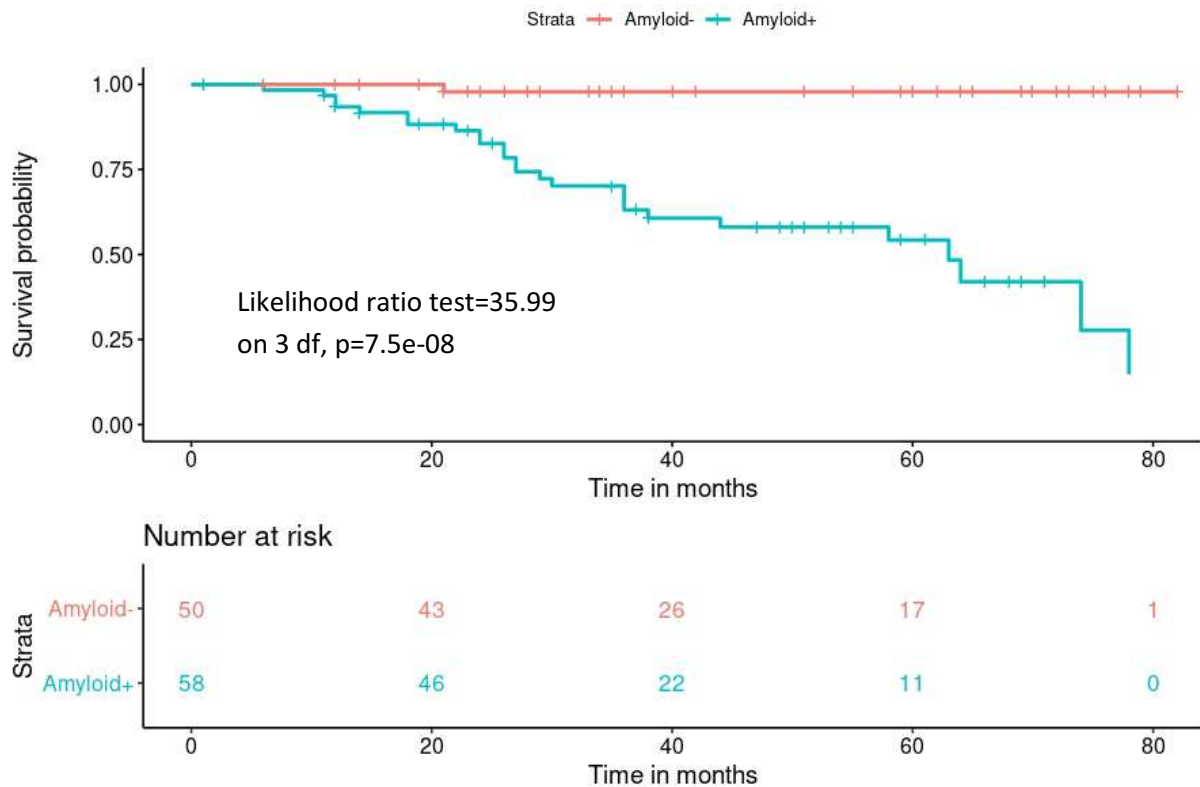


Figure 4: Survival curves for amyloid in the INSIGHT-preAD cohort, adjusted for age and sex

Figure 4a) Amyloid stages – INSIGHT-preAD cohort

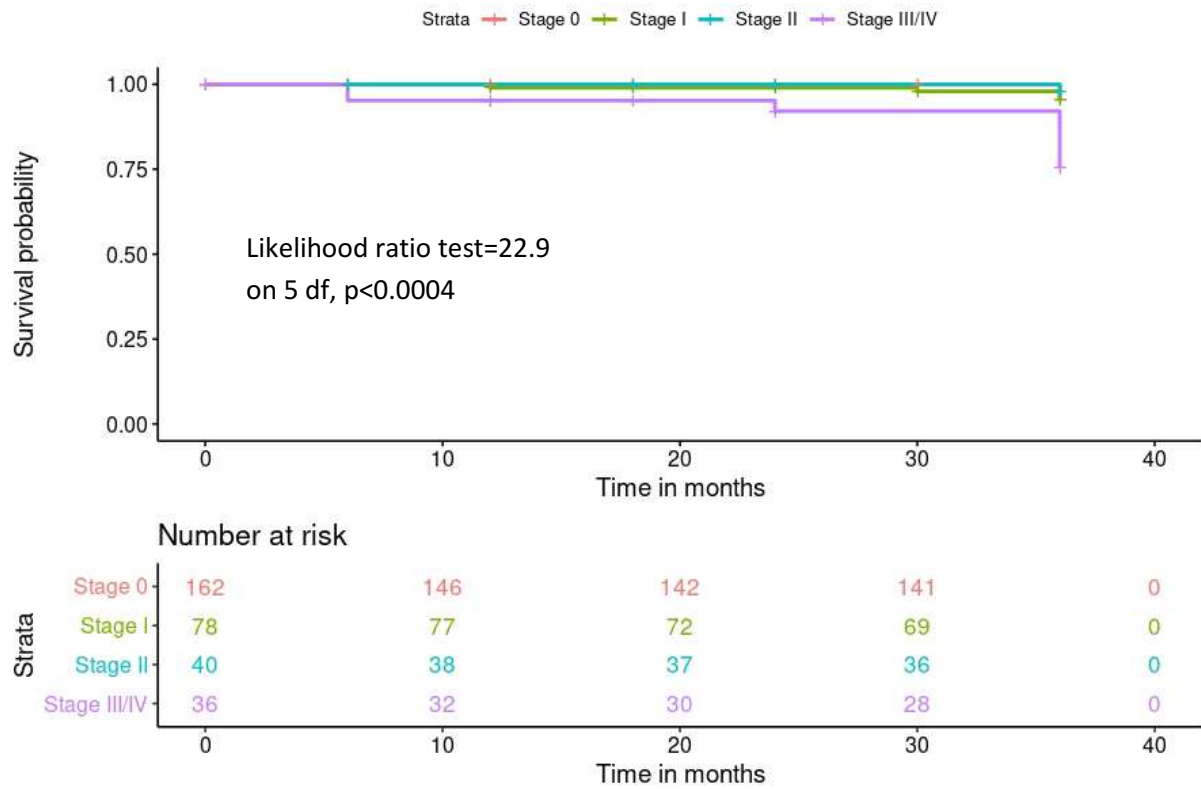
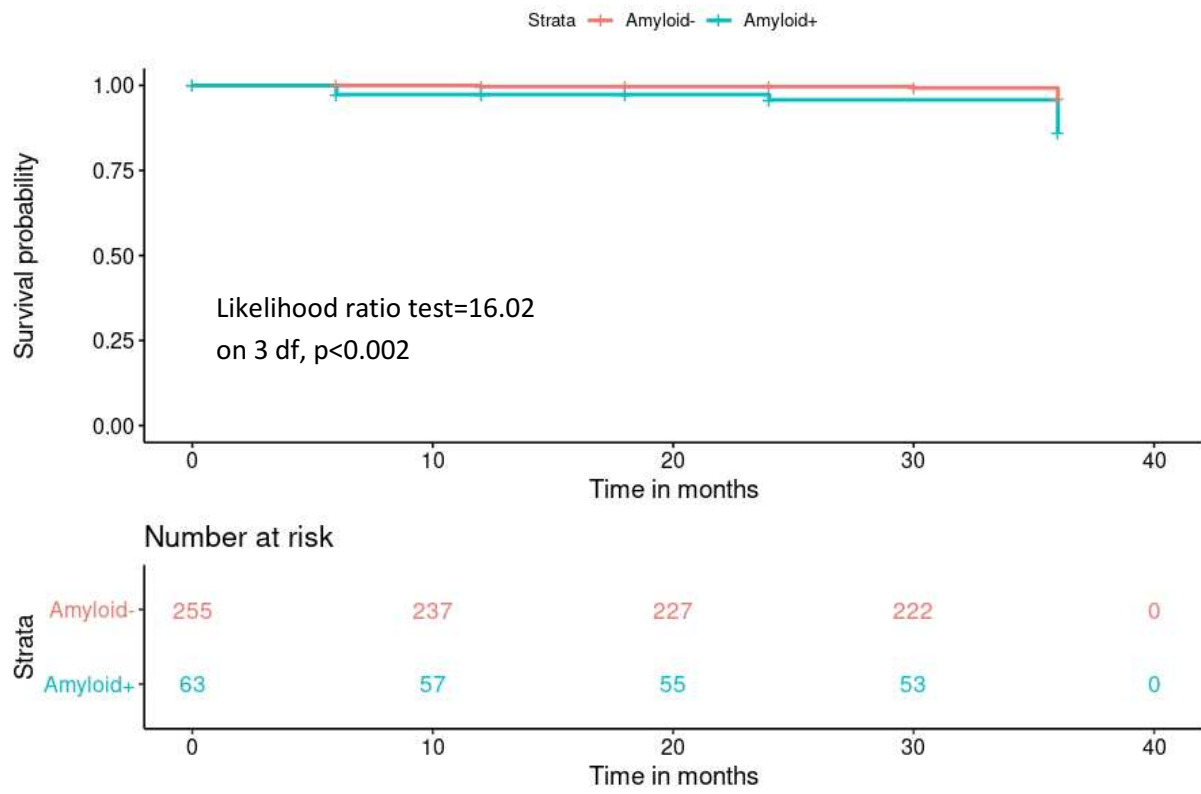


Figure 4b) SUVR binary - INSIGHT-preAD cohort



Highlights

- A confirmatory study in preclinical and prodromal Alzheimer's disease is presented.
- Amyloid stages from amyloid PET identify a high risk group for conversion
- Effects are robustly replicated across three large independent cohorts.
- Identification of high risk converters through amyloid stages has implications for selecting cohorts for clinical trials.

Journal Pre-proof

Association of Lipidomics Signatures in Blood with Clinical Progression in Preclinical and Prodromal Alzheimer's Disease

Fatemah Sakr^{a,b,c,*}, Martin Dyrba^b, Anja Bräuer^{c,d} and Stefan Teipel^{a,b} for the Alzheimer's Disease Neuroimaging Initiative¹

^a*Department of Psychosomatic Medicine, University Medicine Rostock, Rostock, Germany*

^b*German Centre for Neurodegenerative Diseases (DZNE), Rostock, Germany*

^c*Anatomy Research Group, School of Medicine and Health Sciences, Carl von Ossietzky University Oldenburg, Oldenburg, Germany*

^d*Research Centre for Neurosensory Science, Carl von Ossietzky University Oldenburg, Oldenburg, Germany*

Accepted 30 October 2021
Pre-press 9 December 2021

Abstract.

Background: Lipidomics may provide insight into biochemical processes driving Alzheimer's disease (AD) pathogenesis and ensuing clinical trajectories.

Objective: To identify a peripheral lipidomics signature associated with AD pathology and investigate its potential to predict clinical progression.

Methods: We used Bayesian elastic net regression to select plasma lipid classes associated with the CSF pTau/A β ₄₂ ratio as a biomarker of AD pathology in preclinical and prodromal AD cases from the ADNI cohort. Consensus clustering of the selected lipid classes was used to identify lipidomic endophenotypes and study their association with clinical progression.

Results: In the *APOE4*-adjusted model, ether-glycerophospholipids, lyso-glycerophospholipids, free-fatty acids, cholesterol esters, and complex sphingolipids were found to be associated with the CSF pTau/A β ₄₂ ratio. We found an optimal number of five lipidomic endophenotypes in the prodromal and preclinical cases, respectively. In the prodromal cases, these clusters differed with respect to the risk of clinical progression as measured by clinical dementia rating score conversion.

Conclusion: Lipid alterations can be captured at the earliest phases of AD. A lipidomic signature in blood may provide a dynamic overview of an individual's metabolic status and may support identifying different risks of clinical progression.

Keywords: Alzheimer's disease, heterogeneity, lipidomics, risk assessment

¹Data used in the preparation of this article were obtained from the Alzheimer's Disease Neuroimaging Initiative (ADNI) database (<http://adni.loni.usc.edu>). As such, the investigators within the ADNI contributed to the design and implementation of ADNI and provided data but did not participate in the analysis or writing of this report. A complete listing of ADNI investigators can be found at: http://adni.loni.usc.edu/wp-content/uploads/how_to_apply/ADNI_Acknowledgement_List.pdf

*Correspondence to: Fatemah A. Sakr, MSc, PhD candidate, Marie-Curie Early-Stage Researcher under the ITN-ETN H2020 BBDiag; Clinical Dementia Research Department, University Medicine Rostock, Rostock, Germany; German Centre for Neurodegenerative Diseases (DZNE), Gehlsheimer Str. 20, 18147 Rostock, Germany. Tel.: +49 381 494 9487; Fax: +49 381 494 9472; E-mails: fatemah.sakr@dzne.de; fatemah.sakr@gmail.com.

INTRODUCTION

Current diagnostic research criteria for the early detection of Alzheimer's disease (AD) are based on disease-defining biomarkers of amyloidosis, tauopathy, and neurodegeneration [1]. These biomarkers, however, are not precise enough to predict individual clinical trajectories and risk of clinical conversion [2]. More recently, multi-omics approaches have been studied to account for the heterogeneity of clinical courses in AD and identify different clinic-pathological endophenotypes as a potential basis for personalized medicine [3, 4].

As one important example, lipidomics provides insight into metabolic endophenotypes that may modify the effect of AD pathology on neurodegeneration and clinical trajectories. Thus, lipids are involved in many downstream processes of AD pathology, such as membrane remodeling, modulation of transmembrane proteins, including amyloid- β protein precursor (A β PP) and its secretases, maintaining blood-brain barrier function, myelination, cell signaling, and inflammation. In addition, they may even influence upstream events such as oxidative stress pathways and alterations of energy balance [5, 6]. Recent genetic studies supported the role of lipids in AD pathogenesis even beyond the apolipoprotein E ϵ 4 allele (*APOE4*), which is considered the major genetic risk factor for late-onset sporadic AD (LOAD) [7]. Genome-wide association studies (GWAS) have identified associations between disease status and several genes involved in lipid homeostasis, such as *CLU* (clusterin), *SORL1* (sortilin-related receptor 1), *ABCA7* (ATP-binding cassette, subfamily A, member 7), and *PLD3* (phospholipase-D3) [7] in addition to the microglia related *PLCG2* (phospholipase C-gamma) [8].

Our study used targeted lipidomics data from the Alzheimer's Disease Neuroimaging Initiative (ADNI) cohort to identify lipid alterations in the blood associated with AD pathology biomarker, namely cerebrospinal fluid (CSF) pTau/A β ₄₂ ratio, in people with preclinical or prodromal AD. In a secondary exploratory analysis, we determined lipidomic endophenotypes within prodromal and preclinical cases, respectively, using a consensus clustering approach. We investigated whether these lipidomic endophenotypes contributed to predicting subsequent clinical progression as determined by dementia rating score (CDR) conversion in preclinical and prodromal AD cases.

MATERIALS AND METHODS

Cohort overview

This study used data provided by the Alzheimer's Disease Neuroimaging Initiative (ADNI) database (<http://adni.loni.usc.edu>). ADNI is a large, multicenter, longitudinal study of older adults launched in 2003 by the National Institute on Aging, the National Institute of Biomedical Imaging and Bioengineering, the Food and Drug Administration, private pharmaceutical companies, and non-profit organizations. The study was designed to acquire serial neuroimaging, clinical and neuropsychological assessments, and other biologic markers to monitor the progression of mild cognitive impairment (MCI) and early AD. A full description of the study protocols and analytical methods are provided at (<http://www.adni-info.org/>).

The final cohort consisted of 529 participants from the ADNI cohort having a baseline diagnosis of either cognitively normal or mild cognitive impairment along with complete CSF- biomarkers, lipidomics, and body mass index (BMI) data. BMI values were sorted into three categories as follows: BMI_{low} (average weight): 18.5–24.9 or (underweight): < 18.5, BMI_{medium} (overweight): 25–29.9 and BMI_{high} (at least moderately obese): > 30. We further classified our participants into three diagnostic groups based on their CSF pTau/A β ₄₂ status, such that the cognitively normal (CN) group represents cognitively normal participants with CSF pTau/A β ₄₂ below the cut-off (0.025) [9]. Preclinical and prodromal groups had CSF pTau/A β ₄₂ above the optimized cut-off and an initial diagnosis of cognitively normal and MCI, respectively.

APOE genotyping

At the baseline visit, blood samples were obtained from the participants, shipped to the central biomarker analysis lab at the University of Pennsylvania, and processed using an *APOE* genotyping kit, as further described (http://adni.loni.usc.edu/wp-content/uploads/2010/09/ADNI_GeneralProcedures_Manual.pdf). For subsequent analysis, we coded participants' *APOE* genotype according to the presence of ϵ 4 allele present as follows; 0: no ϵ 4 allele, 1 : 1 or 2 ϵ 4 alleles.

CSF biomarkers measurements

CSF amyloid- β (1-42) (CSF A β ₄₂) and CSF Phospho-Tau (181P) (CSF pTau) were measured

using the fully automated Roche Elecsys® immunoassay platform at the UPenn/ADNI Biomarker Laboratory. CSF biomarkers $A\beta_{42}$ and pTau/ $A\beta_{42}$ were binary classified based on the optimized cut-offs 977 pg/ml and 0.025, respectively. These cut-offs were determined on the ADNI cohort then validated against the visual reads of amyloid- β PET, as explained in [9].

Lipidomics data

Targeted Lipidomics analysis was carried out on the plasma samples from ADNI participants using ultra-high-performance liquid chromatography coupled with chromatographic separation to characterize isomeric and isobaric lipid species. Mass spectrometry analysis was performed on an Agilent (6490 QQQ) mass spectrometer in positive ion mode with dynamic scheduled multiple reaction monitoring (MRM). The analysis was conducted following the lipidomics protocol developed by Kevin Huynh and Peter Meikle in Baker Heart and Diabetes Institute, Metabolomics laboratory. A detailed description of their lipidomics platform was provided in the methodology file (ADNI_ADMCLIPIDOMICSMEIKLELABLONG_METHODS_20210121.pdf) and respective articles [10,11].

After applying the standard normalization and batch correction procedures, measurements from 692 lipid species were provided in the file (ADMCLIPIDOMICSMEIKLELABLONG.csv). All the lipid measurements were \log_{10} and z-transformed before any analysis. Lipid species (692) were then merged into one hundred and seven (107) composite scores defined through a hierarchical clustering approach that was applied within each of the lipid subclasses/classes.

Statistical analysis

Selection of salient lipids associated with biomarkers of AD pathology

We used Bayesian elastic net regularized logistic regression to select lipid composite scores associated with the CSF pTau/ $A\beta_{42}$ ratio as a biomarker of AD pathology. Regularized logistic regression methods were developed to carry out simultaneous parameter estimation and variable selection [12, 13]. Elastic net offers an optimum regularization and variable selection, particularly in high dimensional data settings, such as the current lipidomics data, where features are often highly collinear, and their number exceeds the sample size [13, 14]. As one of

the regularization approaches, the elastic net provides a reasonable compromise between both ridge (L2) and lasso (L1) penalties [13, 14]. It performs an effective feature selection via the lasso penalty while better handling correlated features via the ridge penalty [14, 15]. Adopting a Bayesian approach possesses several advantages over classic elastic net regularized regression [12, 16]. First, Bayesian methods provide a straightforward statistical inference for the estimated coefficients through the posterior distributions and credibility intervals [12, 16]. Second, it allows for simultaneous estimation of both penalty parameters (L2 & L1) and model parameters [12, 16]. This is particularly important in controlling the double shrinkage problem (too small, estimated coefficients) due to sequential estimation of penalty parameters through cross-validation procedure in the classic method. Additionally, Bayesian approaches have shown better variable selection in real data examples and simulation studies [12].

Before conducting the analysis, lipid composite scores were transformed into W-scores using regression models estimated on the control group. W-scores are analogous to Z-scores yet adjusted for particular covariates, namely age and sex [17]. An initial filtering step was carried out to include only the top 60% of lipid composite scores correlated with the CSF pTau/ $A\beta_{42}$ status in the regularized logistic regression models. Then, a Bayesian logistic regression model with elastic net regularization was fitted in the *RStan* interface. We adapted the scripts provided by Sara van Erp on GitHub (<https://github.com/sara-vanerp/bayesreg>), implementing elastic net priors in Bayesian regularized regression models using Stan language [16]. A training dataset (80% of the whole cohort) was used for estimation of model parameters through Markov Chain Monte Carlo (MCMC) sampling (No-U-Turn Sampler (NUTS) algorithm). The resulting estimates were then used to predict the outcome in the test dataset (20 % of the whole cohort). Lipid composite scores were selected based on the credible interval criterion, where a variable is excluded if the credibility interval covers 0. A credibility interval level of 50% was used as recommended in [12]. Salient lipid composite scores were determined based on being selected in more than 50% of the cross-validation 100 iterations. Three different models were calculated: 1) Reference model, using the demographic criteria (Age and Sex); 2) Lipid model, using lipid composite W-scores, and 3) Lipid model + *APOE4*, where participants' *APOE4* status was added as a covariate to the Lipid model.

Prediction of clinical progression

Lipidomic endophenotypes based on consensus clustering. We applied a hierarchical clustering on those lipid composite scores that had been found associated with the CSF pTau/A β ₄₂ ratio in the previous regularized regression analysis. The clustering was performed separately in the preclinical and prodromal subgroups, respectively. We employed a consensus clustering approach using data sub-sampling [18, 19], repeated 5,000 times to ensure the stability and robustness of clustering results. During each repetition, 80% of the data samples (participants) were randomly selected for agglomerative hierarchical clustering using Ward's criterion to minimize the total within-cluster variance. A consensus matrix/cluster-based similarity matrix was then constructed. Each element in the matrix is a number between 0 and 1 inclusive, representing the proportion of times that two samples (participants) were clustered together out of the times that the same samples were chosen in the bootstrap sub-sampling process. Then final cluster assignment was defined through the consensus function, cluster-based similarity partitioning algorithm (CSPA), first introduced by Strehl and Ghosh and implemented in diceR library [18]. CSPA is an efficient consensus function that re-clusters the data samples through applying hierarchical clustering on the constructed consensus matrix [18, 19]. Hence the cluster labels are inferred at the hierarchy level of the optimal number of clusters (k) previously defined.

The optimal number of clusters was defined based on a composite score combining the proportion of ambiguous clustering (PAC) score and Dunn's index estimated within the consensus clustering. PAC is a robust estimate of cluster stability, mainly when data samples are not independent [20], an intrinsic feature of omics data. PAC score is the fraction of sample pairs with consensus index values falling in the intermediate interval, i.e., PAC window. In a perfect clustering, the consensus matrix would consist of zeros or ones, and therefore the PAC score would be zero [20]. Thus, the lower the PAC score, the more stable and near perfect the clusters. We used a PAC window of (0.1,0.9) in our analysis.

Conversely, Dunn's index estimates clustering internal validity considering compactness and separation measures [21]. The larger the Dunn's index, the better the inter-cluster separability and intra-cluster compactness. The composite score was computed as PAC score divided by Dunn's index value;

accordingly, the lower the composite score, the better the clustering.

Lipidomic endophenotypes and risk of CDR conversion. We assessed the potential of the defined lipidomic endophenotypes to predict Clinical Dementia Rating score (CDR) conversion from a value of 0 to 0.5 or 0.5 to 1 or higher in the preclinical and prodromal sub-cohorts, respectively. Using Bayesian survival analysis, we estimated the risk of conversion over a follow-up period of six years (average follow-up = 4.15 + 1.72) while accounting for censoring. We further explored the effect of several covariates, namely age, sex, BMI, APOE4, and years of education, on the estimated risk of conversion. Finally, Bayesian multivariate analysis (MANOVA) was conducted to reveal which lipid composite scores distinguished clusters at low versus high risk of clinical progression.

The whole analysis workflow is summarized in Fig. 1. All analyses were performed in R (version 3.6.3) using the following packages: RStan (version 2.21.2), RStanArm, brms, bayestestR, BayesFactor, pROC, diceR.

RESULTS

Demographic characteristics

A summary of the demographic characteristics of our final cohort is provided in (Table 1). The diagnostic groups did not differ in age, sex, or education years. The distribution of BMI categories differed between groups; the preclinical group had the highest proportion of BMI-low category. As expected, the APOE ϵ 4 allele was more prevalent in preclinical and prodromal groups ($\geq 60\%$) compared with the normal control group (pTau/A β ₄₂ -ve) (18%). AD CSF biomarker levels (pTau and pTau/A β ₄₂) were higher in prodromal participants than in the preclinical group.

Selection of salient lipids associated with biomarkers of AD pathology

Bayesian elastic net regularized logistic regression models performance

Using only age and sex as predictors, the performance of the Reference model was not better than random prediction. The Lipid model improved the prediction accuracy. The cross-validated area under the receiver operating curves (CV-AUC),

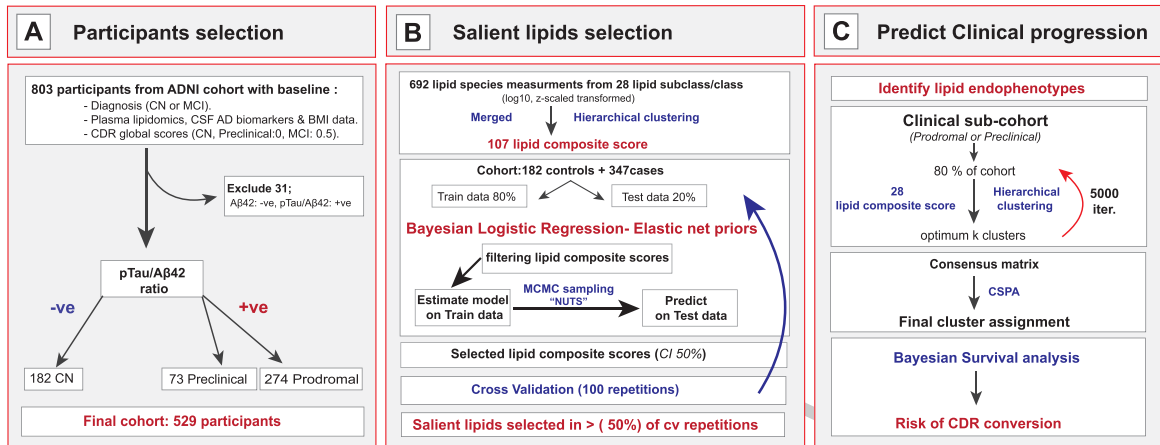


Fig. 1. Overview of the data analysis workflow. This figure summarizes the analysis workflow adopted by this study as described in the Materials and Methods section. Panel A displays the preparation of the final cohort based on the defined inclusion criteria then the classification of the final diagnostic groups based on the CSF pTau/Aβ42 ratio. The statistical analysis is demonstrated in panels B and C. Panel B illustrates the selection of salient lipids associated with biomarkers of AD pathology through Bayesian elastic net regularized logistic regression models. Panel C explains the steps to predict clinical progression in the diagnostic groups, namely prodromal and preclinical. First, we defined clusters of participants having similar lipid profiles within each diagnostic group. Then we explored the defined clusters for the risk of conversion to MCI or dementia.

Table 1
 Overview of cohort demographics

	CN	Preclinical	Prodromal	Whole cohort
N	182	73	274	529
Mean age (sd) ^a	73.2 (5.9)	75.9 (5.2)	73.3 (7.0)	73.6 (6.5)
Sex – Females ^b N (percent %)	88 (48 %)	41 (56 %)	109 (40 %)	238 (45 %)
APOE4 carriers ^{b***} N (percent %)	32 (18 %)	43 (59 %)	195 (71 %)	270 (51 %)
BMI ^{b***} N (percent %)				
Low	50 (27%)	38 (52%)	113 (41%)	201 (38%)
Medium	85 (47%)	21 (29%)	126 (46%)	232 (44%)
High	47 (26 %)	14 (19 %)	35 (13%)	96 (18%)
Mean Education y (sd) ^a	16.3 (2.7)	16.0 (2.8)	15.9 (2.9)	16.1 (2.8)
CSF biomarkers				
Mean Aβ42 (sd) ^{a***}	1727.0 (524.0)	634.0 (185.0)	630.0 (167.0)	1007.8 (620.4)
Mean pTau (sd) ^{a***}	20.1 (6.6)	28.8 (10.4) [#]	35.4 (14.1) [#]	29.2 (13.4)
Mean pTau/Aβ42 ratio (sd) ^{a***}	0.012 (0.003)	0.049 (0.025) [#]	0.059 (0.028) [#]	0.042 (0.03)

Summary of the demographic characteristics of our cohort split into the final three diagnostic groups cognitively normal elderly (CN), preclinical and prodromal. Characteristics are described as Number (N) and the corresponding percentage (percent %) or Mean value and standard deviation (sd) as convenient. Group differences were tested using Bayesian ANOVA (a) and Bayesian test of association (b). Results were interpreted in terms of Bayes Factor (BF) in favor of presence of group differences in the tested variables, where BF of (3–20) represented moderate evidence (*), BF of (20–150) represented strong evidence (**), while BF of (>150) represented very strong evidence (***). Differences in levels of CSF biomarkers levels between Preclinical and Prodromal are marked by (#).

CV-Accuracy, CV-Sensitivity, and CV-Specificity at the optimum threshold were 0.65, 0.66, 0.68, and 0.61, respectively. However, the best performance was achieved by the Lipid + APOE4 model; the estimated CV-AUC, CV-Accuracy, CV-Sensitivity, and CV-Specificity increased to 0.76, 0.71, 0.69, and 0.77, respectively. Supplementary Table 1 provides an overview of all tested models.

Identification of salient lipids

The Lipid + APOE4 model selected a set of twenty-eight lipid composite scores in at least 50% of cross-validation repetitions (Supplementary Table 2). A features' relative importance and stability were determined by the median posterior β-coefficients and frequency of selection across the cross-validations. According to these criteria,

lyso-glycerophospholipids (LPL), alkenyl-glycerophospholipids (plasmalogens), free fatty acids (FFA), cholesterol esters and sphingolipids (complex ceramides) lipid classes/subclasses ranked on top of the list. Both lyso-phosphatidylcholine (LPC_7: poly-unsaturated fatty acid (PUFA)) and lyso-alkyl-phosphatidylcholine (LPC_O_2: long-chain fatty acid (FA)) were positively associated with the CSF pTau/A β 2 ratio. Similarly, phosphatidylcholine (PC_5: arachidonic acid (AA)) harboring arachidonic acid showed a positive association. Conversely, plasmalogens such as alkenyl-phosphatidylcholine (PC_P_5: docosahexaenoic acid (DHA), Eicosapentaenoic acid (EPA) & PC_P_2: saturated and mono-unsaturated FA) and alkenyl-phosphatidylethanolamine (PE_P_5: AA, DHA) showed negative associations.

Except for AA (FA_3), free fatty acids (FA_1: saturated, mono-unsaturated, PUFA) were negatively associated with the AD biomarkers. Cholesterol esters (Chols_ester_3: PUFA & Chols_ester_2) and long-chain acyl-carnitines (AC_4: PUFA) were positively associated with AD biomarkers, while di-acylglycerol (DG_3: EPA, DHA) and alkyl-diacylglycerol (TG_O_3) showed negative relation.

Complex ceramides including hexosyl-ceramides (hexCER_6 & hexCER_7), gangliosides (GM1), and sulfatides were found to be positively associated with AD biomarkers yet di-hydro-ceramides (dhCER_1), gangliosides (GM3_3: very long FA), and sphingomyelin (SM_3: very long FA) were negatively associated. Figure 2 displays the median posterior β -coefficients and their credibility intervals across the cross-validations, as estimated by the Lipid + *APOE4* model. Lipid species, constituting each of the salient lipid composite scores, are listed in Supplementary Table 3.

Prediction of clinical progression

Lipidomic endophenotypes based on consensus clustering

We conducted consensus clustering to identify lipidomic endophenotypes based on the set of lipid composite scores selected by the Lipid + *APOE4* model.

In the prodromal sub-cohort, we determined the optimum number of clusters to be ($k=5$), as demonstrated in Supplementary Figure 1. Of the prodromal participants, 28% fell into the cluster (I), 23% in the cluster (IV), 20% each in the clusters (II) and (V), and 9% in the cluster (III). Apart from the BMI categories distribution, there was no conclusive evidence

for differences in age, sex, years of education, *APOE4* status, or the CSF levels of AD biomarkers between the defined clusters (Supplementary Table 4).

Following the same approach, we determined ($k=5$) the optimal number of clusters for the preclinical sub-cohort, as shown in Supplementary Figure 2. Of these participants, 28% fell into the cluster (I), while the rest were equally distributed over the remaining clusters. Details on the distribution of demographic characteristics, *APOE4* genotype, and BMI categories can be found in Supplementary Table 5.

Lipidomic endophenotypes and risk of CDR conversion

We evaluated the risk of CDR conversion among prodromal sub-cohort clusters with and without adjusting for the effect of covariates as demonstrated in Supplementary Table 6. Cluster (IV) was chosen as the reference group since it exhibited a lower risk of CDR conversion. Moreover, cluster (IV) enclosed a relatively large proportion of participants. As shown in Fig. 3, the clusters (II) (HR = 1.97 (1.26–3.10)) and (V) (HR = 1.99 (1.30–3.00)) had an increased risk of conversion in the *APOE4* adjusted model. To investigate whether these effects differed between sexes, we repeated the Bayesian survival models (*APOE4* adjusted) in the male and female data subsets, respectively (Table 2). In men, the lipid profiles of clusters (II and V) showed an increased risk of conversion, whereas cluster (III) showed a decreased risk of conversion relative to the reference cluster (IV). In women, only cluster (II) had an increased risk of conversion.

Finally, we conducted Bayesian multivariate analysis to identify differences in lipid composite scores between the reference cluster (IV) and the remaining clusters (Supplementary Table 7). Figure 4 shows the specific lipid profile for each cluster of the prodromal sub-cohort.

In the preclinical sub-cohort, there was no evidence of a difference in risk of CDR conversion between the five clusters. Essentially identical results were obtained whether we adjusted or not for covariates.

DISCUSSION

We explored different lipid classes in preclinical and prodromal AD cases to analyze the relationship between lipid metabolism markers and biomarkers of amyloid and tau pathology, as well as clinical progression.

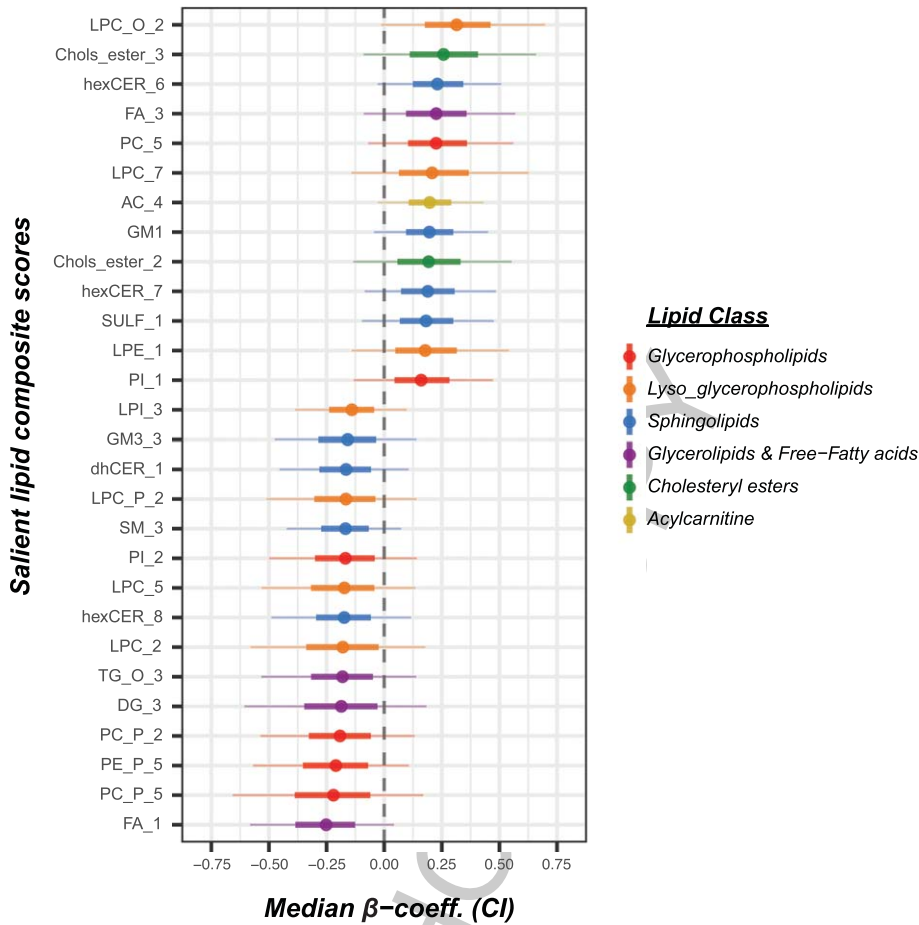


Fig. 2. Salient lipids associated with CSF pTau/A β ₄₂ ratio. We used Bayesian elastic net logistic regression (Lipid+APOE4 model) to select salient lipid composite scores associated with CSF pTau/A β ₄₂ ratio. Estimated posterior β -coefficients are represented as points with their respective 50% and 90% credibility intervals as thick and thin error bars, respectively. The points' color codes for their corresponding lipid class. LPC_O.2: Lyso-alkyl-phosphatidylcholine (long/ very long FA), Choles.ester.3: Cholesteryl ester (PUFA), hexCER: Hexosylceramide, FA.3: Free fatty acid (AA), PC.5: Phosphatidylcholine (AA), LPC.7: Lysophosphatidylcholine (PUFA), AC.4: Acylcarnitine (PUFA), GM1: GM1 gangliosides, Choles.ester.2: Cholesteryl ester, SULF.1: Sulfatides, LPE.1: Lyso-phosphatidylethanolamine (saturated FA), PI.1: Phosphatidylinositol (PUFA), LPI.3: Lyso-phosphatidylinositol (AA), GM3.3: GM3 gangliosides (very long FA), dhCER: Dihydroceramide, LPC.P.2: Lyso-alkenyl-phosphatidylcholine (long FA), SM.3: Sphingomyelin (very long saturated FA), PL.2: Phosphatidylinositol (saturated, monounsaturated FA), LPC.5: Lysophosphatidylcholine (long, very long FA), LPC.2: Lysophosphatidylcholine (odd numbered FA), TG.O.3: Alkyl-diacylglycerol, DG.3: diacylglycerol (EPA & DHA), PC.P.2: Alkenyl-phosphatidylcholine (saturated and mono-unsaturated FA), PE.P.5: Alkenyl-phosphatidylethanolamine (AA, DHA), PC.P.5: Alkenyl-phosphatidylcholine (DHA & EPA) and FA.1: Free fatty acid.

Our first goal was to determine associations between peripheral lipid alterations and pathology markers of AD in the CSF. Ether glycerophospholipids, particularly plasmalogens, showed lower levels in preclinical and prodromal AD participants compared with controls. Conversely, we found arachidonic acid-containing phosphatidylcholine, PUFA (omega-3) lyso-phosphatidylcholine and lyso-alkyl-phosphatidylcholine with predominant saturated/mono-unsaturated long-chain fatty acid to be increased. Low levels of plasmalogens have been

frequently linked to AD pathology [22], whether measured in brain tissue [23–25], CSF [25], or plasma blood samples [26]. Grey matter plasmalogens (DHA and AA at sn-2) depletion was found associated with disease progression and severity in AD patients [27–30]. A recent study by Lim et al. proposed that ether-lipids dysregulation may partly mediate the effect of two major AD risk factors, namely, age and APOE4 [31].

Toledo et al. showed that higher baseline levels of long-chain and PUFA-containing alkyl phosphatidyl-

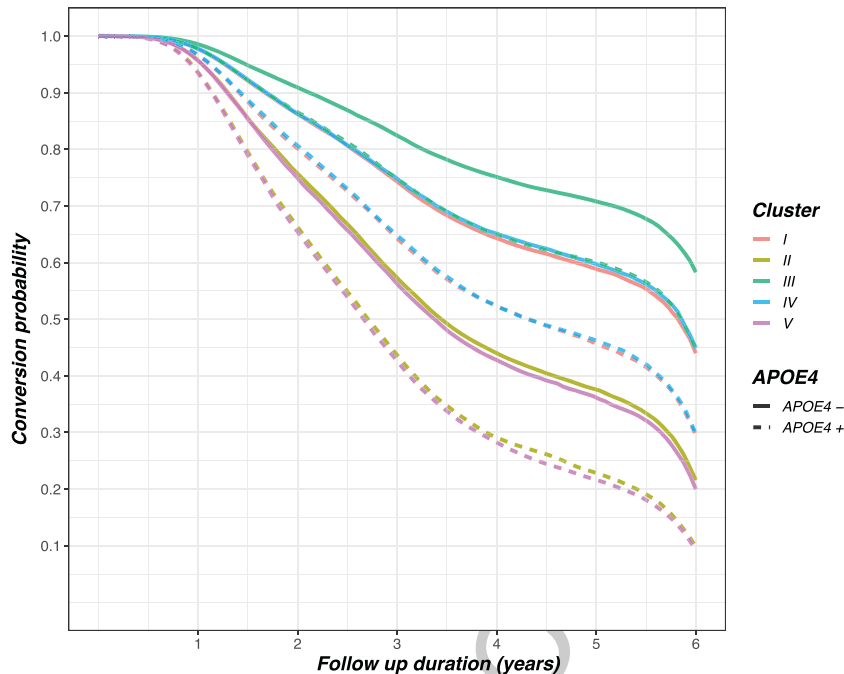


Fig. 3. Lipid endophenotypes predict clinical progression to dementia. We conducted a Bayesian survival analysis to estimate the risk of clinical progression to dementia among the pre-defined clusters of the prodromal sub-cohort. Clinical progression in the prodromal sub-cohort is defined as the conversion of clinical dementia rating score (CDR) from a value of 0.5 to 1. Clusters (II and V) are found to have ≈ 2 folds higher risk of progression to dementia compared to the reference cluster (IV).

Table 2
Risk of clinical progression among prodromal lipidomic endophenotypes

Model	Cluster + <i>APOE4</i>			Male subset			Female subset		
	Median (MAD)	Hazard ratio	HDI	Median (MAD)	Hazard ratio	HDI	Median (MAD)	Hazard ratio	HDI
Intercept: IV	-9.03 (1.80)			-8.46 (2.20)				-9.24 (2.72)	
I	0.02 (0.26)	1.02	0.68–1.52	-0.16 (0.32)	0.85	0.54–1.51	0.28 (0.42)	1.33	0.68–2.72
II	0.68 (0.28)	1.97	1.26–3.10	0.56 (0.35)	1.75	1.04–3.16	0.84 (0.43)	2.32	1.15–4.57
III	-0.41 (0.42)	0.66	0.36–1.22	-1.08 (0.58)	0.34	0.13–0.89	0.09 (0.54)	1.10	0.48–2.56
V	0.69 (0.26)	1.99	1.30–3.00	0.85 (0.34)	2.35	1.38–4.06	0.55 (0.43)	1.74	0.89–3.53
<i>APOE4</i>	0.39 (0.21)	1.48	1.07–2.05	0.40 (0.27)	1.50	1.00–2.25	0.27 (0.33)	1.31	0.76–2.23

Bayesian survival analysis was conducted to estimate the relative risk of progression to dementia among prodromal lipidomic endophenotypes while adjusting for *APOE4*. *APOE4* adjusted model was selected based on the sensitivity analysis provided in Supplementary Table 6, which investigated the relative risk of several covariates. We further replicated the same model on male and female subsets separately to explore sex-specific effect of lipidomic endophenotypes on clinical progression. Throughout the analysis, we set cluster (IV) as our reference group. Results were interpreted in terms of high-density intervals (HDI) of posterior distributions, where hazard ratios with HDI not covering (1) were considered relevant and reported in red.

cholines (PC ae 42 : 4, PC ae 44 : 4) correlated with abnormal levels of CSF A β ₄₂ in preclinical and prodromal AD participants of the ADNI cohort and predicted conversion from MCI to AD dementia [32]. In the current study, we observed high levels of arachidonic acid-containing phosphatidylcholine, and long-chain alkyl lyso-phosphatidylcholines (LPC-O), were associated with the CSF pTau/A β ₄₂

ratio. Results from both studies suggest an early role of arachidonated phosphatidylcholines, particularly long-chain alkyl isomers and their lyso derivatives, in AD pathogenesis, even in cognitively normal individuals with pathological levels of CSF AD biomarkers. These phosphatidylcholine species are known precursors of potent inflammatory mediators, including platelet-activating factor (PAF) and arachidonic

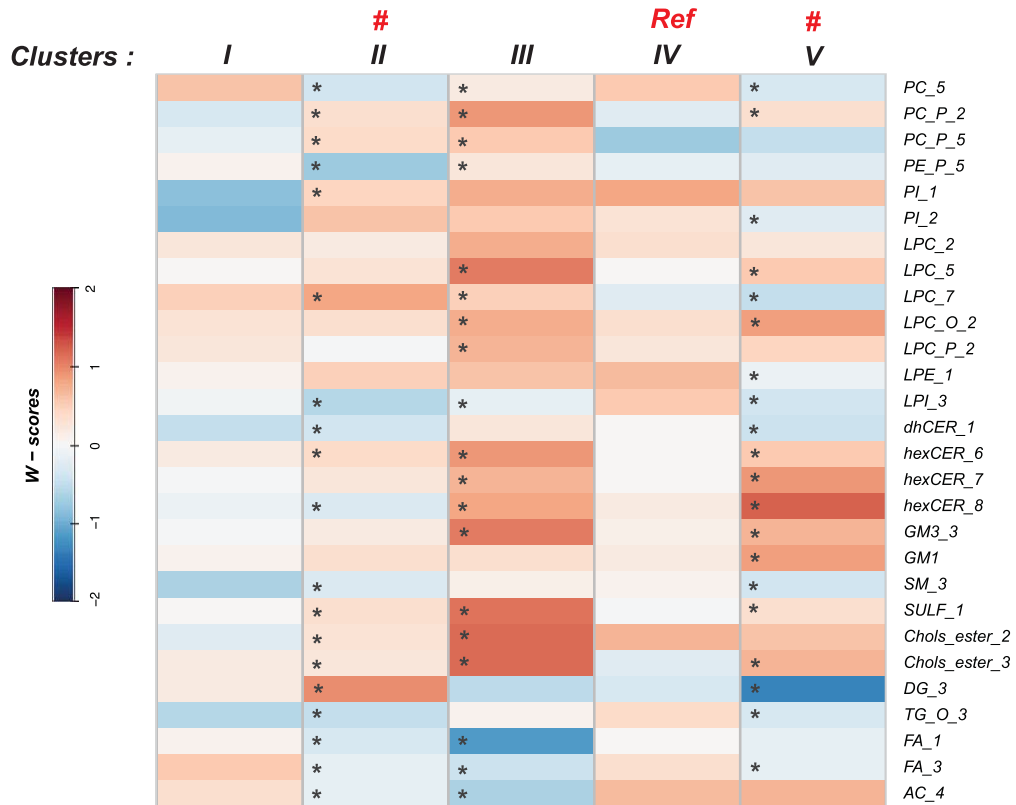


Fig. 4. Heterogeneity of lipidomic endophenotypes among the prodromal sub-cohort. The specific lipid profile of each cluster is demonstrated on a heatmap in terms of average w-scores. On the color scale, red represents scores higher than expected in the age and sex-matched control group, and blue color represents lower scores. Bayesian multivariate analysis was conducted to identify lipid composite scores distinguishing clusters at higher risk of clinical progression from the reference group. Cluster (IV) was set as the reference group and marked by (Ref.). Clusters (II and V) were defined as groups at higher risk of progression and marked by (#). Asterisk (*) points to lipid scores that showed evidence of group differences. PC_5: Phosphatidylcholine (AA), PC_P_2: Alkenyl-phosphatidylcholine (saturated and mono-unsaturated FA), PC_P_5: Alkenyl-phosphatidylcholine (DHA & EPA), PE_P_5: Alkenyl-phosphatidylethanolamine (AA, DHA), PL_1: Phosphatidylinositol (PUFA), PL_2: Phosphatidylinositol (saturated, monounsaturated FA), LPC_2: Lysophosphatidylcholine (odd numbered FA), LPC_5: Lysophosphatidylcholine (long, very long FA), LPC_7: Lysophosphatidylcholine (PUFA), LPC_O_2: Lyso-alkyl-phosphatidylcholine (long/very long FA), LPC_P_2: Lyso-alkenyl-phosphatidylcholine (long FA), LPE_1: Lyso-phosphatidylethanolamine (saturated FA), LPI_3: Lyso-phosphatidylinositol (AA), dhCER: Dihydroceramide, hexCER: Hexosyl-ceramide, GM3_3: GM3 gangliosides (very long FA), GM1: GM1 gangliosides, SM_3: Sphingomyelin (very long saturated FA), SULF_1: Sulfatides, Chols_ester_2: Cholesteryl ester, Chols_ester_3: Cholesteryl ester (PUFA), DG_3: diacylglycerol (EPA & DHA), TG_O_3: Alkyl-diacylglycerol, FA_1: Free fatty acid, FA_3: Free fatty acid (AA) and AC_4: Acylcarnitine (PUFA).

acid. Additionally, they are highly abundant in platelets and immune cells [33, 34]. This points to a potential regulatory role in inflammation processes and would represent a possible link between inflammation and AD [32].

Complex ceramides, including glycosylated ceramides, GM1 gangliosides, and their precursors hexosyl-ceramides and sulfatides, showed higher levels in prodromal and preclinical AD participants, in contrast to di-hydro-ceramides, sphingomyelins, and GM3 gangliosides, which were decreased. Several studies suggested a shift in sphingolipids metabolism

towards ceramides accumulation [35, 36] and depletion of sphingomyelins, particularly those with long-chain FA (C22, C24) [37, 38] and sulfated sphingolipids [35] early in the course of AD [39]. Ceramides, a key bioactive molecule in sphingolipids metabolism, were suggested to contribute to the increased susceptibility of neurons and oligodendrocytes to apoptotic cell death [40]. This hypothesis was further supported by the elevated activity of enzymes involved in ceramides synthesis, namely sphingomyelinases and ceramidases, in brain tissue of AD cases [38]. Consistent with these findings, gene

expression of sphingomyelinases and serine palmitoyl transferase enzymes was found to be upregulated in AD patients' brain tissue [36, 39].

The second goal of our study was to identify distinct lipidomic endophenotypes and assess their association with clinical progression. Lipidomics endophenotyping offers a global mapping of the alterations in biochemical pathways [41]. These alterations may partly reflect underlying AD pathology. Additionally, these endophenotypes can capture complementary information related to an individual's specific comorbidities and/or genomic characteristics that could partly explain the diversity observed in clinical trajectories within AD populations [3]. In the prodromal sub-cohort, the lipid profiles of clusters (II and V) were associated with a higher risk of clinical progression. In both clusters, we observed lower levels of PUFA (mainly AA) containing plasmalogens and phosphatidylcholines associated with a compensatory increase of plasmalogens, mainly alkenyl phosphatidylcholines, containing saturated and mono-unsaturated FAs. Higher levels of cholesterol esters, complex ceramides together with the depletion of long-chain sphingomyelins, and dihydro-ceramides were also noted in clusters (II and V) participants. Cluster (III) lipidomic profile was associated with a lower risk of progression (CDR conversion) yet only in men. Cluster (III) constituted a group of prodromal participants with a higher prevalence of low BMI and a slightly higher proportion of APOE4 carriers compared with the reference cluster (IV).

Previous studies used logistic regression or machine learning algorithms to investigate the association of lipids with dementia risk in cognitively normal individuals [42–44] and people with MCI [32, 45]. Several studies have found higher levels of sphingomyelin, phosphatidylcholines, and lysophosphatidylcholine associated with conversion from MCI to AD/dementia [32, 46, 47]. Conversely, Mapstone et al. [43] and Ma et al. [45] showed that lower baseline levels of phosphatidylcholines and lysophosphatidylcholine were significantly associated with accelerated cognitive decline [45] and risk of conversion to MCI/AD compared to cognitively stable participants [43].

In a different approach, Wood et al. [48] addressed heterogeneity in lipid alterations patterns within groups of MCI and AD cases. They defined subgroups within each diagnostic group according to their Mini-Mental State Examination score (low versus high). Based on the literature, they focused on two

lipid classes, ethanolamine plasmalogens and diacylglycerols. MCI and AD cases had elevated levels of diacylglycerols and plasmalogens depletion compared with controls [48]. Low and high Mini-Mental State Examination MCI cases, however, showed no differences in both lipid classes [48]. In contrast to such a hypothesis-driven approach, here we explored the diversity of lipidomic endophenotypes within prodromal cases using an unsupervised clustering approach. Thus, our findings serve to generate rather than confirm hypotheses on the association of lipid profiles with the risk of conversion.

Recent evidence suggested that sex has an effect on the association of lipids with AD pathology and rates of cognitive decline [31, 49, 50]. In our study, cluster (III) showed a decreased risk of conversion in men but not in women. This cluster had high levels of long-chain fatty acids lysophosphatidylcholine (both acyl and ether) and plasmalogens together with low levels of acylcarnitines. Sex-specific remodeling of lipid metabolism was suggested before, where high levels of sphingomyelins and phosphatidylcholines were reported in women [49, 50]. Conversely, lysophosphatidylcholine and ceramides were found at higher levels in men [49]. Thus, phospholipases may have higher activity in men and sphingomyelin synthetase may have a higher activity in women [49]. Consequently, we adjusted lipid scores for age and sex based on the control group in an attempt to control for the complex interaction of lipids with sex during different stages of AD. Although we started with a substantial number of cases, the sample size within preclinical and prodromal sub-cohorts and their respective lipid endophenotypes clusters was small, so that it was not feasible to conduct the full analysis in a sex-stratified fashion, as recommended in [49, 50].

Lack of consistency across metabolomics studies' results always was and still is a major limitation that hinders including lipid markers into diagnostic biomarker panels of AD [50, 51]. This heterogeneity is related to many factors, among them variability in data processing procedures and analytical platforms [51], as well as studies' design, sample size, distribution of relevant risk factors, and used statistical approaches [50]. Another factor probably is the lack of strong effects which contributes to inconsistent findings across studies. In our Bayesian regression models, we observed overall small contributions from individual lipid composite scores to the association with AD pathology CSF biomarkers as indicated by poor model performance as well as small posterior coefficients with large credibility

intervals. In addition, metabolomics data are inherently highly collinear. This could contribute to high variance observed within the models and difficulty assessing variables' relative importance [52]. Taken together, a wide range of variance is observed in metabolomics data that limits their integration in the first line of diagnostic workflow and renders them likely more useful in adding to the accuracy of other prognostic markers [48].

Several limitations need to be acknowledged in this study. Instead of using raw lipid scores, we used composite scores based on hierarchical clustering applied within each lipid class. Such an approach could have masked the effects of some individual lipid species. Our objective was to reduce data dimensionality and overcome the drawback of variables' multicollinearity, particularly on regression coefficients estimation and model stability. Concurrently we wanted to maintain the representation of all investigated lipid subclasses/classes and identify subsets of functionally similar lipid species. Finally, given the heterogeneity of lipidomics data, particularly in early AD individuals, even larger cohorts are needed to identify endophenotypes robustly. In future analysis, we would like to tune and then validate our approach on a larger sample derived from multiple cohorts and particularly enriched with participants in the preclinical stage of AD.

CONCLUSION

Through our study, we have shown that alterations in lipids, particularly those harboring polyunsaturated fatty acids and ether bonds, can be captured at the earliest stages of AD. Lipidomics profiles provide an overview of an individual's metabolic status whilst incorporating the balance within and between interacting biochemical pathways. Hence, identifying distinct lipidomic endophenotypes could contribute to AD risk and clinical trajectories. Refining and validating this approach could open a new avenue to adjuvant interventions modulating lipid metabolic pathways and allow for targeting subjects with the largest expected benefit.

ACKNOWLEDGMENTS

This study was supported by the Marie-Curie Innovative Training Network BBdiag (EU-Horizon 2020, Project ID: 721281).

Data collection and sharing for this project was funded by the Alzheimer's Disease Neuroimaging Initiative (ADNI) (National Institutes of Health Grant U01 AG024904) and DOD ADNI (Department of Defense award number W81XWH-12-2-0012). ADNI is funded by the National Institute on Aging, the National Institute of Biomedical Imaging and Bioengineering, and through generous contributions from the following: AbbVie, Alzheimer's Association; Alzheimer's Drug Discovery Foundation; Araclon Biotech; BioClinica, Inc.; Biogen; Bristol-Myers Squibb Company; CereSpir, Inc.; Cogstate; Eisai Inc.; Elan Pharmaceuticals, Inc.; Eli Lilly and Company; EuroImmun; F. Hoffmann-La Roche Ltd and its affiliated company Genentech, Inc.; Fujirebio; GE Healthcare; IXICO Ltd.; Janssen Alzheimer Immunotherapy Research & Development, LLC.; Johnson & Johnson Pharmaceutical Research & Development LLC.; Lumosity; Lundbeck; Merck & Co., Inc.; Meso Scale Diagnostics, LLC.; NeuroRx Research; Neurotrack Technologies; Novartis Pharmaceuticals Corporation; Pfizer Inc.; Piramal Imaging; Servier; Takeda Pharmaceutical Company; and Transition Therapeutics. The Canadian Institutes of Health Research is providing funds to support ADNI clinical sites in Canada. Private sector contributions are facilitated by the Foundation for the National Institutes of Health (<http://www.fnih.org>). The grantee organization is the Northern California Institute for Research and Education, and the study is coordinated by the Alzheimer's Therapeutic Research Institute at the University of Southern California. ADNI data are disseminated by the Laboratory for Neuro Imaging at the University of Southern California.

Authors' disclosures available online (<https://www.j-alz.com/manuscript-disclosures/20-1504r2>).

SUPPLEMENTARY MATERIAL

The supplementary material is available in the electronic version of this article: <https://dx.doi.org/10.3233/JAD-201504>.

REFERENCES

- [1] Sperling RA, Aisen PS, Beckett LA, Bennett DA, Craft S, Fagan AM, Iwatsubo T, Jack CR, Kaye J, Montine TJ, Park DC, Reiman EM, Rowe CC, Siemers E, Stern Y, Yaffe K, Carrillo MC, Thies B, Morrison-Bogorad M, Wagster M V., Phelps CH (2011) Toward defining the preclinical stages of Alzheimer's disease: Recommendations from the National

- Institute on Aging-Alzheimer's Association workgroups on diagnostic guidelines for Alzheimer's disease. *Alzheimers Dement* **7**, 280-292.
- [2] Dumurgier J, Hanseeuw BJ, Hatling FB, Judge KA, Schultz AP, Chhatwal JP, Blacker D, Sperling RA, Johnson KA, Hyman BT, Gómez-Isla T (2017) Alzheimer's disease biomarkers and future decline in cognitive normal older adults. *J Alzheimers Dis* **60**, 1451-1459.
 - [3] Badhwar AP, McFall GP, Sapkota S, Black SE, Chertkow H, Duchesne S, Masellis M, Li L, Dixon RA, Bellec P (2020) A multiomics approach to heterogeneity in Alzheimer's disease: Focused review and roadmap. *Brain* **143**, 1315-1331.
 - [4] Hampel H, O'Bryant SE, Molinuevo JL, Zetterberg H, Masters CL, Lista S, Kiddle SJ, Batrla R, Blennow K (2018) Blood-based biomarkers for Alzheimer disease: Mapping the road to the clinic. *Nat Rev Neurol* **14**, 639-652.
 - [5] Chew H, Solomon VA, Fonteh AN (2020) Involvement of lipids in Alzheimer's disease pathology and potential therapies. *Front Physiol* **11**, 598.
 - [6] Wong MW, Braidy N, Poljak A, Pickford R, Thambisetty M, Sachdev PS (2017) Dysregulation of lipids in Alzheimer's disease and their role as potential biomarkers. *Alzheimers Dement* **13**, 810-827.
 - [7] Giri M, Zhang M, Lü Y (2016) Genes associated with Alzheimer's disease: An overview and current status. *Clin Interv Aging* **11**, 665-681.
 - [8] Magno L, Lessard CB, Martins M, Lang V, Cruz P, Asi Y, Katan M, Bilsland J, Lashley T, Chakrabarty P, Golde TE, Whiting PJ (2019) Alzheimer's disease phospholipase C-gamma-2 (PLCG2) protective variant is a functional hypermorph. *Alzheimers Res Ther* **11**, 16.
 - [9] Hansson O, Seibyl J, Stomrud E, Zetterberg H, Trojanowski JQ, Bittner T, Lifke V, Corradini V, Eichenlaub U, Batrla R, Buck K, Zink K, Rabe C, Blennow K, Shaw LM (2018) CSF biomarkers of Alzheimer's disease concord with amyloid- β PET and predict clinical progression: A study of fully automated immunoassays in BioFINDER and ADNI cohorts. *Alzheimers Dement* **14**, 1470-1481.
 - [10] Huynh K, Barlow CK, Jayawardana KS, Weir JM, Mellett NA, Cinel M, Magliano DJ, Shaw JE, Drew BG, Meikle PJ (2019) High-throughput plasma lipidomics: Detailed mapping of the associations with cardiometabolic risk factors. *Cell Chem Biol* **26**, 71-84.
 - [11] Huynh K, Lim WLF, Giles C, Jayawardana KS, Salim A, Mellett NA, Smith AAT, Olshansky G, Drew BG, Chatterjee P, Martins I, Laws SM, Bush AI, Rowe CC, Villemagne VL, Ames D, Masters CL, Arnold M, Nho K, Saykin AJ, Baillie R, Han X, Kaddurah-Daouk R, Martins RN, Meikle PJ (2020) Concordant peripheral lipidome signatures in two large clinical studies of Alzheimer's disease. *Nat Commun* **11**, 5698.
 - [12] Li Q, Lin N (2010) The Bayesian elastic net. *Bayesian Anal* **5**, 151-170.
 - [13] Zou H, Hastie T (2005) Regularization and variable selection via the elastic net. *J R Stat Soc B Stat Methodol* **67**, 301-320.
 - [14] Hastie T, Tibshirani R, Wainwright M (2015) Statistical learning with sparsity. In *Statistical Learning with Sparsity: The Lasso and Generalizations*, Chapman and Hall/CRC, pp. 55-93.
 - [15] Kuhn M, Johnson K (2013) *Applied Predictive Modeling*, Springer New York, New York.
 - [16] van Erp S, Oberski DL, Mulder J (2019) Shrinkage priors for Bayesian penalized regression. *J Math Psychol* **89**, 31-50.
 - [17] Dyrba M, Mohammadi R, Grothe MJ, Kirste T, Teipel SJ (2020) Gaussian graphical models reveal inter-modal and inter-regional conditional dependencies of brain alterations in Alzheimer's disease. *Front Aging Neurosci* **12**, 99.
 - [18] Strehl A, Ghosh J (2002) Cluster ensembles - A knowledge reuse framework for combining multiple partitions. *J Mach Learn Res* **3**, 583-617.
 - [19] Hennig C, Meila M, Murtagh F, Rocci R (2015) *Handbook of Cluster Analysis*, Chapman and Hall/CRC.
 - [20] Şenbabaoğlu Y, Michailidis G, Li JZ (2014) Critical limitations of consensus clustering in class discovery. *Sci Rep* **4**, 6207.
 - [21] Dunn JC (1974) Well-separated clusters and optimal fuzzy partitions. *J Cybern* **4**, 95-104.
 - [22] Su XQ, Wang J, Sinclair AJ (2019) Plasmalogens and Alzheimer's disease: A review. *Lipids Health Dis* **18**, 100.
 - [23] Ginsberg L, Rafique S, Xuereb JH, Rapoport SI, Gershfeld NL (1995) Disease and anatomic specificity of ethanolamine plasmalogen deficiency in Alzheimer's disease brain. *Brain Res* **698**, 223-226.
 - [24] Grimm MOW, Kuchenbecker J, Rothhaar TL, Grösgen S, Hundsdoerfer B, Burg VK, Friess P, Müller U, Grimm HS, Riemenschneider M, Hartmann T (2011) Plasmalogen synthesis is regulated via alkyl-dihydroxyacetonephosphate-synthase by amyloid precursor protein processing and is affected in Alzheimer's disease. *J Neurochem* **116**, 916-925.
 - [25] Wood PL, Barnette BL, Kaye JA, Quinn JF, Woltjer RL (2015) Non-targeted lipidomics of CSF and frontal cortex grey and white matter in control, mild cognitive impairment, and Alzheimer's disease subjects. *Acta Neuropsychiatr* **27**, 270-278.
 - [26] Yamashita S, Kiko T, Fujiwara H, Hashimoto M, Nakagawa K, Kinoshita M, Furukawa K, Arai H, Miyazawa T (2016) Alterations in the levels of amyloid- β , phospholipid hydroperoxide, and plasmalogen in the blood of patients with Alzheimer's disease: Possible interactions between amyloid- β and these lipids. *J Alzheimers Dis* **50**, 527-537.
 - [27] Goodenowe DB, Cook LL, Liu J, Lu Y, Jayasinghe DA, Ahiahonu PWK, Heath D, Yamazaki Y, Flax J, Krenitsky KF, Sparks DL, Lerner A, Friedland RP, Kudo T, Kamino K, Morihara T, Takeda M, Wood PL (2007) Peripheral ethanolamine plasmalogen deficiency: A logical causative factor in Alzheimer's disease and dementia. *J Lipid Res* **48**, 2485-2498.
 - [28] Han X (2005) Lipid alterations in the earliest clinically recognizable stage of Alzheimer's disease: Implication of the role of lipids in the pathogenesis of Alzheimer's disease. *Curr Alzheimer Res* **2**, 65-77.
 - [29] Han X, Holtzman DM, McKeel Jr DW (2001) Plasmalogen deficiency in early Alzheimer's disease subjects and in animal models: Molecular characterization using electrospray ionization mass spectrometry. *J Neurochem* **77**, 1168-1180.
 - [30] Wood PL, Mankidy R, Ritchie S, Heath D, Wood JA, Flax J, Goodenowe DB (2010) Circulating plasmalogen levels and Alzheimer Disease Assessment Scale-Cognitive scores in Alzheimer patients. *J Psychiatry Neurosci* **35**, 59-62.
 - [31] Lim WLF, Huynh K, Chatterjee P, Martins I, Jayawardana KS, Giles C, Mellett NA, Laws SM, Bush AI, Rowe CC, Villemagne VL, Ames D, Drew BG, Masters CL, Meikle PJ, Martins RN (2020) Relationships between plasma lipid species, gender, risk factors, and Alzheimer's disease. *J Alzheimers Dis* **76**, 303-315.
 - [32] Toledo JB, Arnold M, Kastenmüller G, Chang R, Baillie RA, Han X, Thambisetty M, Tenenbaum JD, Suhre K, Thompson JW, John-Williams LS, MahmoudianDehkordi

- S, Rotroff DM, Jack JR, Motsinger-Reif A, Risacher SL, Blach C, Lucas JE, Massaro T, Louie G, Zhu H, Dallmann G, Klavins K, Koal T, Kim S, Nho K, Shen L, Casanova R, Varma S, Legido-Quigley C, Moseley MA, Zhu K, Henrion MYR, van der Lee SJ, Harms AC, Demirkan A, Hankemeier T, van Duijn CM, Trojanowski JQ, Shaw LM, Saykin AJ, Weiner MW, Doraiswamy PM, Kaddurah-Daouk R (2017) Metabolic network failures in Alzheimer's disease: A biochemical road map. *Alzheimers Dement* **13**, 965-984.
- [33] Wykle RL (2004) Arachidonate remodeling and PAF synthesis in human neutrophils. In *Arachidonate Remodeling and Inflammation*, Birkhäuser, Basel, Basel, pp. 73-87.
- [34] Prescott SM, Zimmerman GA, Stafforini DM, McIntyre TM (2000) Platelet-activating factor and related lipid mediators. *Annu Rev Biochem* **69**, 419-445.
- [35] Han X, Holtzman DM, McKeel DW, Kelley J, Morris JC (2002) Substantial sulfatide deficiency and ceramide elevation in very early Alzheimer's disease: Potential role in disease pathogenesis. *J Neurochem* **82**, 809-818.
- [36] Filippov V, Song MA, Zhang K, Vinters H V, Tung S, Kirsch WM, Yang J, Duerksen-Hughes PJ (2012) Increased ceramide in brains with Alzheimer's and other neurodegenerative diseases. *J Alzheimers Dis* **29**, 537-547.
- [37] Han X, Rozen S, Boyle SH, Hellegers C, Cheng H, Burke JR, Welsh-Bohmer KA, Doraiswamy PM, Kaddurah-Daouk R (2011) Metabolomics in early Alzheimer's disease: Identification of altered plasma sphingolipidome using shotgun lipidomics. *PLoS One* **6**, e21643.
- [38] He X, Huang Y, Li B, Gong CX, Schuchman EH (2010) Deregulation of sphingolipid metabolism in Alzheimer's disease. *Neurobiol Aging* **31**, 398-408.
- [39] Katsel P, Li C, Haroutunian V (2007) Gene expression alterations in the sphingolipid metabolism pathways during progression of dementia and Alzheimer's disease: A shift toward ceramide accumulation at the earliest recognizable stages of Alzheimer's disease? *Neurochem Res* **32**, 845-856.
- [40] Jana A, Hogan EL, Pahan K (2009) Ceramide and neurodegeneration: Susceptibility of neurons and oligodendrocytes to cell damage and death. *J Neurol Sci* **278**, 5-15.
- [41] Trushina E, Mielke MM (2014) Recent advances in the application of metabolomics to Alzheimer's disease. *Biochim Biophys Acta* **1842**, 1232-1239.
- [42] Mielke MM, Bandaru VVR, Haughey NJ, Rabins P V, Lyketsos CG, Carlson MC (2010) Serum sphingomyelin and ceramides are early predictors of memory impairment. *Neurobiol Aging* **31**, 17-24.
- [43] Mapstone M, Cheema AK, Fiandaca MS, Zhong X, Mhyre TR, Macarthur LH, Hall WJ, Fisher SG, Peterson DR, Haley JM, Nazar MD, Rich SA, Berlau DJ, Peltz CB, Tan MT, Kawas CH, Federoff HJ (2014) Plasma phospholipids identify antecedent memory impairment in older adults. *Nat Med* **20**, 415-418.
- [44] Casanova R, Varma S, Simpson B, Kim M, An Y, Saldana S, Riveros C, Moscato P, Griswold M, Sonntag D, Wahrheit J, Klavins K, Jonsson P V., Eiriksdottir G, Aspelund T, Launer LJ, Gudnason V, Legido Quigley C, Thambisetty M (2016) Blood metabolite markers of preclinical Alzheimer's disease in two longitudinally followed cohorts of older individuals. *Alzheimers Dement* **12**, 815-822.
- [45] Ma YH, Shen XN, Xu W, Huang YY, Li HQ, Tan L, Tan CC, Dong Q, Tan L, Yu JT (2020) A panel of blood lipids associated with cognitive performance, brain atrophy, and Alzheimer's diagnosis: A longitudinal study of elders without dementia. *Alzheimers Dement (Amst)* **12**, e12041.
- [46] Li D, Misialek JR, Boerwinkle E, Gottesman RF, Sharrett AR, Mosley TH, Coresh J, Wruck LM, Knopman DS, Alonso A (2017) Prospective associations of plasma phospholipids and mild cognitive impairment/dementia among African Americans in the ARIC Neurocognitive Study. *Alzheimers Dement (Amst)* **6**, 1-10.
- [47] Varma VR, Oommen AM, Varma S, Casanova R, An Y, Andrews RM, O'Brien R, Pletnikova O, Troncoso JC, Toledo J, Baillie R, Arnold M, Kastenmueller G, Nho K, Doraiswamy PM, Saykin AJ, Kaddurah-Daouk R, Legido-Quigley C, Thambisetty M (2018) Brain and blood metabolite signatures of pathology and progression in Alzheimer disease: A targeted metabolomics study. *PLOS Med* **15**, e1002482.
- [48] Wood PL, Locke VA, Herling P, Passaro A, Vigna GB, Volpato S, Valacchi G, Cervellati C, Zuliani G (2016) Targeted lipidomics distinguishes patient subgroups in mild cognitive impairment (MCI) and late onset Alzheimer's disease (LOAD). *BBA Clin* **5**, 25-28.
- [49] Barupal DK, Zhang Y, Fan S, Hazen SL, Tang WHW, Cajka T, Irvin MR, Arnett DK, Kind T, Kaddurah-Daouk R, Fiehn O (2019) The circulating lipidome is largely defined by sex descriptors in the GOLDN, GeneBank and the ADNI studies. *bioRxiv* 731448.
- [50] Arnold M, Nho K, Kueider-Paisley A, Massaro T, Huynh K, Brauner B, MahmoudianDehkordi S, Louie G, Moseley MA, Thompson JW, John-Williams LS, Tenenbaum JD, Blach C, Chang R, Brinton RD, Baillie R, Han X, Trojanowski JQ, Shaw LM, Martins R, Weiner MW, Trushina E, Toledo JB, Meikle PJ, Bennett DA, Krumsiek J, Doraiswamy PM, Saykin AJ, Kaddurah-Daouk R, Kastenmüller G (2020) Sex and APOE ε4 genotype modify the Alzheimer's disease serum metabolome. *Nat Commun* **11**, 1148.
- [51] Jiang Y, Zhu Z, Shi J, An Y, Zhang K, Wang Y, Li S, Jin L, Ye W, Cui M, Chen X (2019) Metabolomics in the development and progression of dementia: A systematic review. *Front Neurosci* **13**, 343.
- [52] Dormann CF, Elith J, Bacher S, Buchmann C, Carl G, Carré G, Marquéz JRG, Gruber B, Lafourcade B, Leitão PJ, Munkemüller T, McClean C, Osborne PE, Reineking B, Schröder B, Skidmore AK, Zurell D, Lautenbach S (2013) Collinearity: A review of methods to deal with it and a simulation study evaluating their performance. *Ecography (Cop)* **36**, 27-46.